ASEANO

ASEAN-NORWEGIAN COOPERATION PROJECT ON LOCAL CAPACITY BUILDING FOR REDUCING PLASTIC POLLUTION IN THE ASEAN REGION (ASEANO) 2020 – 2021

SUBPROJECT 1:

MAPPING AND CHARACTERIZATION OF IMUS RIVER WATERSHED USING GEOGRAPHIC INFORMATION SYSTEM AND REMOTE SENSING TECHNOLOGY

Sedigo, N.A., Creencia, G.B.A., Dizon, J.C.R., and Mojica, D.Z.P.
Cavite State University (CvSU)

Editor: Thomas Bell
Formatter: John Castillo
Partnerships in Environmental Management for the Seas of East Asia (PEMSEA

Abstract

River systems have been identified as major pathways and transporters of wastes, including plastics, that ultimately end up in the oceans. The Imus River Watershed (IRW) is located in the Philippine Province of Cavite, one of the provinces in the CALABARZON Region of southern Luzon. This study delineated and mapped the physical boundaries of the Imus River watershed and determined the topographic features, stream characteristics, geomorphology, political subdivisions, barangay communities, population distribution, land use and land cover, and hydro-climatic characteristics of the watershed. Both primary and secondary data sources were used in making comprehensive land use maps, population maps, and hydroclimatic data analyses.

The boundary of the Imus River Watershed was initially established through an unsupervised delineation process using a digital elevation model of Cavite with a 5-meter resolution in ArcGIS. Sangley Point Synoptic Station in Cavite City and the CvSU-PAGASA Agrometeorological Station in Indang were used to define the general hydroclimatic condition of IRW due to their close proximity to the watershed. The total drainage area of IRW is 11,259.80 hectares, covering portions of Tagaytay City, Amadeo, Silang, Dasmariñas, Imus City, Bacoor City and Kawit. Elevation within the watershed ranges from 0 to 655 meters above sea level. The lowland area covers parts of Kawit, Imus City, and Bacoor City; a central hilly area covers parts of Imus City, Bacoor City, and the majority of communities in Dasmariñas and Silang. The upland area covers parts of Silang, Amadeo, and Tagaytay City. There were 56 perennial streams identified with a total length of 186.15 km and 36 river segments. The Imus river system is a combination of headwaters and medium-sized streams. The sub-watersheds, labeled A, B, and C, have drainage densities of 1.15 km/km^2, 1.95 km/km^2, and 1.41 km/km^2, respectively. The sub-watersheds A and C have stream frequencies of 0.20/km^2 and 0.25/km^2 while sub-watershed B has a stream frequency of 0.39/km^2. In alphabetical order, these sub-watersheds have bifurcation ratios of 5, 3.31, and 2.5, elongation ratios of 0.33, 0.26, and 0.43, and circulatory ratios of 0.18, 0.11, and 0.26.

A total of 222 barangay communities are located within the boundaries of the watershed with a total population of 1,351,057 in 2015. 90.67% of the province is classified as alienable and disposable land, while the remaining forest land represents only 9.33%. Alienable and disposable lands are further classified as production land (55.24%) and built-up areas (44.76%). The Sangley Point Synoptic Station has a normal mean temperature of 28.53°C while the CvSU-PAGASA Agromet Station has a normal mean temperature of 26.20°C. The average total annual rainfall recorded at Sangley Point Synoptic station and CvSU Agromet Station were 2,265.69 mm and 2,483.05 mm, respectively. The average flow during wet season was 1,601.84 liters per second, while the average flow during dry season was 1,337.42 liters per second.

Acronyms/Abbreviations

ASTI	Advanced Science and Technology Institute
CALABARZON Region	Cavite, Laguna, Batangas, Rizal and Quezon Region
CLUP	Comprehensive Land Use Plan
CvSU	Cavite State University
DENR	Department of Environment and Natural Resources
DOST	Department of Science and Technology
GIS	Geographic Information System
IRW	Imus River Watershed
LGU	Local Government Unit
LULC	Land Use, Land Cover
MSL	Mean Sea Level
NAMRIA	National Mapping and Resource Information Authority
NIVA	Norwegian Institute for Water Research
PAGASA	Philippine Atmospheric, Geophysical, Astronomical Services Administration
PEMSEA	Partnerships in Environmental Management for Seas of East Asia
POPCEN	Population Census
PPDO	Provincial Planning and Development Office
RBCO	River Basin Control Office
RS	Remote Sensing

Contents

List of Tables

List of Figures

Glossary of Terms

Agrometeorological Station. A derivative station using the advanced remote data-acquisition unit (arQ) geared with multi-parameter weather sensors which can simultaneously measure wind speed and direction; air temperature; air humidity; air pressure, rain amount, duration and intensity, soil moisture and temperature, solar radiation, and sunshine duration.

Barangay. Historically referred to as barrio, the smallest administrative division in the Philippines and the native Filipino term for a village, district, or ward. In metropolitan areas, the term often refers to an inner city neighborhood, a suburb or a suburban neighborhood.

Census. A survey conducted on the full set of observation objects belonging to a given population or universe.

Delineation. The process of establishing the boundary of a watershed using topographic maps.

Discharge/Streamflow. The volume of water that moves over a designated point over a fixed period.

Diurnal temperature range. The difference between the maximum and minimum temperatures within a day.

Geomorphology. The study of physical features of the surface of the earth and their relation to its geological structures.

Land Cover. The surface cover of the ground, whether vegetation, urban, infrastructure, water, bare soil or other.

Land use. The purpose to which land serves.

Maximum Temperature. The highest temperature recorded in a given period of observation or the highest temperature of the entire record.

Minimum Temperature. The lowest temperature recorded in a given period of observation or the lowest temperature of the entire record.

Raster file. An image file of rectangular array of regularly sampled values known as pixels.

Rating Curve. A graph of discharge versus stage for a given point on a stream, usually at gauging stations, where the stream discharge is measured across the stream channel with a flow meter.

Shapefile. A simple, non-topological format for storing the geometric location and attribute information of geographic features.

Sub-watershed. A small watershed delineated within a larger watershed, often for purposes of describing and managing local conditions.

Synoptic Station. A station at which meteorological observations are made for the purposes of synoptic analysis.

Temperature Anomaly. The difference from an average or baseline temperature.

Watershed. Also called as drainage basin or catchment, it is a land area that channels rainfall to creeks, streams, and rivers and eventually to outflow points such as reservoirs, bays and the ocean.

Executive Summary

River systems acts as major pathways for the transport of waste, particularly non-biodegradable plastics. Of the land-based waste which enters rivers, most ends up in our oceans.

The Imus River watershed is located in the Philippine province of Cavite, south of Manila. It flows into Manila Bay, a pollution hotspot. This study delineated and mapped the physical boundaries of the watershed. It studied aspects of physical geography, such as topographic features, stream characteristics, geomorphology, land cover, and hydro-climatic characteristics of the watershed, as well as human geography, such as political subdivisions, population distribution, and land use.

Both primary and secondary data sources were used to make comprehensive land use maps, population maps, and hydro-climatic data analyses. The boundary of the Imus River watershed was established using a digital elevation model of the province of Cavite in ArcGIS. Sangley Point Synoptic Station in Cavite and the CvSU-PAGASA Agrometeorological Station in Indang were used to assess the general hydro-climatic condition of IRW due to their close proximity to the watershed.

The total drainage area of the Imus River watershed is 11,259.80 hectares, and its elevation ranges from 0 to 655 meters above sea level. Areas considered lowland include parts of Kawit, Imus and Bacoor. A centrally hilly area covers parts of Imus, Bacoor and the majority of communities in Dasmariñas and Silang. The upland area covers parts of Silang, Amadeo and Tagaytay. There were 56 perennial streams identified with a total length of 186.15 km and 36 river segments. These can be divided into three sub-watersheds, each with their own characteristics.

A total of 222 barangay communities are situated fully or partially within the boundaries of the watershed, and as of 2015 the estimated population of the watershed is 1,351,057 people. 90.67% of the province is classified as alienable and disposable land, divided into production land (55.24%) and built-up areas (44.76%).

Normal mean temperatures ranged from 26.20°C to 28.53°C, while average total annual rainfall ranged from 2,265.69 mm to 2,483.05 mm. The average flow during wet season was 1,601.84 liters per second, while the average flow during dry season was 1,337.42 liters per second.

Introduction

The Philippines Province of Cavite is located within the CALABARZON region in the south of Luzon Island known as the CALABARZON Region. Cavite is bound by Metro Manila and Manila Bay in the north, Batangas in the south, Laguna in the east and the West Philippines sea in the west (Provincial Government of Cavite, 2017). The land area of the province is 142,706 ha, which comprises 0.4% of the total land area of the Philippines. The province is composed of 7 cities and 16 municipalities, which together are made up of a total of 829 barangays (PEMSEA and Provincial Government of Cavite, 2017). In the 2020 census of the Philippines Statistics Authority, the total population of Cavite was 4,344,829. Cavite was the fastest growing province in CALABARZON with an annual population growth rate of 3.57% from 2015 to 2020, higher than the national average of 1.63%. There is significant economic development in the province due to its proximity to Metro Manila, with the provincial government estimating GDP to be PHP 42,000 per capita (PEMSEA, 2020). Economic activity in the province include agriculture, mining, forestry, grazing, gathering fishing and quarrying. Cavite is also a highly industrialized and urbanized province in the country and is the best-loved destination of investors next to Metro Manila as manifested by increasing number of industries. According to the Department of Trade and Industry (DTI) the average annual revenue of the province amounted to PHP 9,220,374,201.26 from 2016 to 2020.

There are six major river systems in Cavite namely; Maragondon, Labac-Alemang, Timalan, Cañas, San Juan, and Imus River (**Figure 1**). These river systems provide crucial natural ecological functions and ecological services. In addition to sustaining local biodiversity, these river systems also sustain the needs of the population of the province in terms of water, food, livelihood, and recreation (Sedigo *et al*., 2015). Due to the rapid agro-industrialization, commercialization, and urbanization in the province, these river systems are increasingly exposed to waste generation from households, commercial establishments, industries, and agriculture. Waste entering the river further risks being transported downstream into Bacoor Bay and other sections of the wider Manila Bay coastline. These wastes include non-degradable plastics, which go on to produce secondary plastics (e.g. microplastics) through

fragmentation. Accumulating in rivers and the ocean, microplastics may pose a greater and less visible threat to ecosystems (Andrady, 2011).

Imus River originates in the upland city of Tagaytay. It traverses the upland municipalities of Amadeo and Silang before passing the densely urbanized cities of Dasmarinas, Imus, Bacoor, and the coastal municipality of Kawit. It finally drains into Bacoor Bay, a sheltered part of the wider Manila Bay. As with other rivers running parallel to Imus River in Cavite, this route conveys waste that finds its way into the river from homes, commercial centers, industries and agricultural farms, towards the ocean. Significant waste is transferred by periodic flooding in the river, especially during the rainy season.

The monitoring of rivers is an essential component of the effective monitoring and management of plastic pollution. The Imus River system has been identified as the Philippine study site of the ASEANO project. As a site of a growing population and economy, it is a likely hotspot for increasing waste output. The ASEANO project is a project led by the Norwegian Institute for Water Research (NIVA) and financed by the *Norwegian Development Assistance Program Against Marine Litter and Microplastics*. The aim of the ASEANO project is to strengthen knowledge, capacity, and awareness to deal with plastic pollution in the ASEAN region. To achieve this aim, having a good understanding of local conditions is crucial. This study seeks to gather baseline data of the Imus river basin such as drainage area, river morphology, hydro-climatic data, as well as the socio-economic characteristics of communities located within its boundaries.

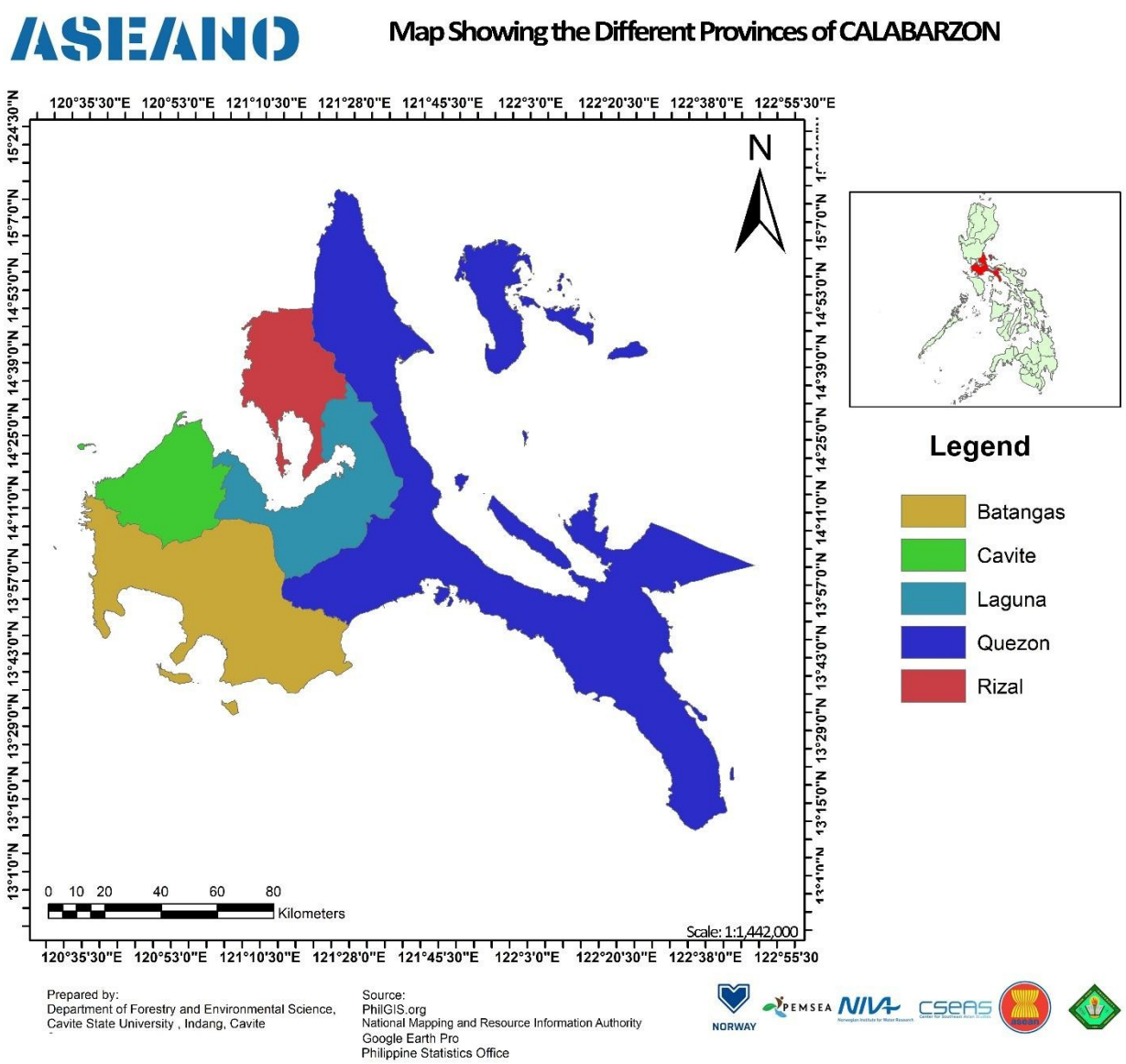

Figure 1. Cavite (green) within the CALABARZON region

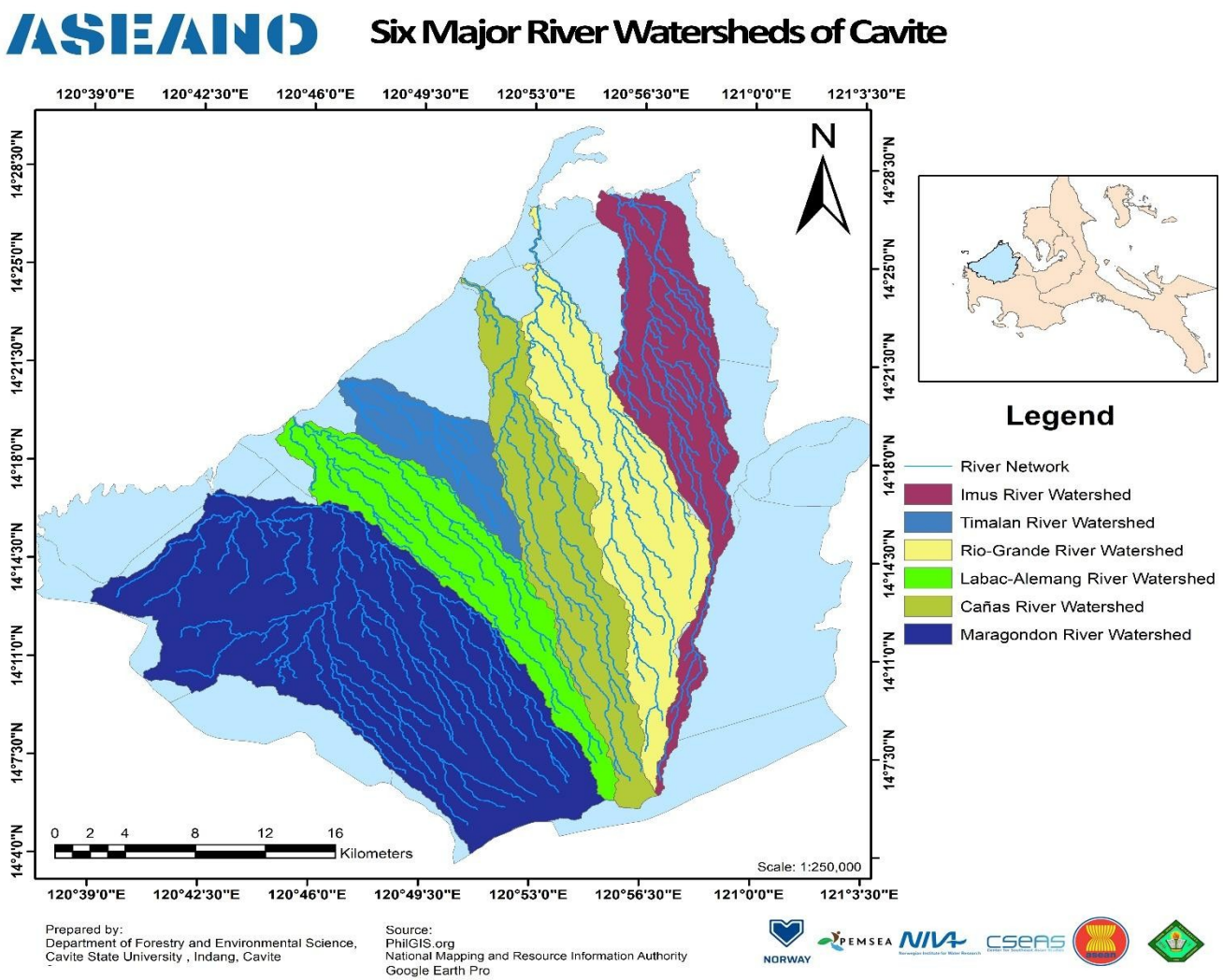

Figure 2. The six major river watersheds in Cavite. The Imus River Watershed (IRW) 60is shown in purple.

Objectives of the Study

This project aimed to delineate the boundaries of Imus River Watershed and characterize the watershed through GIS and RS technologies.

It specifically aimed to:

1. delineate and map the physical boundaries of the Imus River watershed;
2. determine the topographic features of the watershed in terms of:
    2.1. contour;
    2.2. elevation; and
    2.3. slope;
3. determine the stream characteristics and geomorphology of the watershed in terms of:
    3.1. river network;
    3.2. stream order;
    3.3. drainage density;
    3.4. stream frequency;
    3.5. bifurcation ratio;
    3.6. elongation ratio; and
    3.7. circulatory ratio;
4. identify the political subdivisions and barangay communities within the watershed;
5. determine the population distribution within the watershed in terms of:
    5.1. total population per barangay; and
    5.2. population density per barangay
6. determine the land use and land cover of the watershed; and
7. determine the hydro-climatic characteristics of the watershed in terms of:
    7.1. air temperature;
    7.2. rainfall; and
    7.3. streamflow

Methodology

Study Site

The main body of the Imus River is 38.4 kilometers long. Counting its smaller streams and segments, the complete river system spans a total of 186.15 kilometers. It originates from the mountains of Tagaytay and flows through the communities of Balite, Sabutan, Biga, Silang, Palapala, Dasmariñas, Pasong Bayog and San Agustin. A connection to Pasong Bayog passes through the communities of Salitran, Baluctot, Anabu II, Anabu I, Tanzang Luma, Palico, Imus, Salinas, Mabolo and Bacoor before draining out at Bacoor Bay. Baluctot also has a separate connection to the Imus River. Another connection from Pasong Bayog flows through the communities of San Agustin and Bucal. The Imus River system flows through some of the most densely-populated cities in Cavite, including Dasmariñas, Imus, Kawit and Bacoor, before emptying its contents in Manila Bay, one of the world's most polluted bodies of water. (Cavite Ecological Profile, 2017). According to DENR-RBCO (2015) as cited by Paringit and Uy (2017), the outlet of the watershed is located at 14°27'31.16"N, 120°55'34.00"E where the estimated annual runoff is 168 million cubic meters.

Data Gathering

The project performed primary baseline and secondary data gathering procedures. A 5-meter resolution Digital Elevation Map (DEM) and the 2015 land use map of the province of Cavite were requested from the National Mapping and Resource Information Authority (NAMRIA). Comprehensive land use maps of all the municipalities and cities within the Imus River Watershed were requested from the Provincial Planning and Development Office (PPDO) of the Province of Cavite. The DEM was used to establish the boundary and other physiographic characteristics of the watershed. The land use/land cover (LULC) maps were used to characterize the general land cover and land appropriation of the watershed. The latest published population census in 2015 was requested from the Philippine Statistics Authority.

The climate data from Sangley Point Synoptic Station and CvSU-PAGASA Agrometeorological Station were requested from the Philippine Atmospheric, Geophysical and Astronomical Services Administration (PAGASA) while the water level data was requested from the Department of Science and Technology - Advanced Science and Technology Institute (DOST-ASTI).

Delineation and Topographic Characterization of Imus River Watershed

The boundary of the Imus River Watershed was initially established through a delineation process using a digital elevation model of the province of Cavite with 5-meter resolution in ArcGIS. Through the hydrology toolbox in the spatial analyst extension of ArcGIS, the sinks of the DEM were filled to remove data imperfections. To establish how water flowed through the local topography, flow direction was determined in individual cells. A flow accumulation path was built through the flow accumulation raster, and pour points (flow outlets) were identified to determine the watershed pertaining to the flow path. Using the flow direction raster and the pour point shape file as the input, the watershed was delineated using watershed tool in hydrology tool box. This was validated through field visits on the ground and using remote sensing technology to test the consistency of the established boundary. The topographic features such as contour, elevation, and slope of the Imus River Watershed were also extracted from the digital elevation model.

Watershed Geomorphology

The geomorphological characterization of the Imus River Watershed was done to further analyze and understand its structures and dynamics. Its geomorphology together with its hydroclimatic characteristics determine the structure and composition of the watershed and its biotic communities. Such characterization also provides a basis for the prediction of watershed products transported in its channels, such as sediments, woody debris, and plastics.

Sub-watershed and river network. The Imus River Watershed was divided into three sub-watersheds for more detailed geomorphological characterization. Analysis of the river network segments looked at length, confluence, and bed slope.

Stream ordering. Stream ordering is a method of assigning a numeric order to links in a stream network, allowing for the identification and classification of types of streams based on their numbers of tributaries. Some characteristics of streams can

be inferred by simply knowing their order. Using the stream order, the rivers within the watershed were identified as headwaters, medium-sized river channels, or large river channels.

Drainage density. This was calculated as the length of perennial channels divided by their drainage area. It is usually expressed in kilometers per square kilometer (km/km^2).

Stream frequency. This refers to the number of river segments over the total drainage area. The river segments or the river confluence is a point where two or more flowing bodies of water join to form a single channel.

Bifurcation ratio. This is the relationship between the number of stream segments of a given order and the number of streams of the next higher given order. This measures how a single stream order discharges water into another (Horton, 1945). Bifurcation ratio can be computed using the formula:

$$R_b = \frac{N_u}{N_u + 1}$$

Where:

R_b = Bifurcation ratio
N_u = number of the given stream order
N_{u+1} = number of the next higher stream order

Elongation ratio. A dimensionless property which is the ratio of the diameter of a circle of the same area as the basin to the maximum basin length (Sukristiyanti, Maria, & Lestiana, 2018). It was calculated using the formula:

$$R_e = \frac{2\sqrt{}}{}$$

Where:

R_e = Elongation Ratio
A = Area of the watershed/basin
L_b = Watershed length

Circulatory ratio. A dimensionless property which is the ratio between the area of a watershed and the area of a circle with the same circumference as the perimeter of the watershed (Sukristiyanti, Maria, & Lestiana, 2018). It can be calculated using the formula:

$$R_c = \frac{4\pi A}{P^2}$$

Where:

R_c = Circulatory Ratio
A = Area of the watershed/basin
P = Perimeter of the watershed/basin

Mapping of Barangay's and Population Distribution

The barangays within each of the municipalities and cities covered by the Imus River watershed were overlaid with established watershed boundary and river network to identify all the barangay's within the IRW. Using the population data from the Philippine Statistics Authority, total population and population density maps of the IRW were created to identify the population variations among barangay communities. For those barangays that were partially covered by the IRW, the population considered in the study was obtained by allocating a percentage of the barangay population equivalent to the land area covered by the IRW.

Mapping of the Land Use/Land Cover (LULC) of Imus River Watershed

A general land cover map for the IRW showing the presence of crops, grasslands, water bodies, open/barren areas and built-up areas was generated using the 2015 land cover map from NAMRIA. The comprehensive land use maps of the cities/municipalities were requested from the PPDO and then overlaid with the watershed boundary to show the land use and appropriation of the watershed.

Hydroclimatic Characterization of Imus River Watershed

Two weather stations in close proximity to the watershed were used to assess hydroclimatic condition: Sangley Point Synoptic Station in Cavite City (14° 29' 29.94" N, 120° 53' 54.96"E) and the CvSU-PAGASA Agrometeorological Station in Indang (14° 11' 52.39" N, 120° 53' 0.80"E). The watershed was divided into two approximate areas of influence relating to each weather station through the Thiessen Polygon Method. In this method, perpendicular bisectors are constructed at the midpoint of the line segment connecting the two stations. These bisectors determined the boundary between the area of influence of each station. Sangley Point Synoptic

Station generally covers the lowland area whilst the CvSU-PAGASA Agro-met Station represents the upland area of the watershed.

Air temperature. Air temperature data from Sangley Point Synoptic Station cover up to 26 years (1995 – 2020) and those from CvSU-PAGASA Agromet Station about 14 years (2007 – 2020). The daily measurements of air temperature (daily maximum and minimum air temperature) from each station were used to analyze temperature variation. The maximum and minimum readings were used to determine the diurnal temperature range for each station.

Rainfall. Available rainfall data from Sangley Point Synoptic Station cover 26 years (1995 – 2020) and those from CvSU-PAGASA Agromet Station cover 14 years (2007 – 2020). The rainfall data was used to determine rainfall normal, areal distribution, and seasonal variation. Data augmentation using a correlation technique was used to lengthen the rainfall data for CvSU-PAGASA Agrometeorological Station (See Annex A).

Streamflow. The Water Level Station installed by DOST-ASTI at Daang Hari Bridge, Imus, Cavite was used to measure streamflow of the IRW. It is located at 14° 22' 22.49"N, 120° 56' 31.66" E and was installed in February 2017.The cross-sectional survey done by Paringit and Uy (2017) at Daang Bridge, Imus, Cavite was used to develop a rating curve to translate the water level readings into discharge (Figure 1). The elevation at the left bank of the river is 37.91m at Mean Sea Level (MSL) while the elevation at the right bank of the river is 37.82m at MSL. The lowest part of the cross-section (Zero Datum) is at 25.91m at MSL.

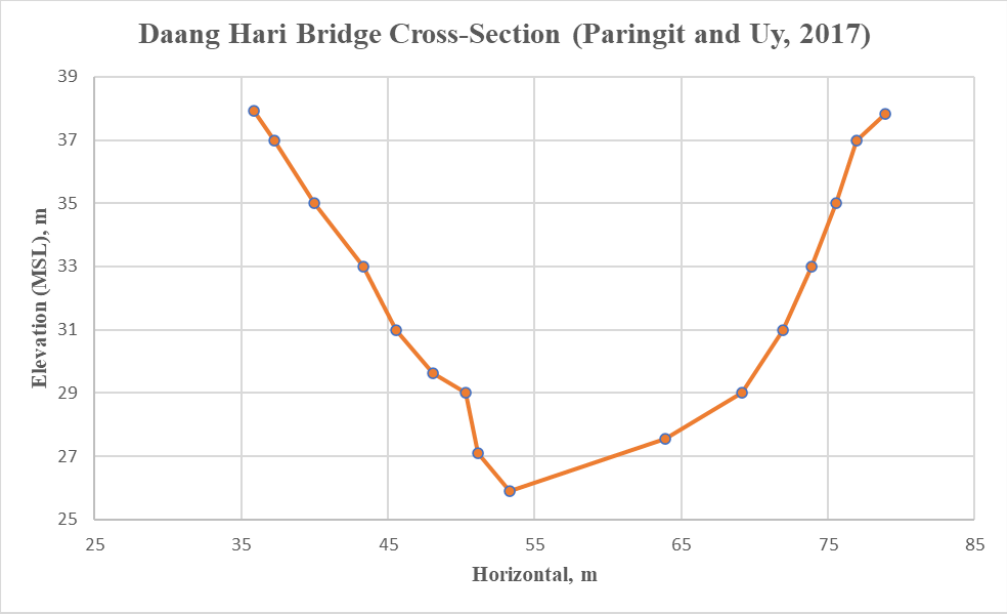

Figure 3. Cross-sectional area of the outlet at Daang Hari Bridge

The relationship between known discharge and the water level (Figure 4) shows a trend line of the rating curve is y=0.2078$x^{3.1002}$, where y = discharge and x = water level. This allows an approximation of streamflow discharge readings from water level readings.

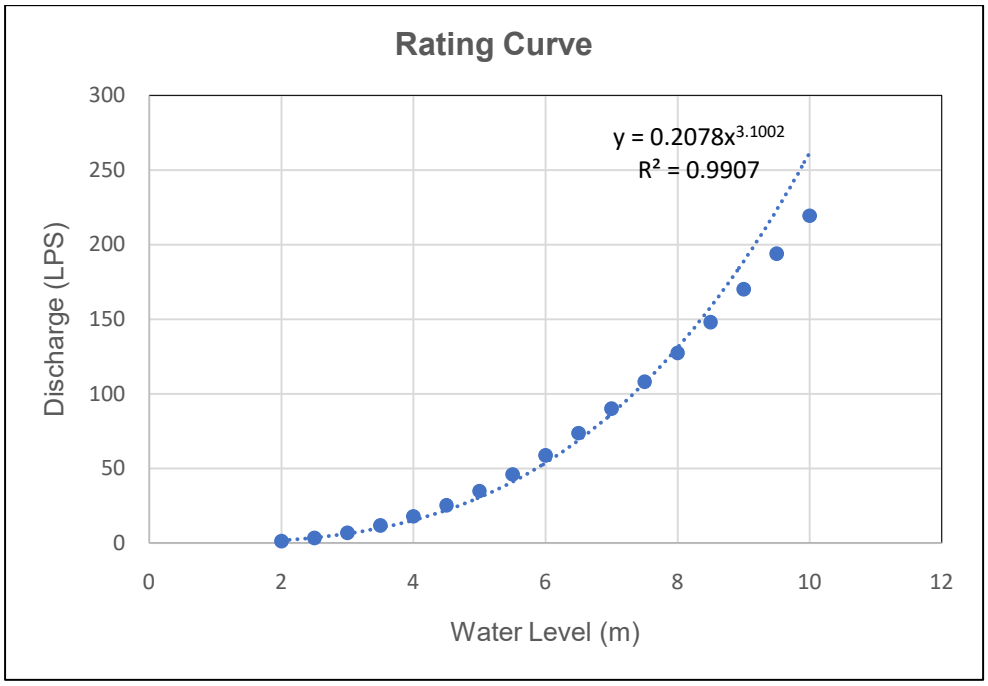

Figure 4. Developed rating curve of the outlet at Daang Hari Bridge.

Results and Discussion

Delineation and Mapping of the Physical Boundaries of Imus River Watershed

Based on the final boundary established (**Figure 5**), the total drainage area of the IRW is 11,259.80 hectares. It covers portions of three municipalities, namely: Amadeo, Kawit and Silang, and portions of four cities, namely: Bacoor, Dasmariñas, Imus, and Tagaytay. Among these municipalities and cities, Dasmariñas City has the largest area within the watershed, around 4,830.42 ha, or 42.92% of the total watershed. Amadeo has the least area covered by the watershed, only 4.09 ha or 0.03% of the watershed (**Table 1**).

Table 1. Municipalities and cities located within Imus River Watershed

Municipality/City	Area (ha)	Share of Watershed (%)
Amadeo	4.09	0.03
Bacoor	1,880.31	16.70
Dasmariñas	4,830.42	42.92
Imus	2,993.66	26.60
Kawit	137.74	1.21
Silang	1,263.36	11.22
Tagaytay	150.19	1.32
Total	**11,259.80**	**100**

Determination of the Topographic Features of Imus River Watershed

The elevation within the watershed ranges from 0 to 655 meters above sea level (**Figure 6**). The Imus River Watershed is divided into three distinct areas: the lowland area has an elevation of 0 – 30 meters above sea level which is relatively flat; central hilly area has an elevation of 30.01 – 400 meters above sea level and a slope of 0.5% to 2%; and upland area has an elevation of 400.01 – 655 meters above sea level and a slope greater than 2% (**Figure 7**, **Figure 8**). The lowland area covers parts of Kawit, Imus City and Bacoor City; centrally hilly area covers parts of Imus City and Bacoor City and the majority of the communities found in Dasmariñas and Silang; the upland area includes parts of Silang, Amadeo, and Tagaytay City.

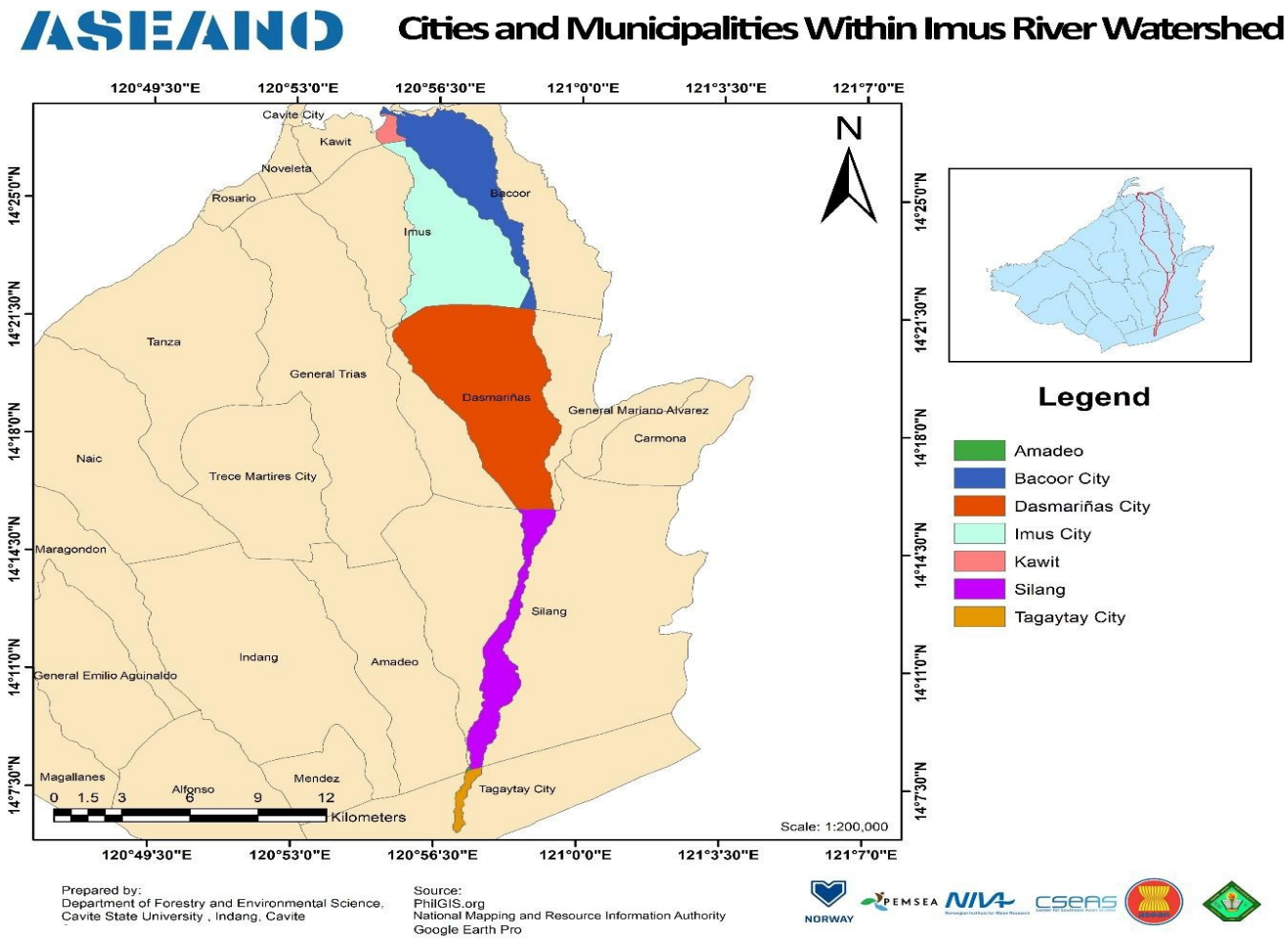

Figure 5. Cities and municipalities partially covered by the Imus River Watershed.

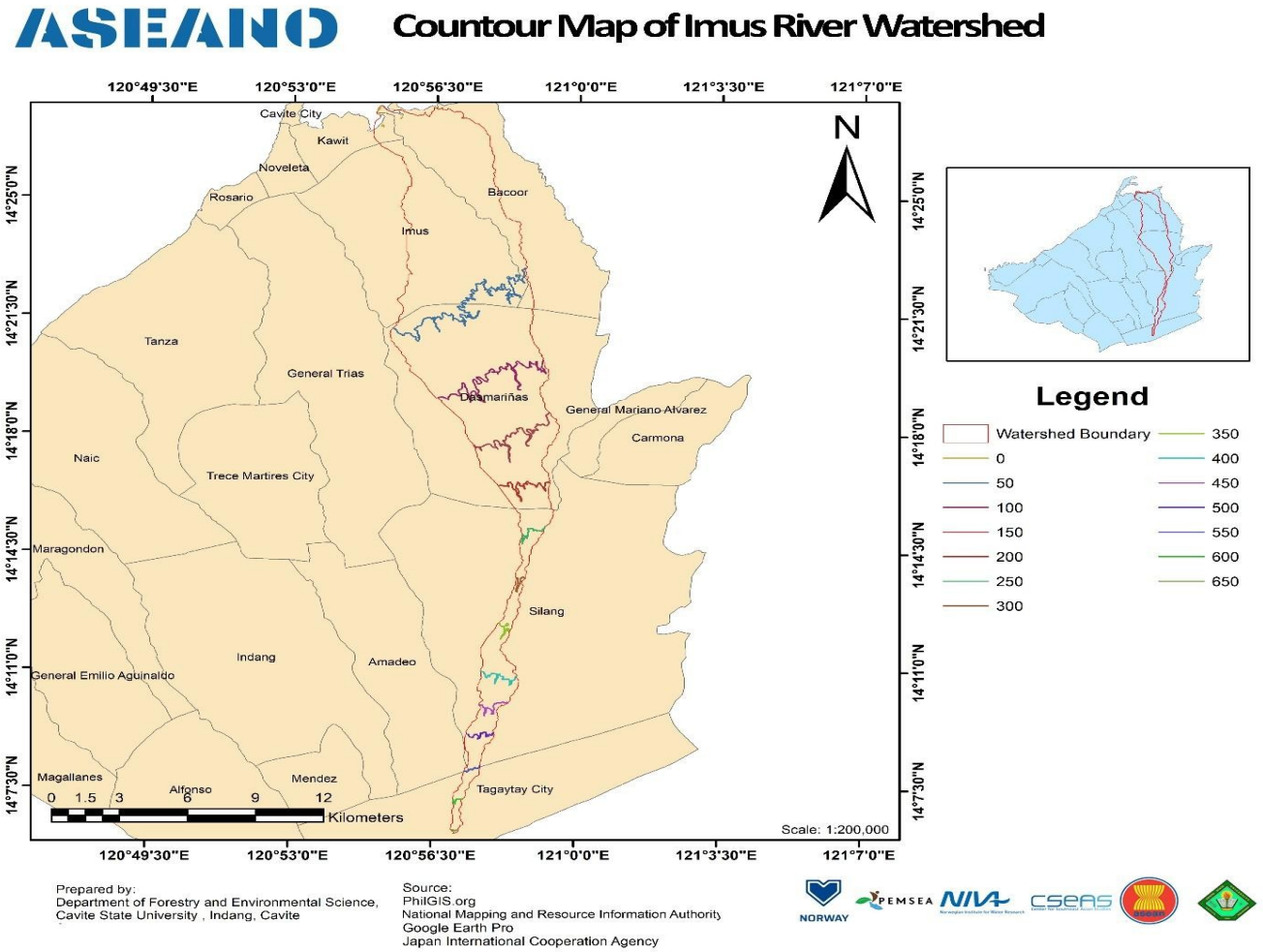

Figure 6. Topographic contours of the Imus River Watershed.

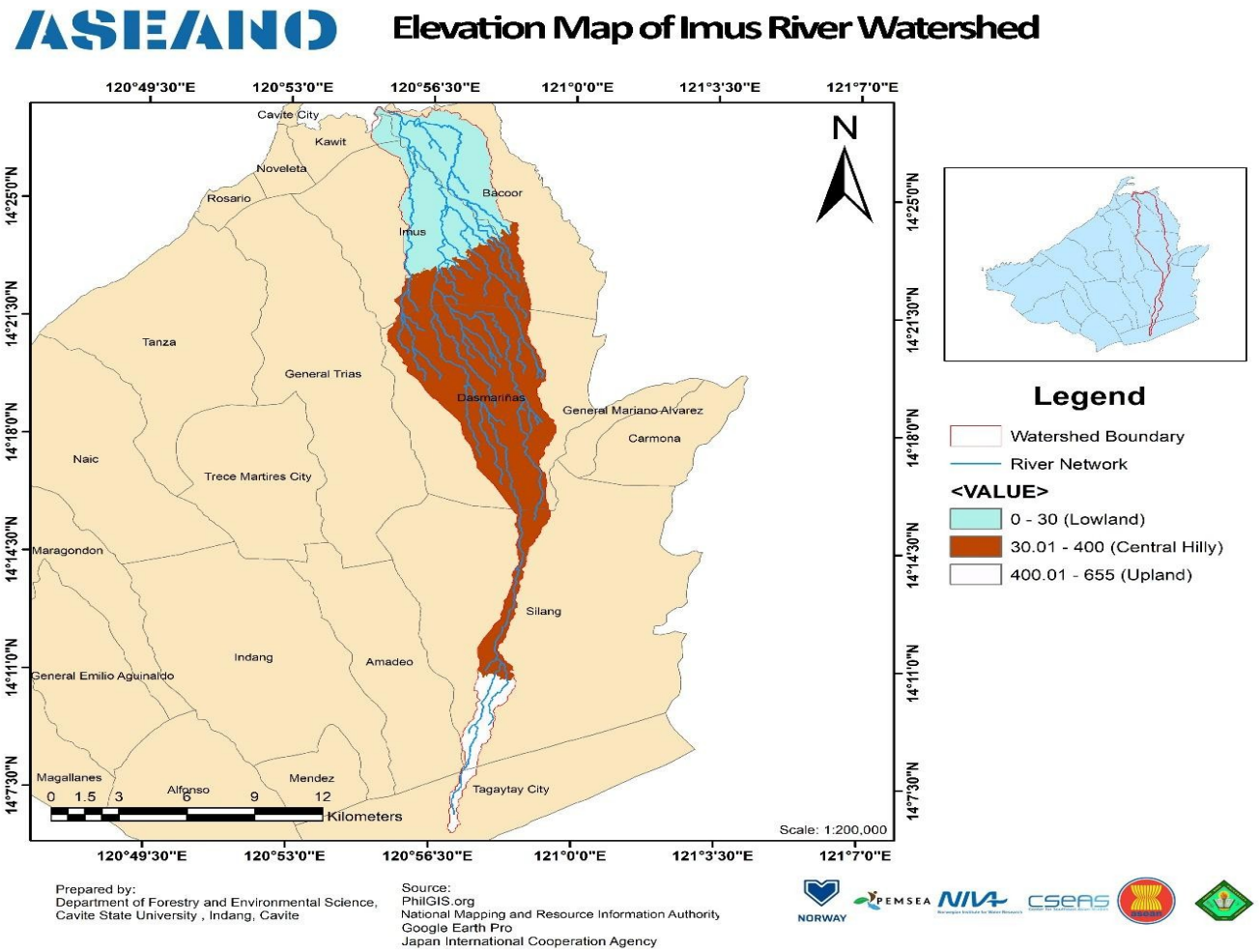

Figure 7. Division of the Imus River Watershed by elevation.

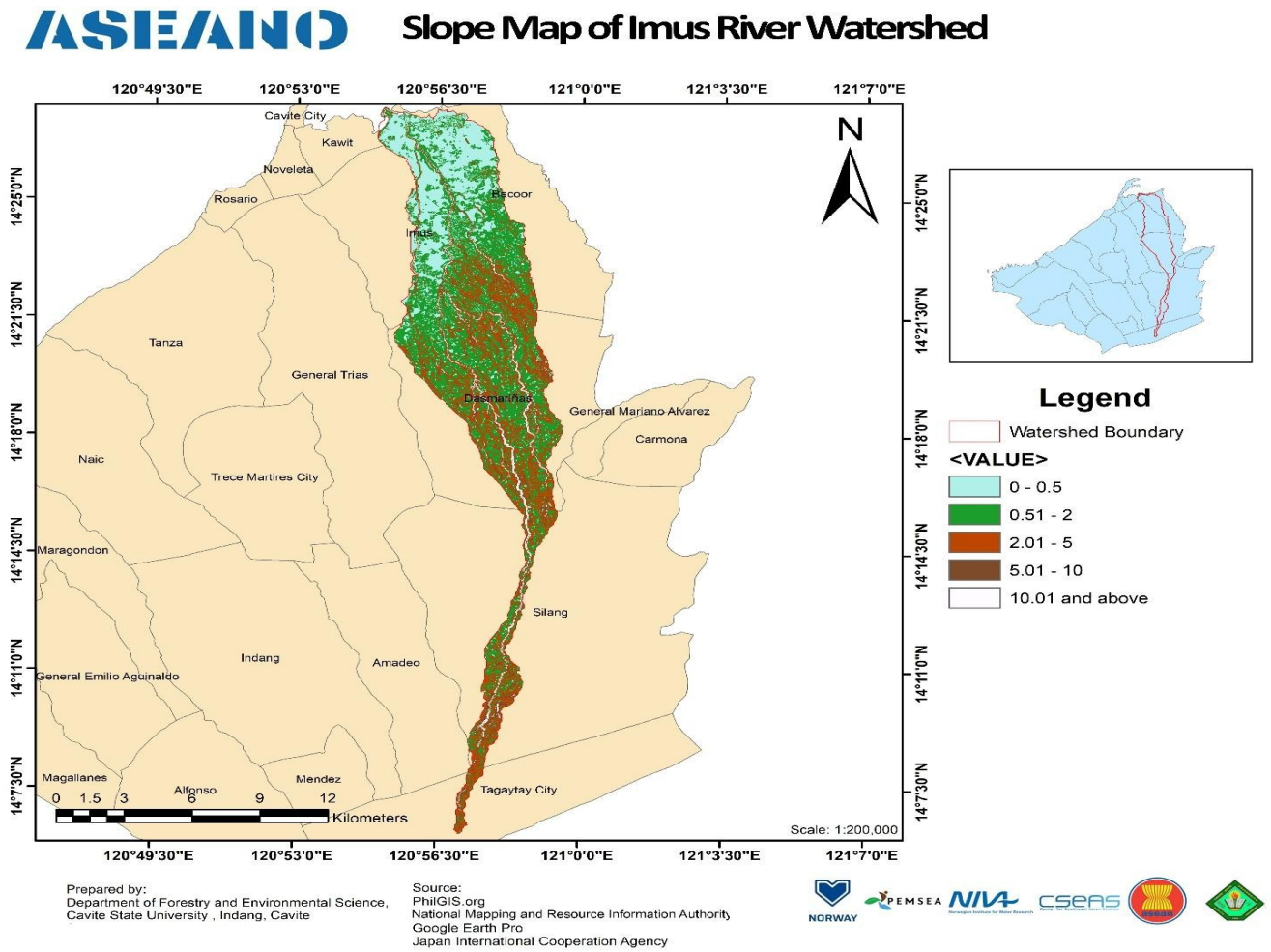

Figure 8. Slope of land within the Imus River Watershed.

Geomorphology of Imus River Watershed

The geomorphology of a watershed influences the dynamics of streams and rivers that are important in understanding the formation and alteration of the stream or river channels, flood plains, and associated upland transitional zones. This information is useful for an effective, long-term watershed management (O'Keefe, Elliot, & Naiman, 2020).

Sub-watershed and river network. There were 56 perennial streams identified with a total length of 186.15 km. 36 river segments were identified (Figure 9), along with their highest and the lowest points (Figure 10). The elevations of the identified points were extracted and used in determining the bed slope of each river (**Table 2**). The watershed was divided into three major sub-watersheds (**Figure 11**). Sub-watershed A has a total drainage area of 2,034.87 ha and a perimeter of 37.37 km, covering portions of Imus, Dasmariñas, and Kawit. Sub-watershed B has a total drainage area of 6,873.79 ha and a perimeter of 90.26 km which covers portions of Imus, Dasmarinas, Silang, Amadeo and Tagaytay; and sub-watershed C has a total drainage area of 2,025.62 ha and a perimeter of 31.20 km which covers Bacoor.

Stream order. Based on river category, rivers with stream order ranging 1 to 3 are considered as headwaters while those ranging from 4 to 6 are medium sized rivers. Based upon this, the river system of the Imus River Watershed is characterized by a combination of headwaters and medium-sized streams.

Table 2. Stream ordering of each sub-watershed of Imus River Watershed.

Sub-watershed	Stream Order	Number of Streams	Total Length
A	1	5	10.13
	2	1	13.41
B	1	31	68.87
	2	7	44.46
	3	2	9.71
	4	1	11.09
C	1	6	15.65
	2	2	12.09
	3	1	0.76

Drainage density. According to Sukritiyani *et al.* (2017), there are five classes of drainage area based on its drainage density: very coarse (<2 km/km^2); coarse (2 – 4 km/km^2); moderate (4 – 6 km/km^2); fine (6 – 8 km/km^2); and very fine (>8 km/km^2).

In the case of IRW, sub-watersheds A, B, and C have values of 1.15 km/km^2, 1.95 km/km^2, and 1.41 km/km^2, respectively. These values classify as very coarse or very low-density drainage areas that may indicate a poorly drained basin with a slow hydrologic response, making them more susceptible to flooding and erosion.

Stream frequency. According to Prabhakaran & Raj (2018), watersheds can be grouped into three classes based on their stream frequency: low frequency (< 2.5 per km^2); moderate frequency (2.6 – 3.5 per km^2); and high frequency (>3.5 per km^2). In the case of IRW, sub-watersheds A and C have values of 0.20/km^2 and 0.25/km^2, which classify as low stream frequency. This indicates lower permeability, less relief, and a gentler slope, which is consistent with sub-watersheds A and C covering relatively flatter lowland areas. On the other hand, sub-watershed B has a value of 0.39/km^2, which falls under a high stream frequency, indicating a steep slope and greater rainfall, consistent with what is common in mountainous areas.

Bifurcation ratio. The values of bifurcation ratio range from 2 to 5 with an average of 3.5. According to Yangchan (2015), high bifurcation ratios ranging from 3 to 5 indicate a structurally more disturbed watershed with prominent distortion in drainage pattern. These values may indicate mountainous or highly dissected drainage basins (Horton, 1945). On the other hand, low bifurcation ratios (<3) indicate a more structurally stable watershed and a clearer drainage pattern (Yangchan, 2015). These range of values may indicate a flat or rolling drainage basins (Horton, 1945).

In the case of IRW, sub-watersheds A and B have bifurcation ratios of 5 and 3.31 respectively, which indicates that the majority of these sub-watersheds are mountainous and highly dissected, with lower flood susceptibility. On the other hand, sub-watershed C has a bifurcation ratio of 2.5, indicating a flat or rolling basin that has a higher possibility of flooding.

Elongation ratio. The elongation ratio is classified into two classes: low value (<1), which indicates an elongated watershed having high relief and steep slope, and high value (>1), which indicates a circular watershed with low relief and low slope. Watersheds with high relief are more susceptible to erosion (Sukristiyanti, Maria, & Lestiana, 2018). In the case of the IRW, sub-watersheds A, B, and C have values of 0.33, 0.26, and 0.43 respectively, indicating that they are all highly elongated and susceptible to erosion due to high relief and steeper slope.

Circulatory ratio. The value of circulatory ratio varies from 0 (minimum circulatory) to 1 (maximum circulatory). It is used to determine the geomorphological stages of development of any basin or watershed. The high, medium, and low values of circulatory ratios are indicative of old, mature, or young stages of the geomorphological adjustment of any basin (Mahala, 2020). In the case of the IRW, sub-watersheds A, B, and C have values of 0.18, 0.11, and 0.26 respectively. These are low values indicating the watershed is in a young dendric stage.

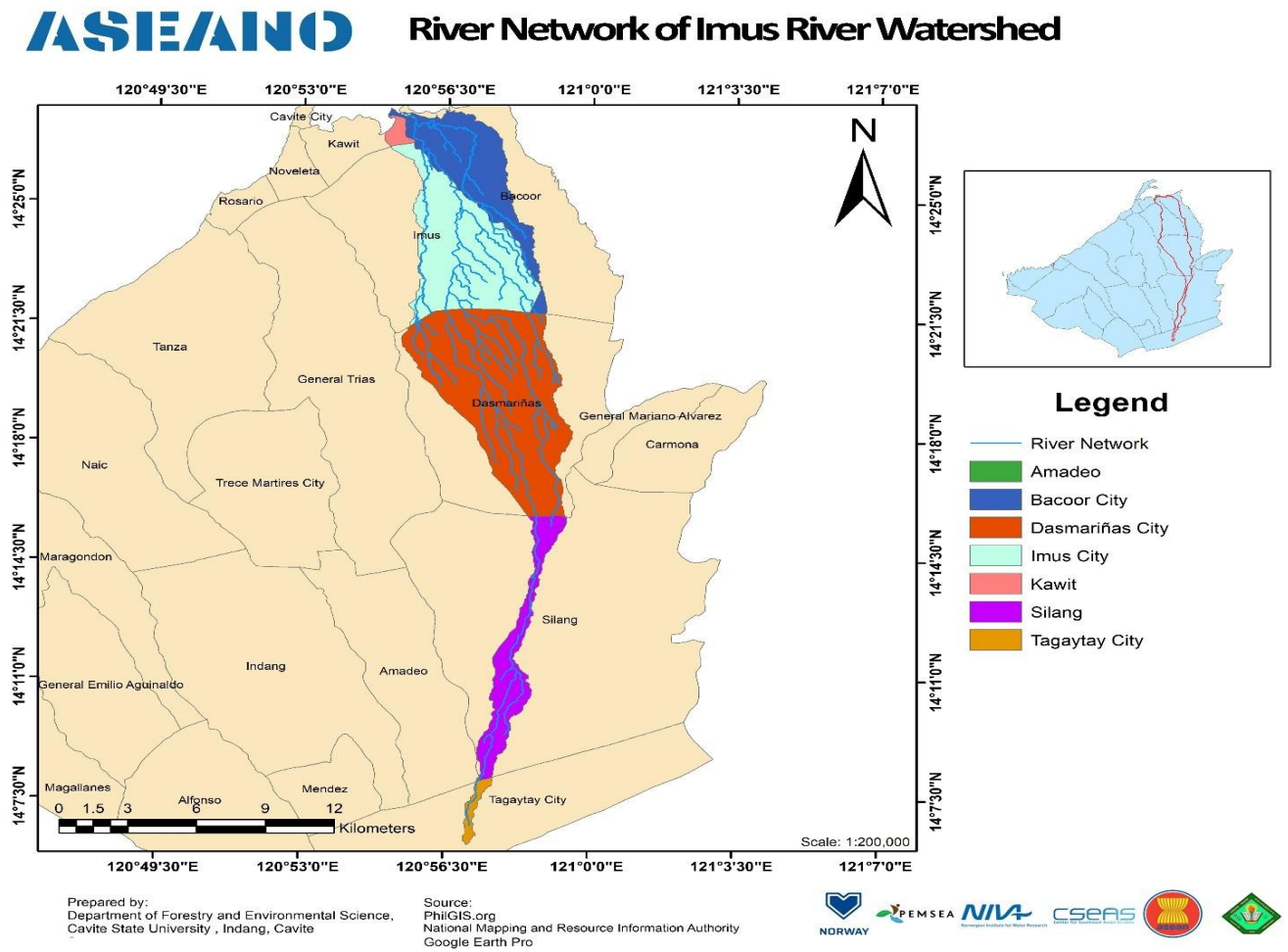

Figure 9. The river network of Imus River Watershed overlaid onto local government units (cities and municipalities)

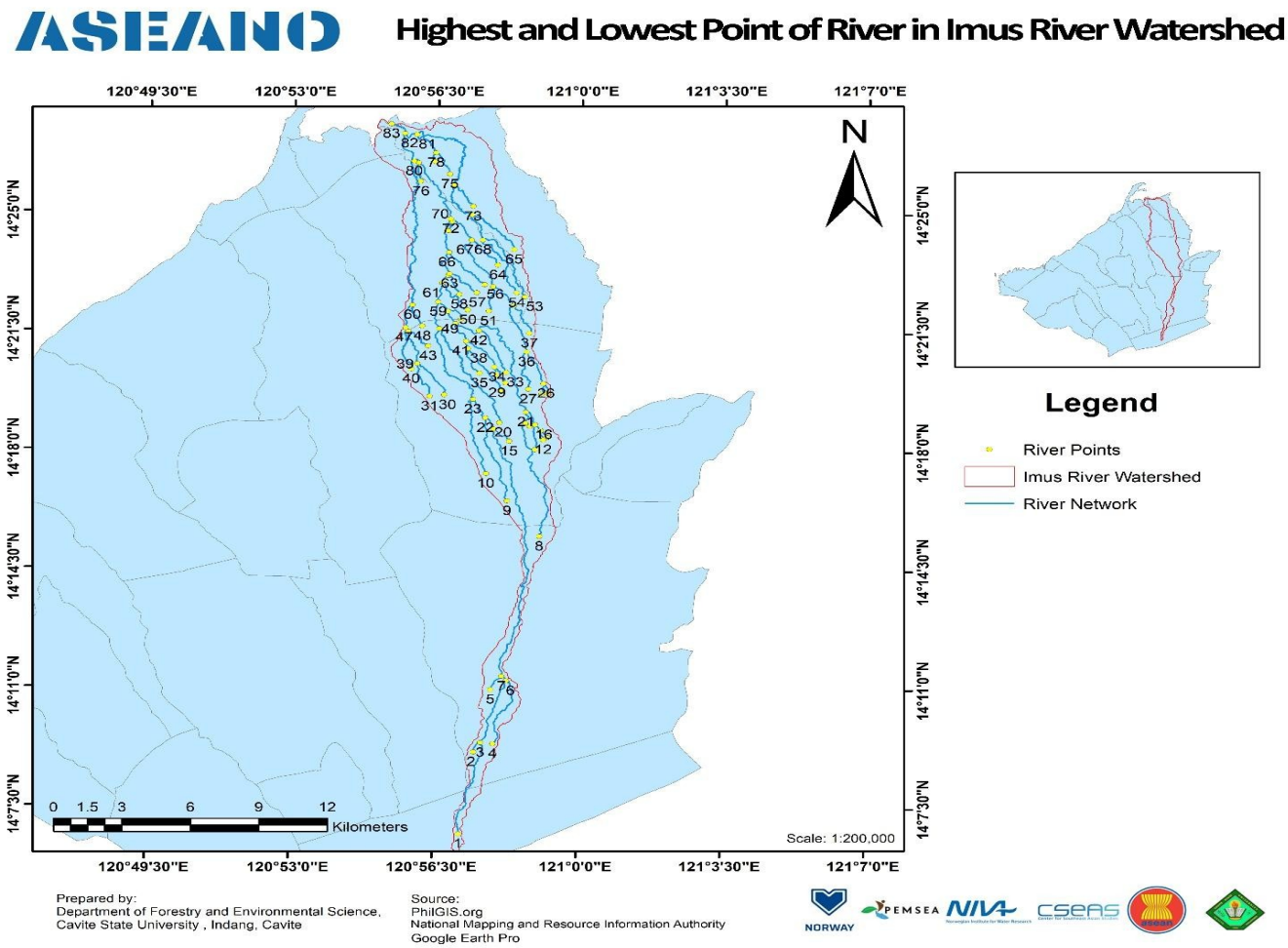

Figure 10. The highest and lowest points within the Imus River Watershed.

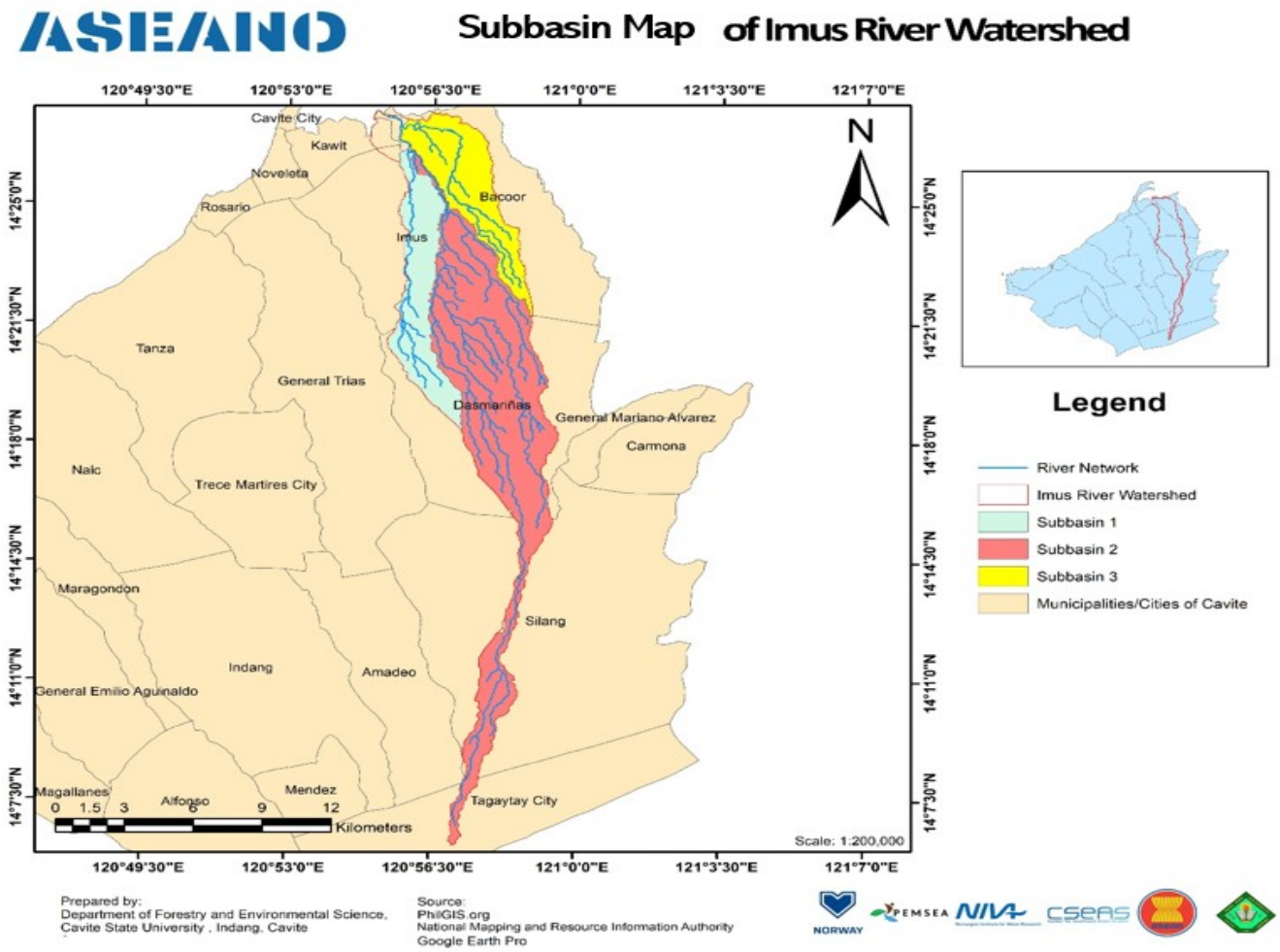

Figure 11. Sub-watersheds of the Imus River Watershed.

Political Subdivisions and Barangay Communities within the Imus River Watershed

The province of Cavite has seven cities and sixteen municipalities, with 829 barangay communities subdivided into eight legislative districts. The barangay communities within IRW have been identified based on the established physical boundary of the watershed (**Figures 12** to **18**). Dasmariñas has the highest number of barangay's (69) located within the watershed, while Amadeo has only one barangay inside the watershed (**Table 3**).

Table 3. List of barangay communities within the Imus River Watershed.

Municipality/City	List of Barangays Within IRW
Tagaytay *(See Figure 12)*	(7 barangays) Kaybagal East, Mag-Asawang Ilat, Maharlika East, Maitim 2nd Central, Maitim 2nd West, Silang Junction North, Silang Junction South
Amadeo *(See Figure 13)*	(1 barangay) Buho
Silang *(See Figure 14)*	(19 barangays) Balite I & II, Barangay I – IV, Biga II, Buho, Iba, Lalaan I & II, Malabag, Malaking Tatyao, Mataas Na Burol, Sabutan, San Vicente II, Toledo, Tubuan I & III
Dasmariñas *(See Figure 15)*	(69 barangays) Zone IV, Burol I – III, Burol, Datu Esmael, Emmanuel Bergado I & II, Fatima I – III, Luzviminda I & II, Paliparan I – III, Sabang, Saint Peter I & II, Salawag, Salitran I – IV, Sampaloc I – V, San Agustin I – III, San Andres I & II, San Antonio de Padua I & II, San Dionisio, San Esteban, San Francisco I & II, San Isidro, Labrador I & II, San Jose, San Juan, San Lorenzo Ruiz I & II, San Luis I & II, San Manuel I & II, San Mateo, San Miguel II, San Miguel, San Nicolas I & II, San Roque, San Simon, Santa Cristina I & II, Santa Cruz I & II, Santa Fe, Santa Lucia, Santa Maria, Santo Cristo, Santo Niño I & II, Zone I-B, Zone I

Table 3. Continued…

Municipality/City	List of Barangays Within IRW
Imus *(See Figure 16)*	(73 barangays) Anabu I (A – G), Anabu II (A – F), Bagong Silang, Bayan Luma I – IX, Bucandala I, II, V, Buhay na Tubig, Carsadang Bago I, Magdalo, Maharlika, Malagasang I (F&G), Malagasang II (E, F, G), Mariano Espeleta I – III, Medicion I (C&D), Medicion II (C – F), Palico I – III & V, Pasong Buaya I & II, Pinagbuklod, Poblacion I (A – C), Poblacion II (A & B), Poblacion III (A & B), Poblacion IV (A–D), Tanzang Luma I – IV, Toclong I (A–C), Toclong II (A&B)
Bacoor *(See Figure 17)*	(48 Barangays) Alima, Aniban I, Banalo, Bayanan, Campo Santo, Daang Bukid, Digman, Dulong Bayan, Habay I & II, Kaingin, Ligas III, Mabolo I – III, Maliksi I, Mambog I – V, Molino II – V & VII, Niog I & II, P.F. Espiritu I – VIII, Queens Row East, Real I & II, Salinas I – IV, Sineguelasan, Tabing Dagat
Kawit *(See Figure 18)*	(8 Barangays) Toclong, Balsahan-Bisita, Binakayan-Aplaya, Binakayan-Kanluran,Congbalay-Legaspi, Manggahan-Lawin, Pulvorista, Samala-Marquez

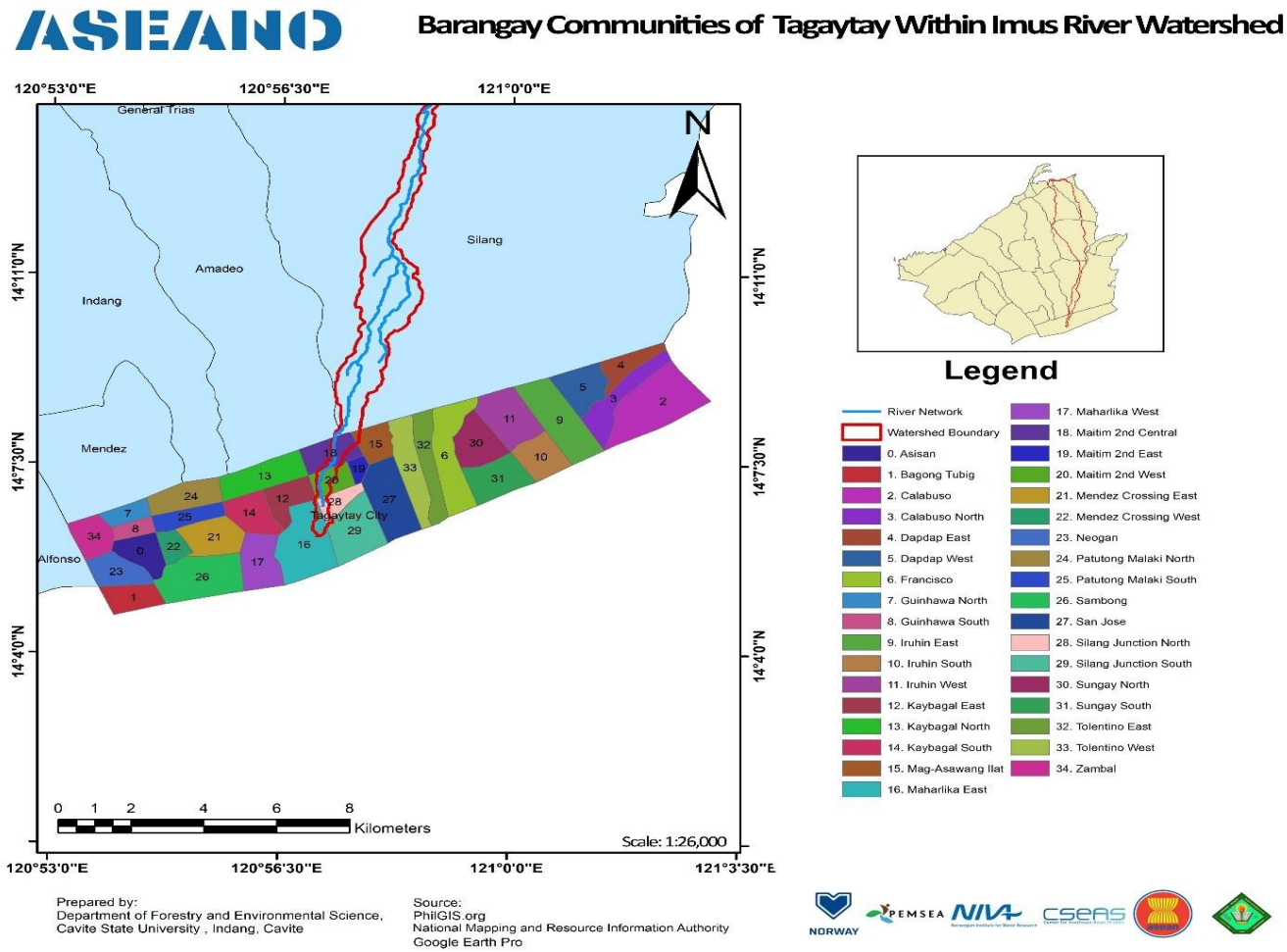

Figure 12. Barangay communities of Tagaytay City overlaid against the Imus River Watershed.

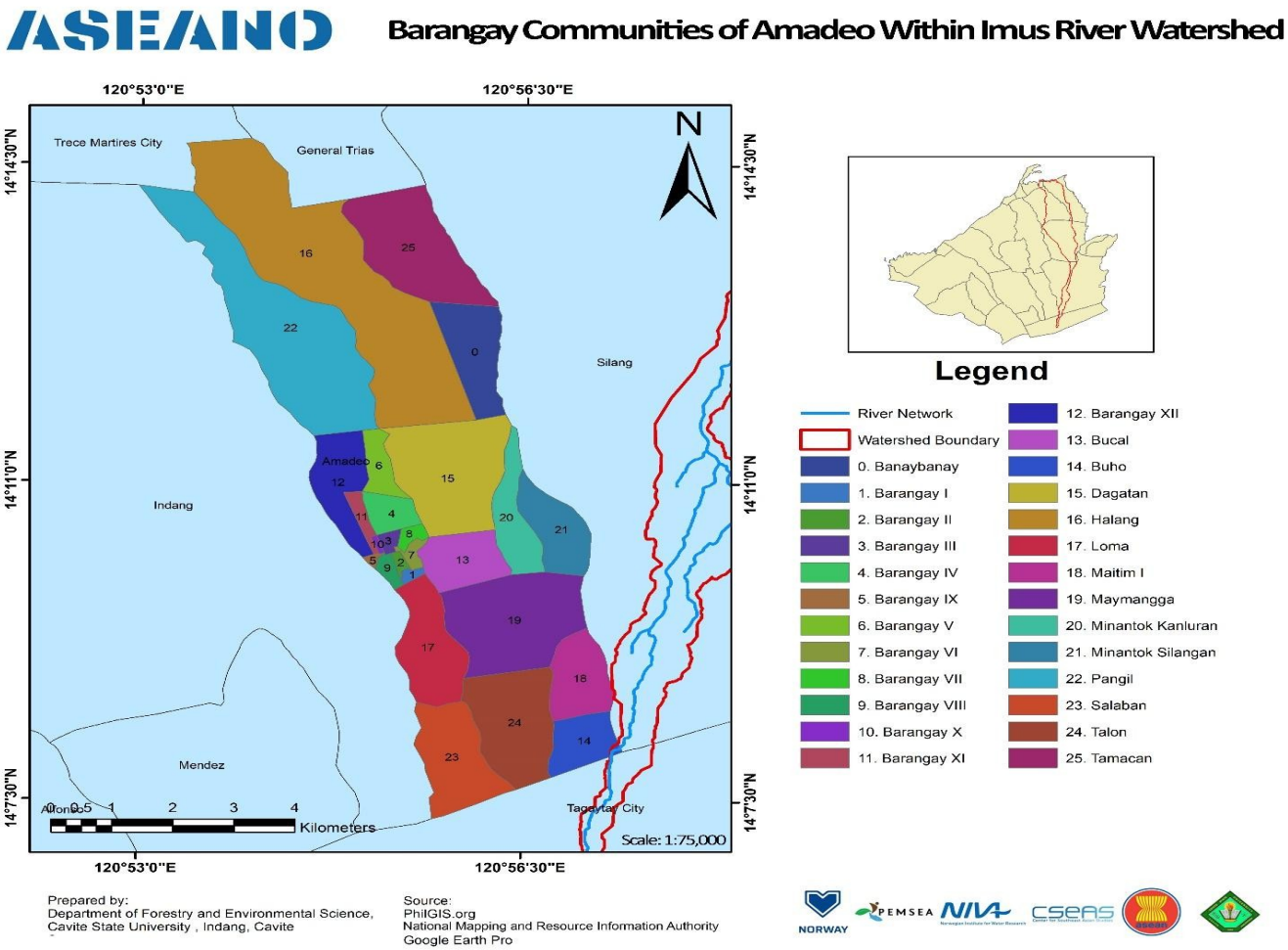

Figure 13. Barangay communities of Amadeo overlaid against the Imus River Watershed.

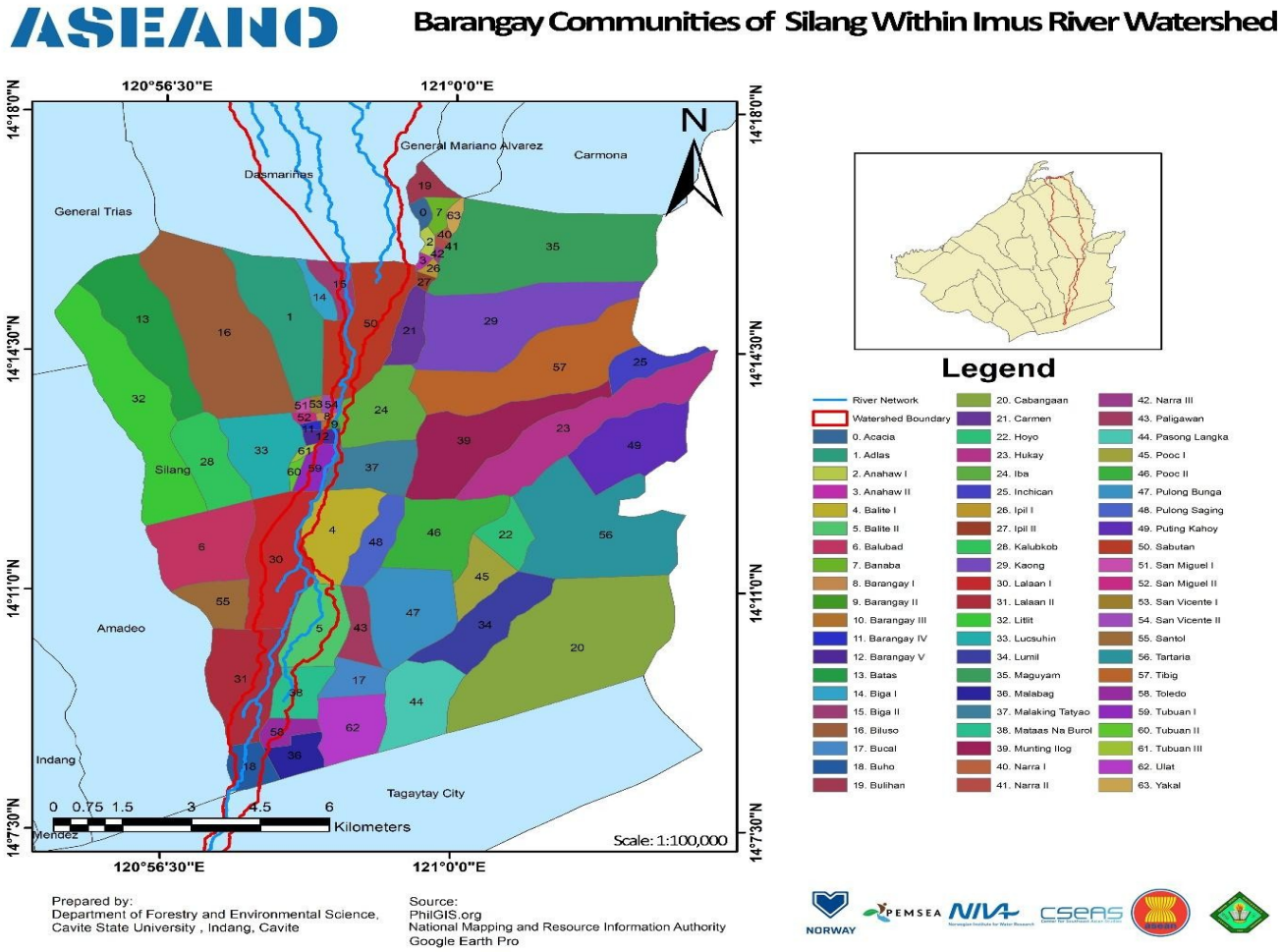

Figure 14. Barangay communities of Silang overlaid against the Imus River Watershed.

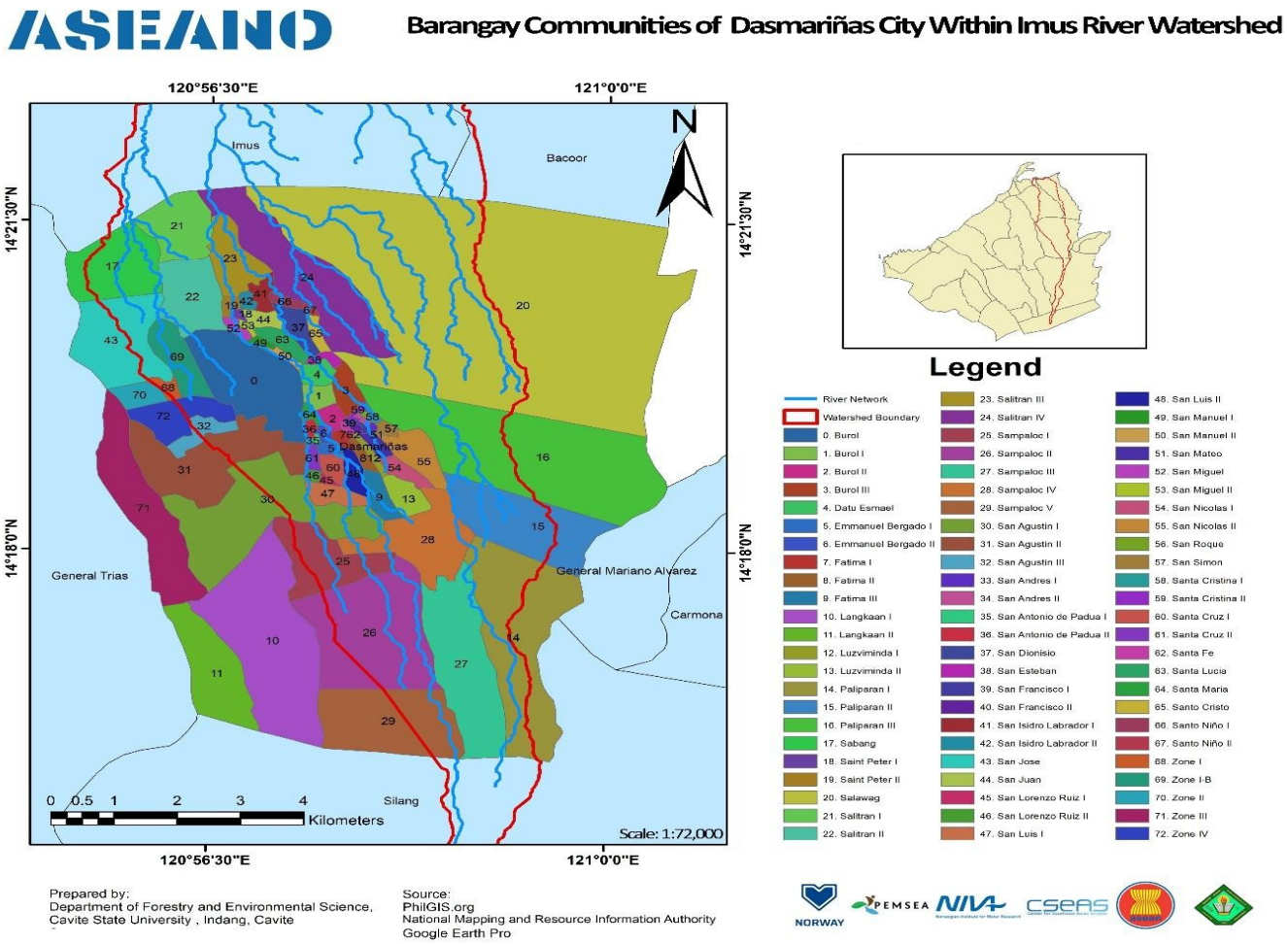

Figure 15. Barangay communities of Dasmariñas City overlaid against the Imus River Watershed.

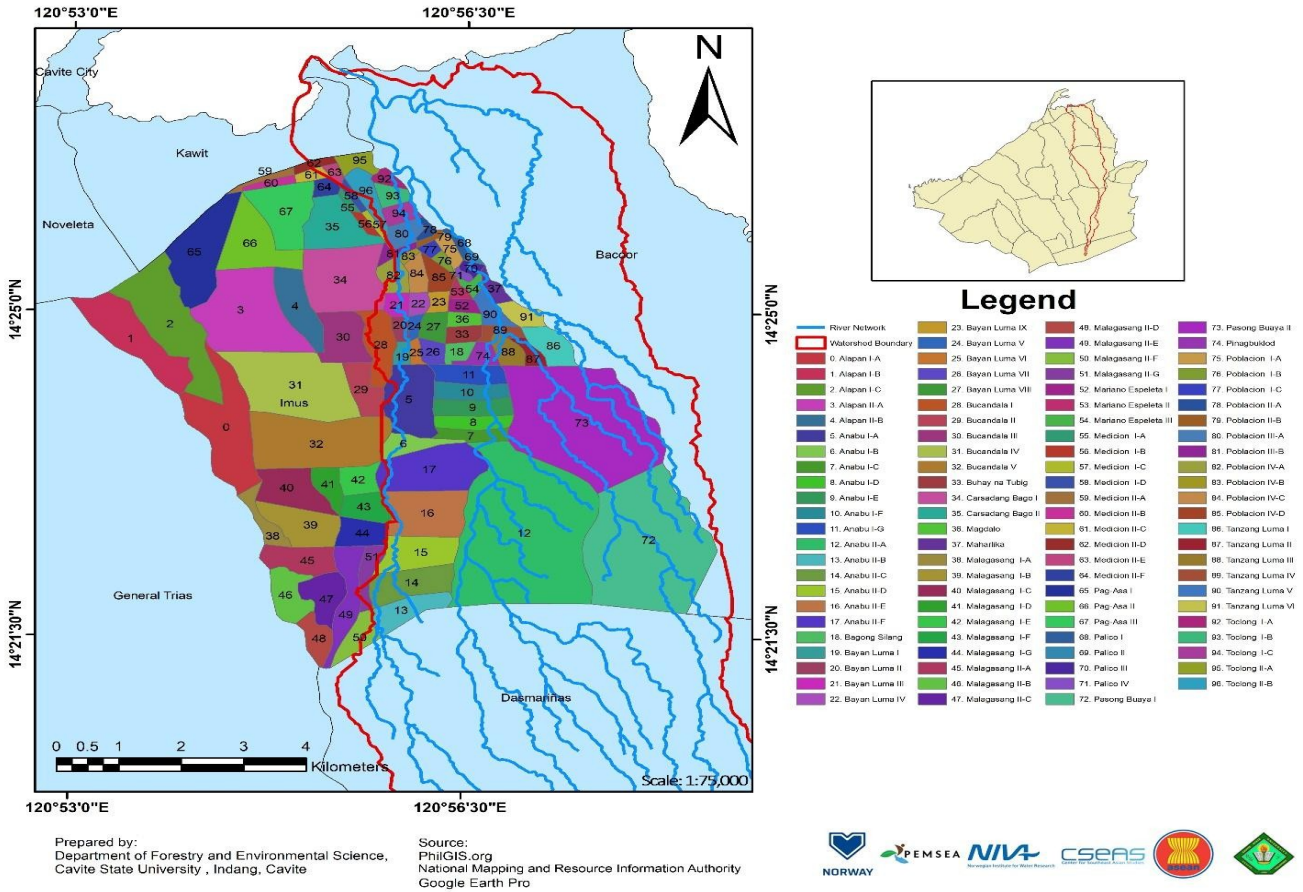

Figure 16. Barangay communities of Imus City overlaid against the Imus River Watershed.

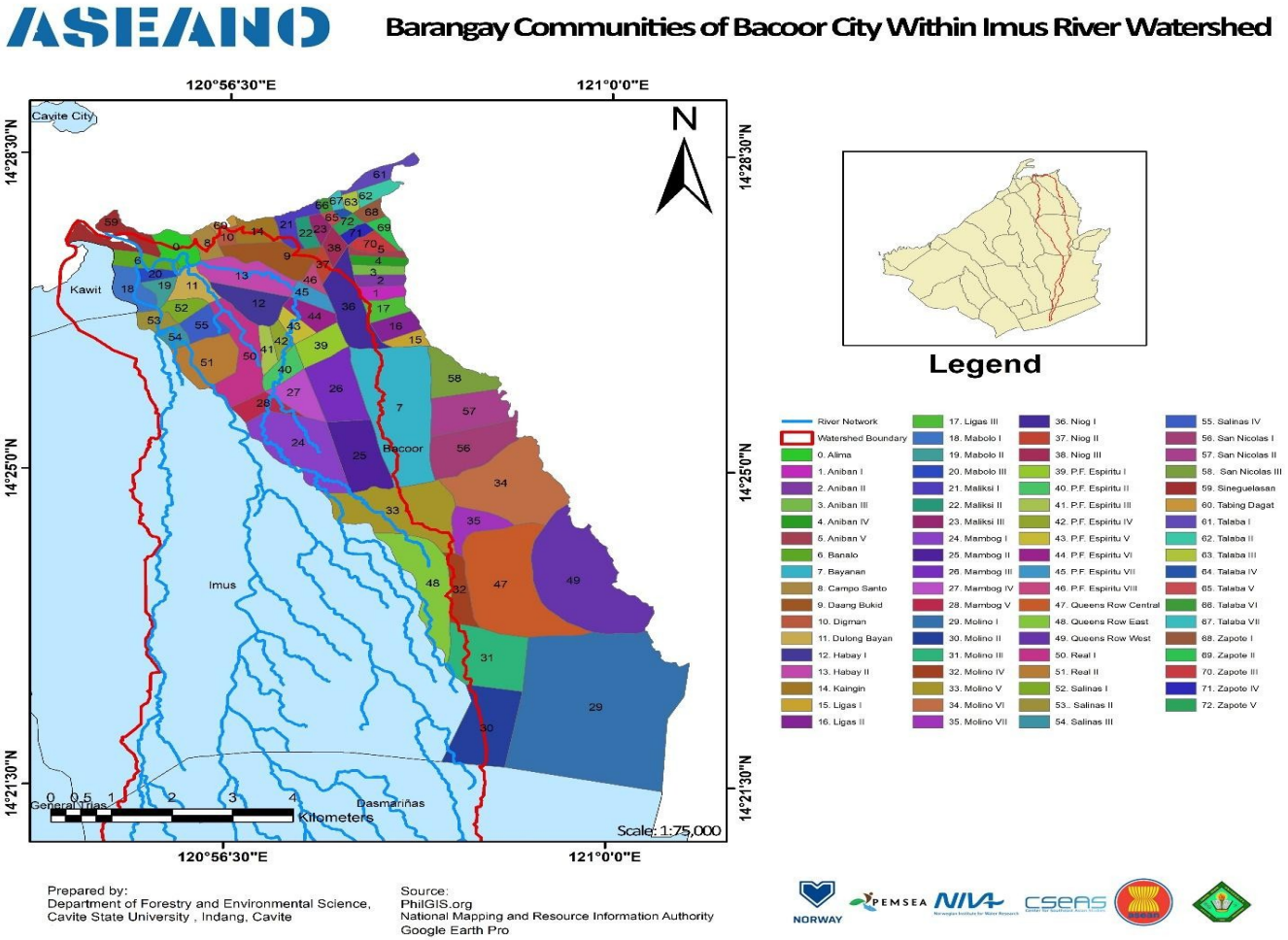

Figure 17. Barangay communities of Bacoor City overlaid against the Imus River Watershed.

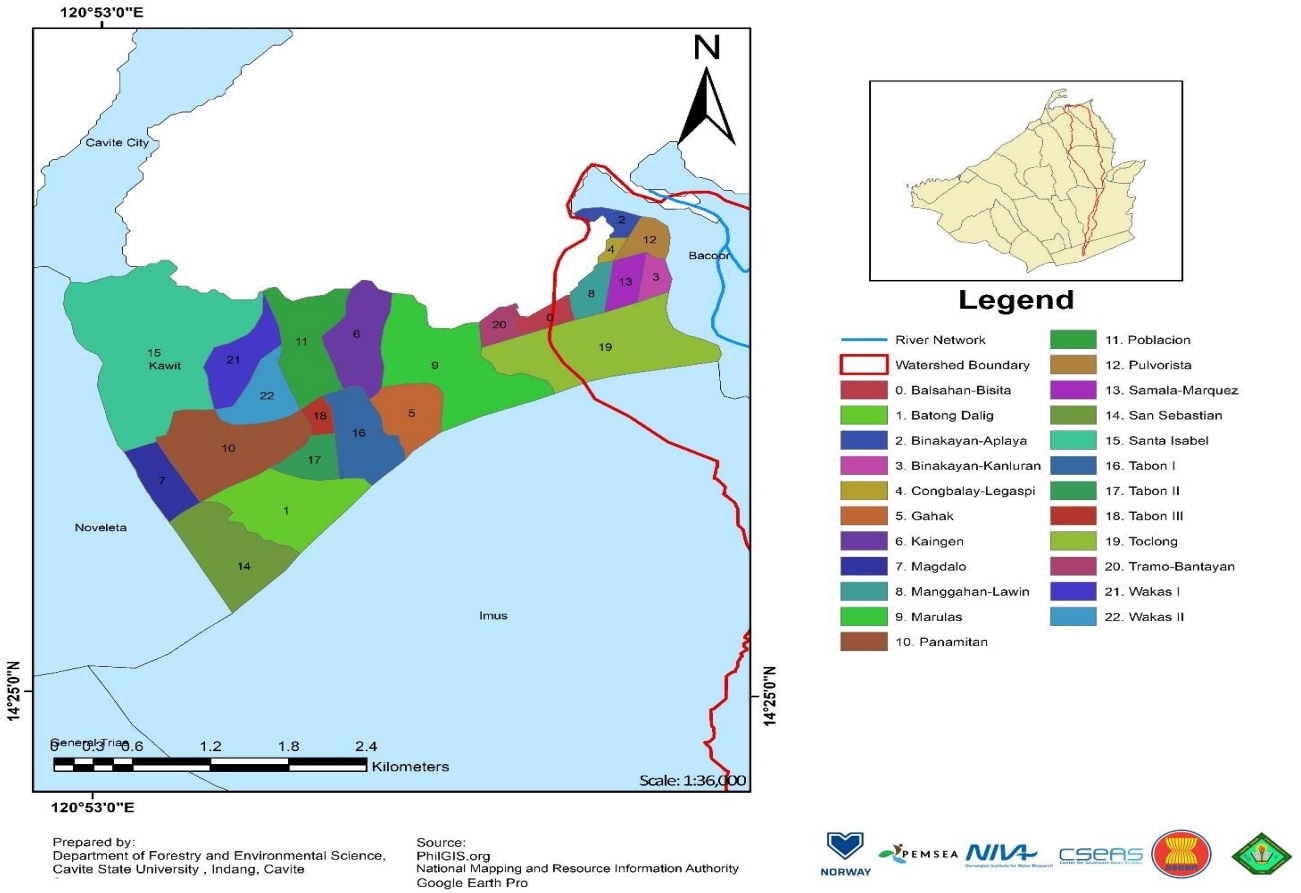

Figure 18. Barangay communities of Kawit overlaid against the Imus River Watershed.

Population Distribution within Imus River Watershed

The total population of Cavite based on the POPCEN 2020 is 4,344,829, making it the most populous province in the Philippines. There was a significant increase in the population from 2015 to 2020 with a 3.57% growth rate representing an increase of 587,610. Due to its proximity to Metro Manila, this population increase can be attributed to the migration of people from Metro Manila and other nearby provinces to the province of Cavite seeking employment opportunities. The top three cities in terms of population in the province are the City of Dasmariñas, contributing 17.92 percent to the total population of the province, followed by the City of Bacoor (16.33%) and City of Imus (10.9%). Major portions of these three populous cities are within the boundary of the Imus River Watershed.

There are 222 barangay communities located within the watershed with a total population of 1,351,057 in 2020. The biggest barangay in terms of land area is Barangay Salawag in Dasmarinas with an area of 21,193,476 m^2, while San Roque in Dasmarinas is the smallest with an area of 15,337.36 m^2. Barangay Salawag was also the most populous barangay with 80,136 inhabitants, while Barangay Poblacion 1-B in Imus was the least populous with only 316 inhabitants. In terms of population density, the densest barangay is Sta. Fe (20.10 per 100 sqm) in Dasmarinas, while the least dense barangay is Pasong Buaya (0.03 per 100 sqm) in Imus. **Figures 19** and **20** shows the total population and population density map of Imus River Watershed.

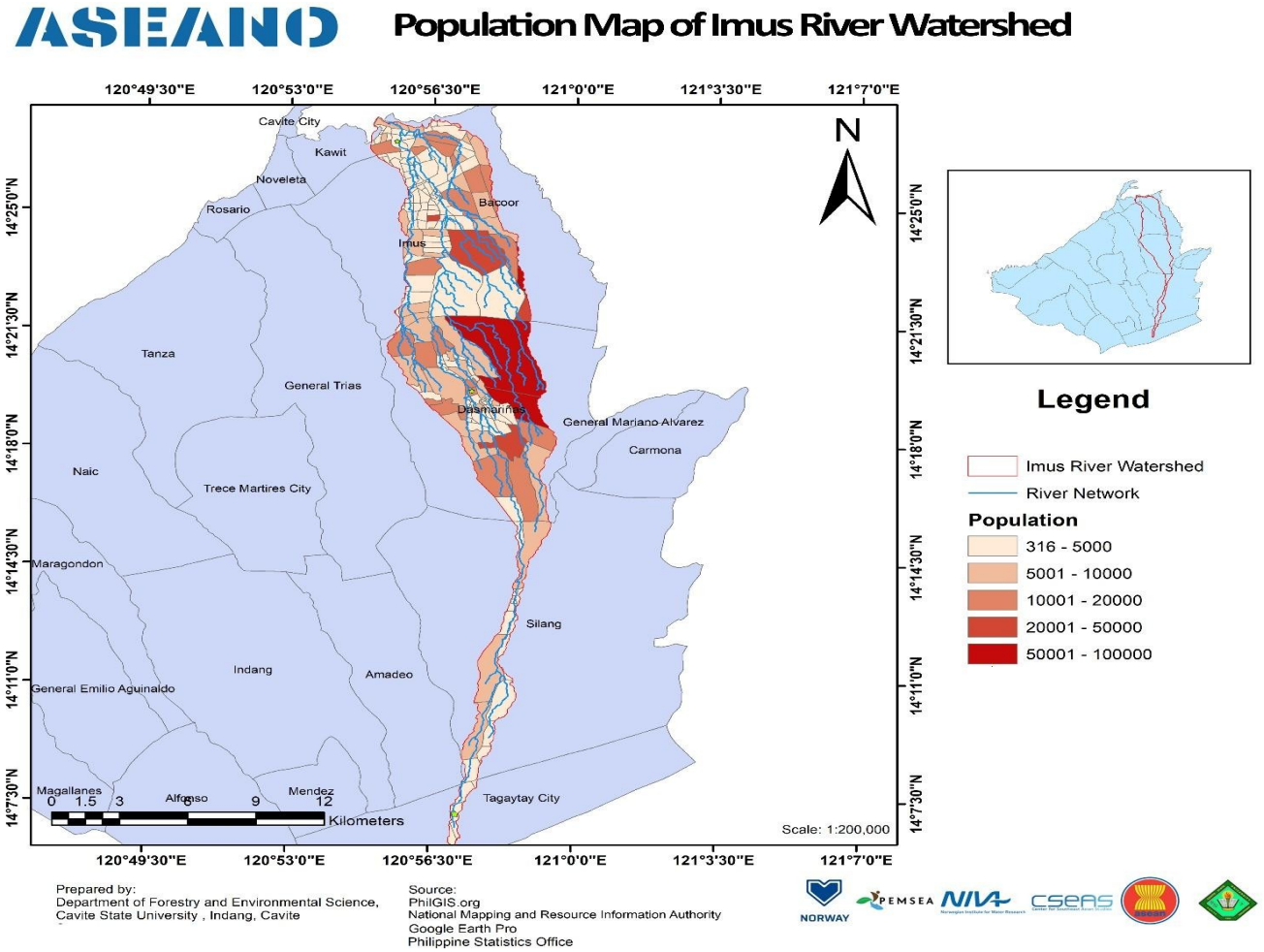

Figure 19. Map showing the population of the barangay communities within the Imus River Watershed.

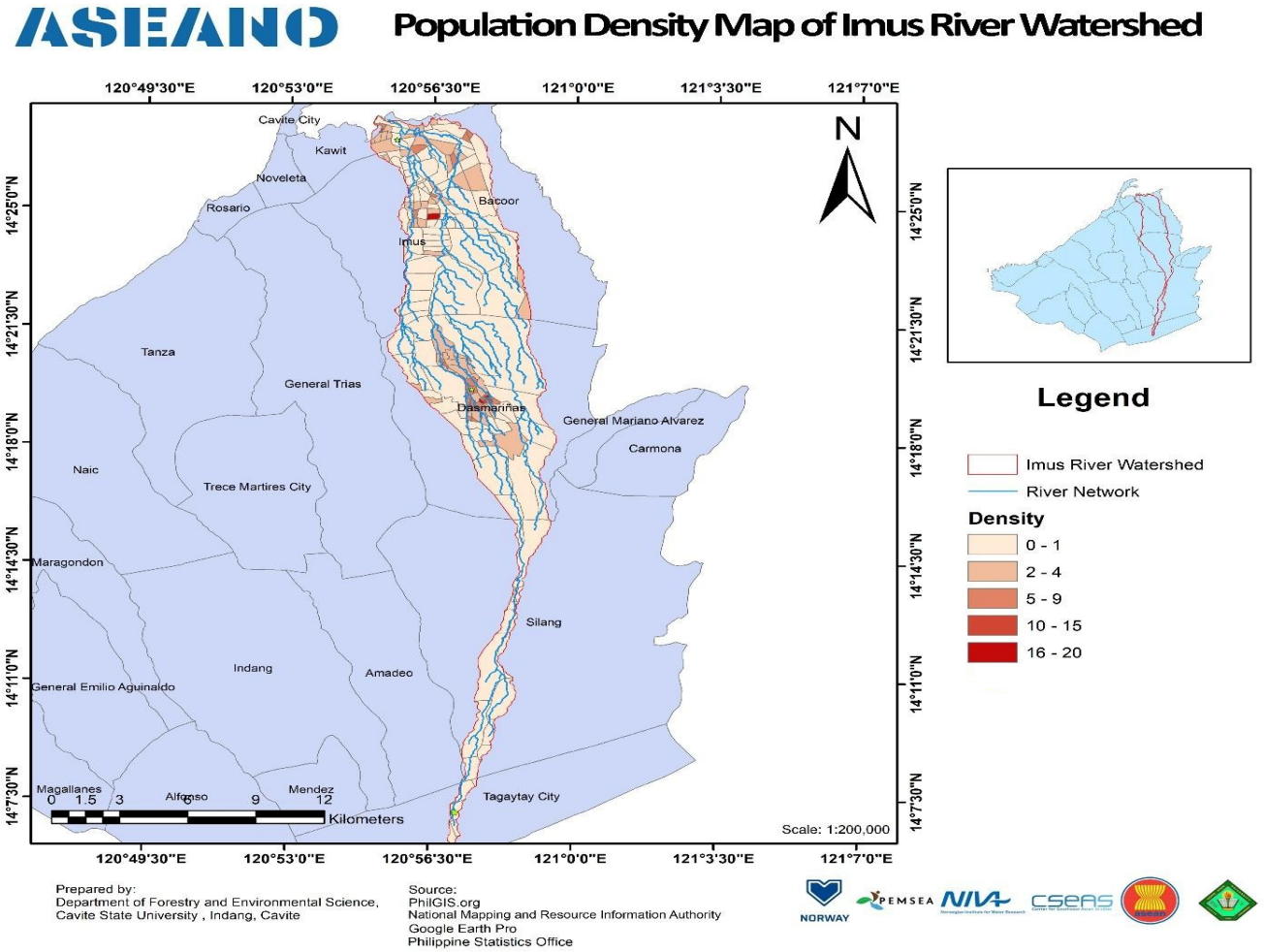

Figure 20. Map showing the population density of barangay communities within Imus River Watershed.

General Land Cover, Vegetation and Comprehensive Land Uses of Imus River Watershed

The assessment of land use/land cover helps to determine the anthropogenic influence on natural systems and is significant in understanding natural settings and socioeconomic conditions at local, regional, and global levels (Chowdhury, Hasan, & Abdullah-Al-Mamun, 2020). Changes in land use and land cover can be caused by socio-economic development, population expansion, and conversion to agriculture (Lambin, Geist, & Lepers, 2013). The multiple land uses within a typical watershed have significant impact on the watershed's hydrological characteristics (Haque, 2013). Vegetative and forest cover loss is accompanied by an increase in stream discharge and surface runoff. This may cause intense flooding, soil erosion, and landslides within the watershed (Guzha, Rufino, Okoth, Jacobs, & Nobrega, 2018).

In total, 90.67% of the province is classified as alienable and disposable land, while the remaining forest land represents only 9.33%. Alienable and disposable lands are further classified as production land (55.24%) and built-up areas (44.76%). The built-up areas include residential, industrial, commercial, and tourism areas. Built-up areas constitute more than half of the total drainage area of the watershed, followed by areas devoted to annual and perennial crops (**Table 4**).

Table 4. Land Classification of Imus River Watershed.

Land Cover	Area (ha)	Percent Share
Annual Crop	2,110.70	18.759
Brush and Shrubs	77.87	0.692
Built-up	6,754.90	60.034
Fishpond	134.19	1.193
Grassland	1,034.47	9.194
Inland Water	18.37	0.163
Mangrove Forest	1.86	0.016
Open/Barren	0.54	0.005
Perennial Crop	1,118.89	9.944
Total	**11, 259.80**	**100**

The Vegetative Index map of IRW shows that most of the upland area (including Tagaytay and Silang) is highly vegetated. The majority of the areas in Dasmariñas and the lowland areas such as Imus, Bacoor, and Kawit have less vegetation (**Figure 21**). Isolated areas of high vegetation found in Imus and Dasmariñas mainly represent rice fields.

The Comprehensive Land Use Plan (CLUP) is a planning document prepared by Local Government Units (LGUs) to rationalize the allocation and proper use of land resources. It projects public and private land uses in accordance with the future spatial organization of economic and social activities. The land use maps from each city and municipality were overlaid with the boundary map and river system map of the IRW to show the public and private land uses within the watershed (**Figures 23** to **29**).

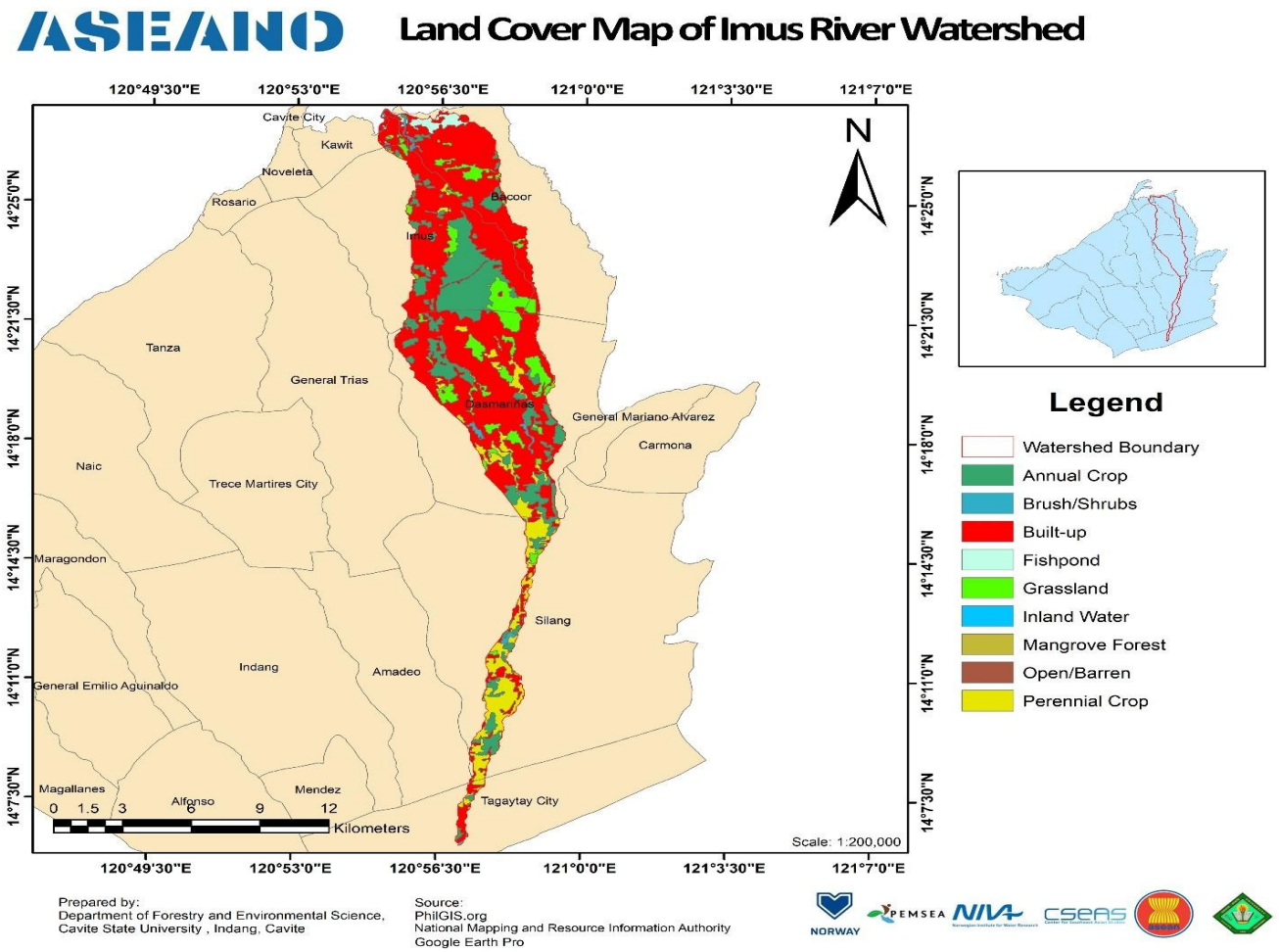

Figure 21. Land cover of the Imus River Watershed.

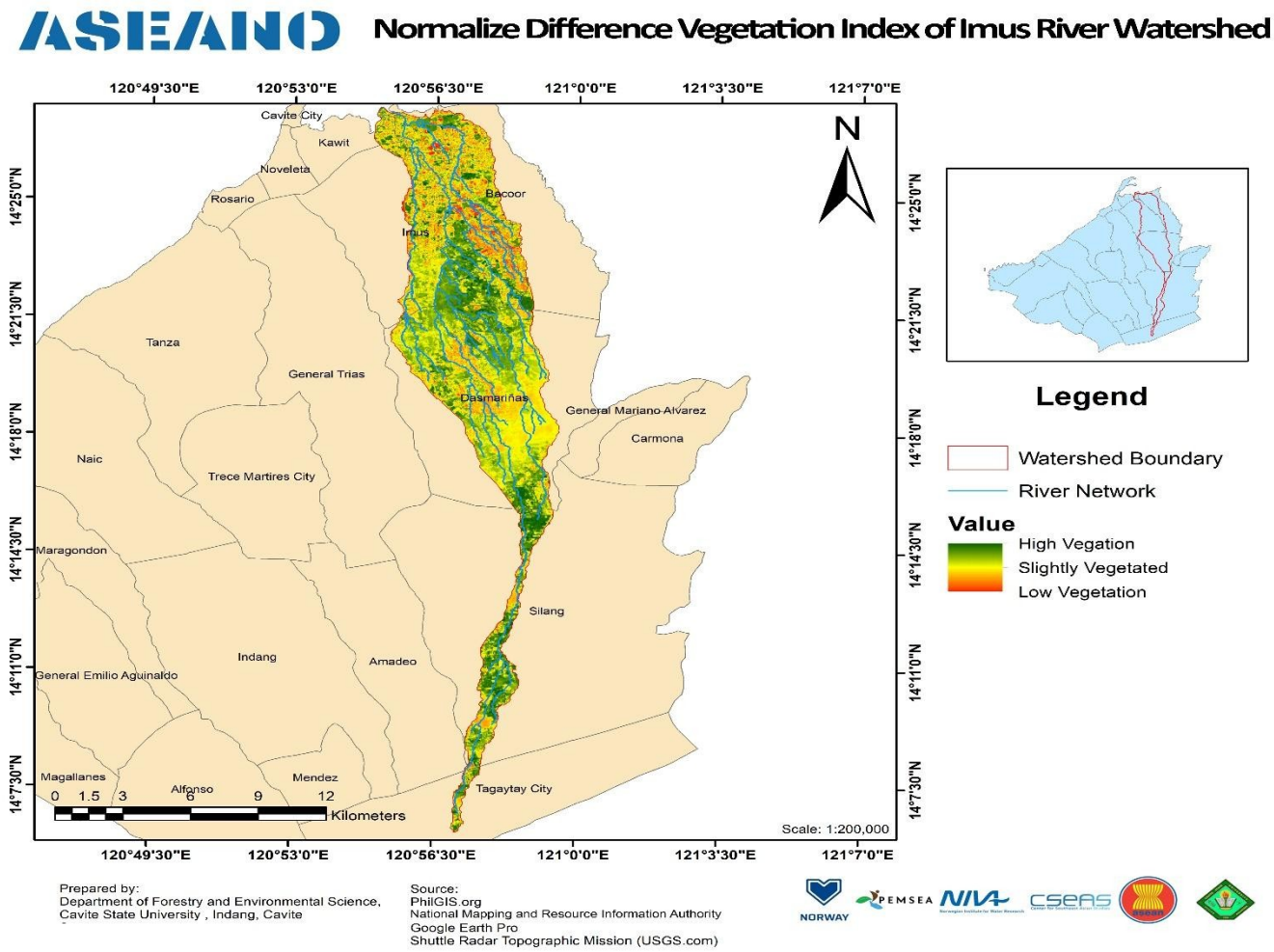

Figure 22. Normalized difference vegetation index of the Imus River Watershed.

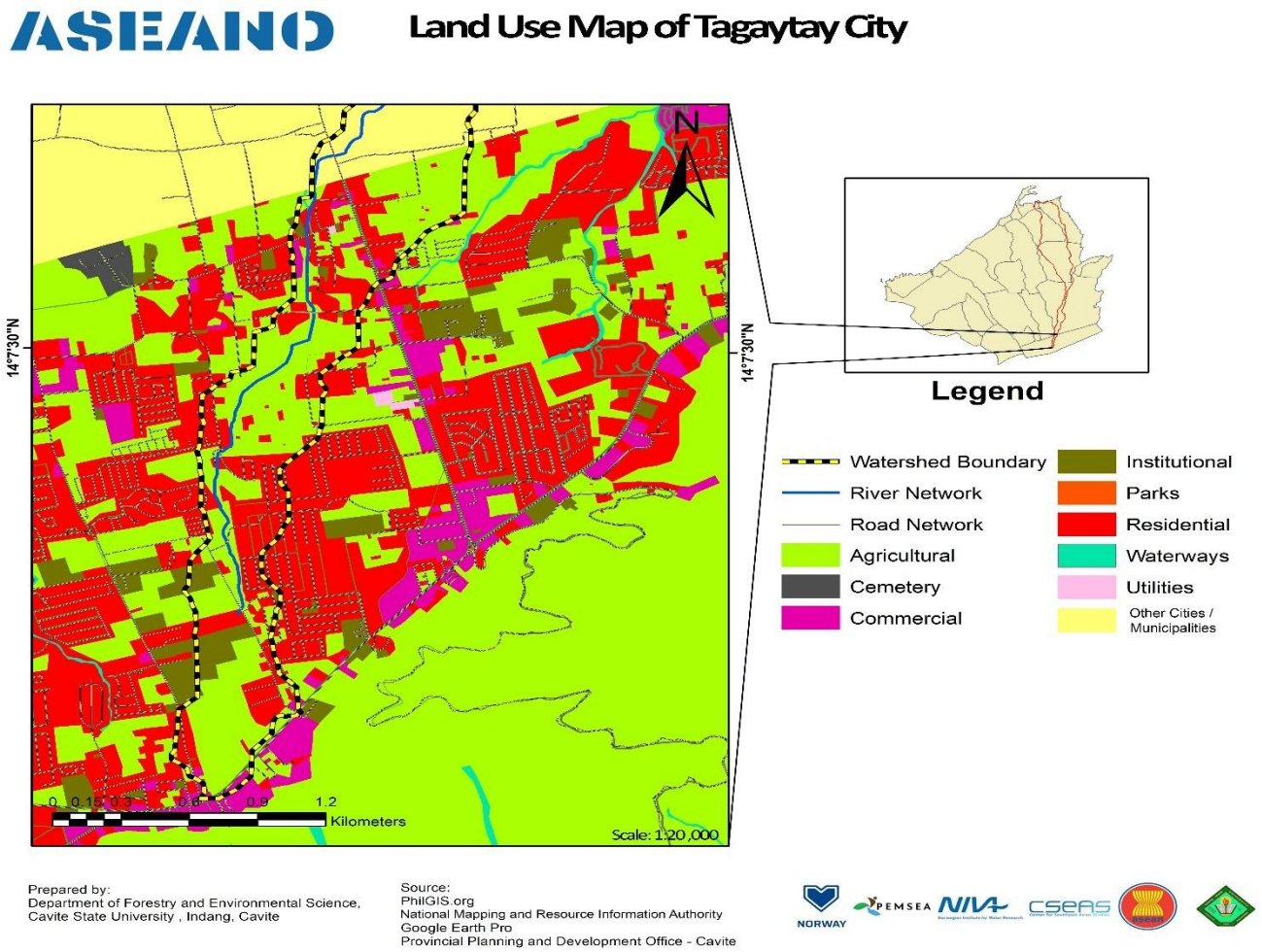

Figure 23. Land use within Tagaytay City.

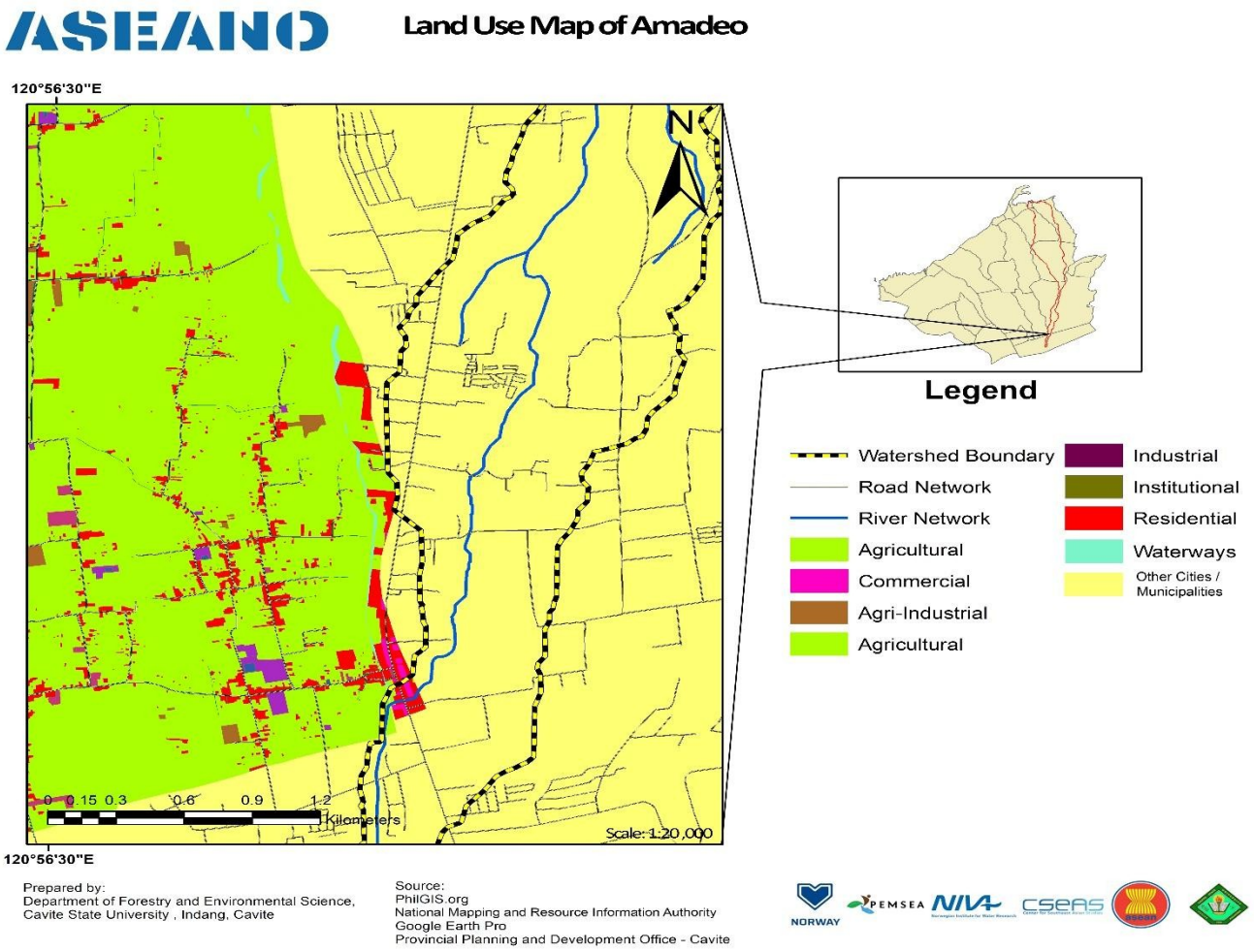

Figure 24. Land use within Amadeo.

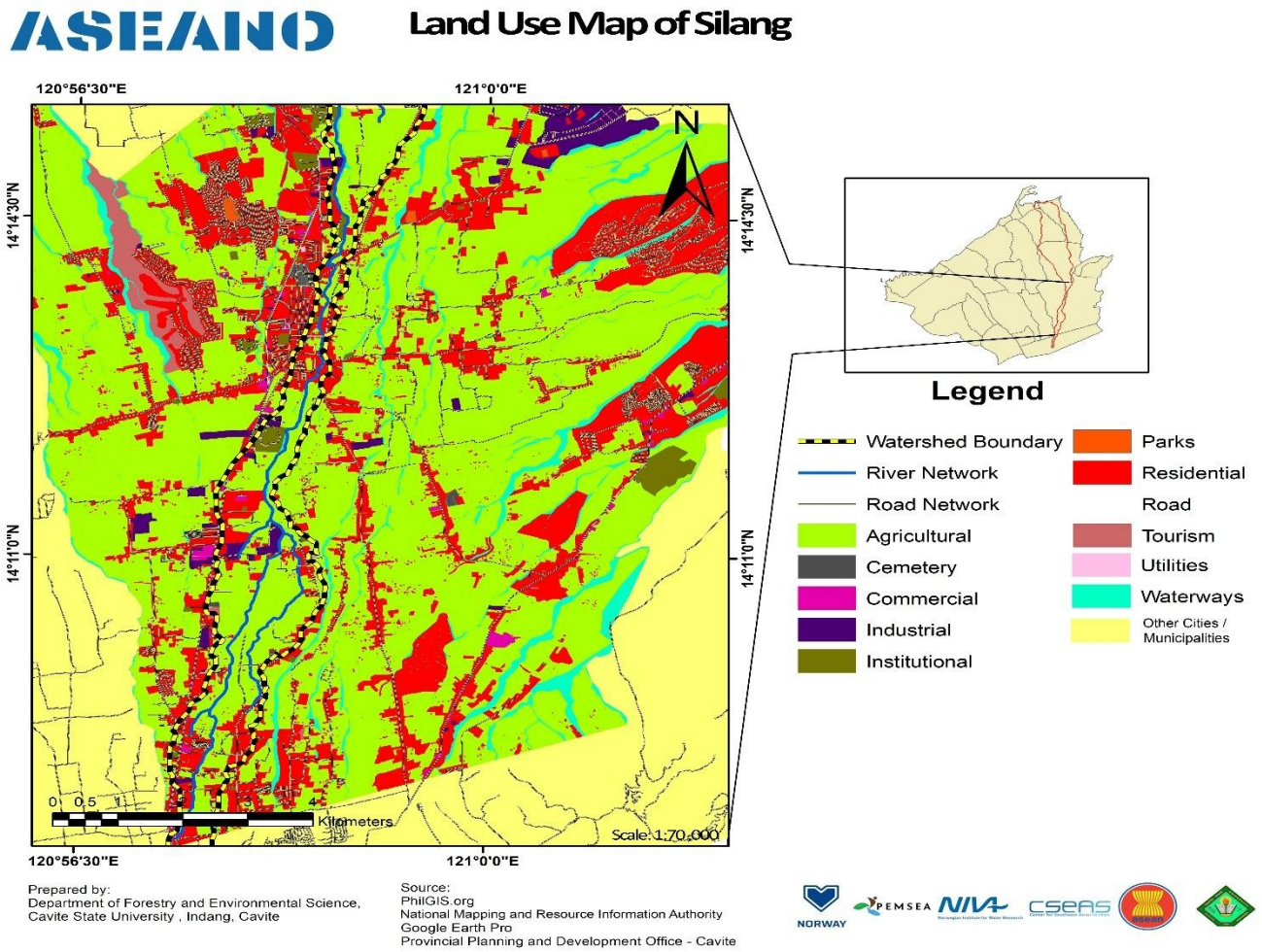

Figure 25. Land use within Silang.

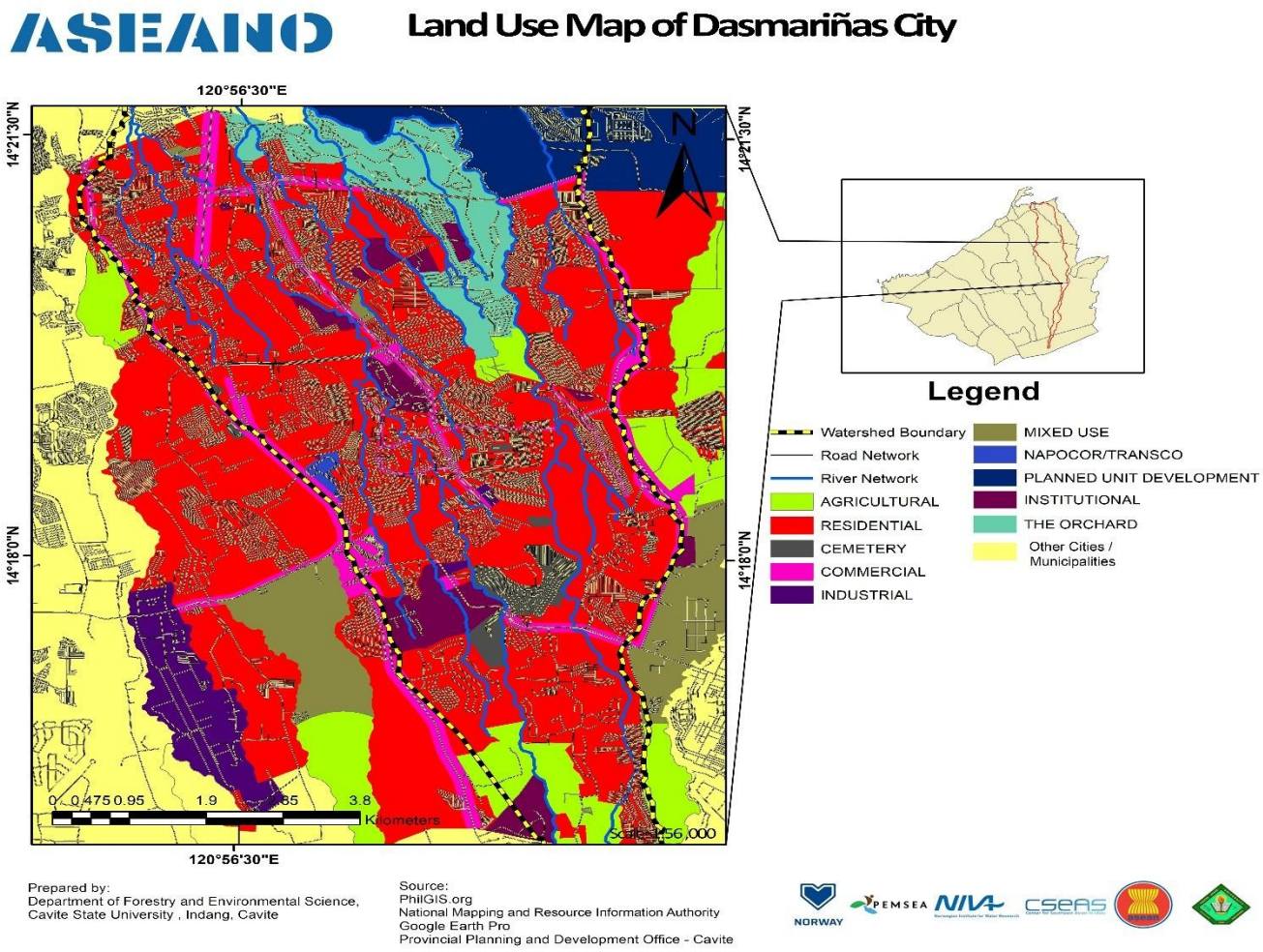

Figure 26. Land use within Dasmariñas City.

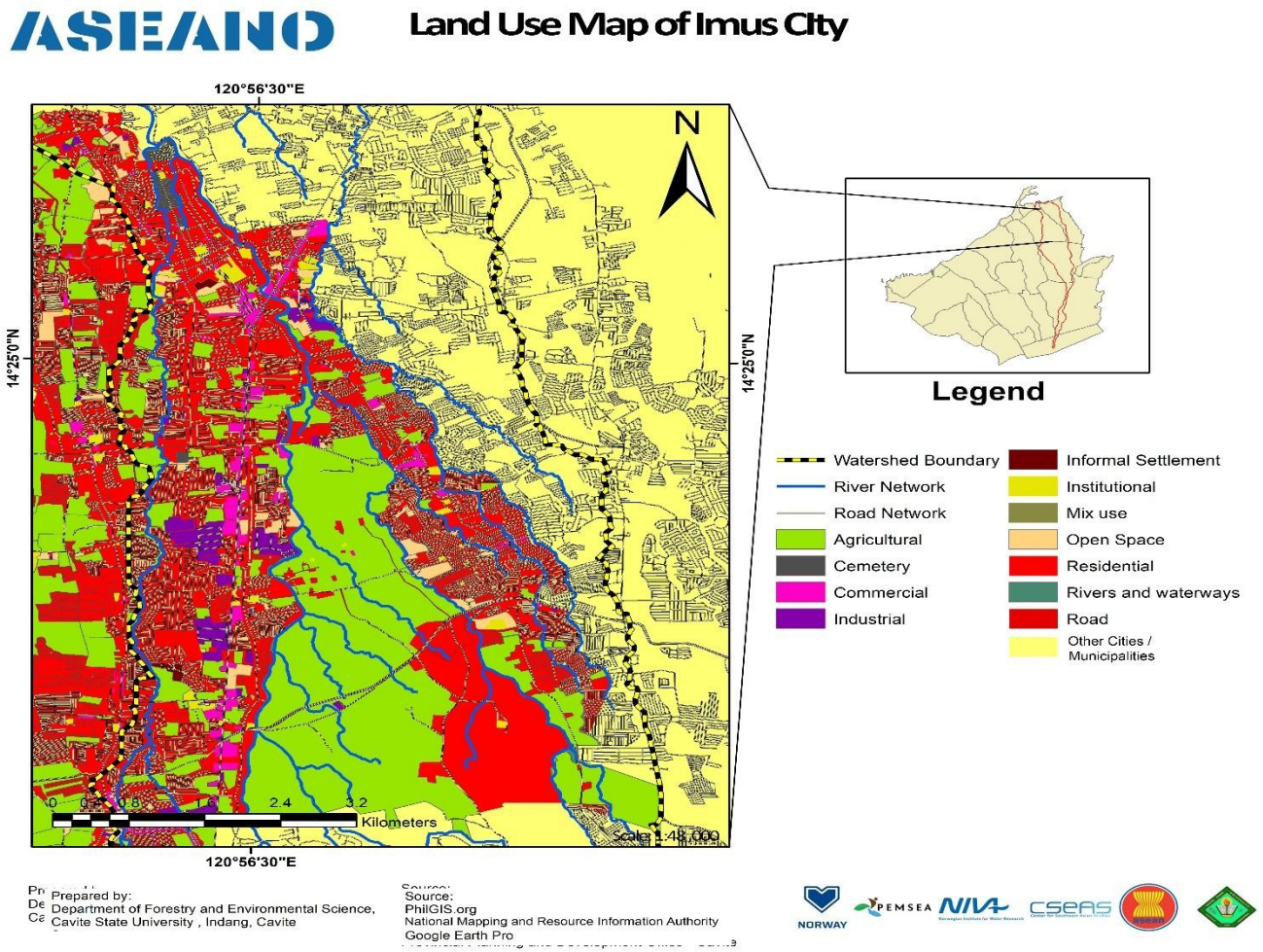

Figure 27. Land use within Imus City.

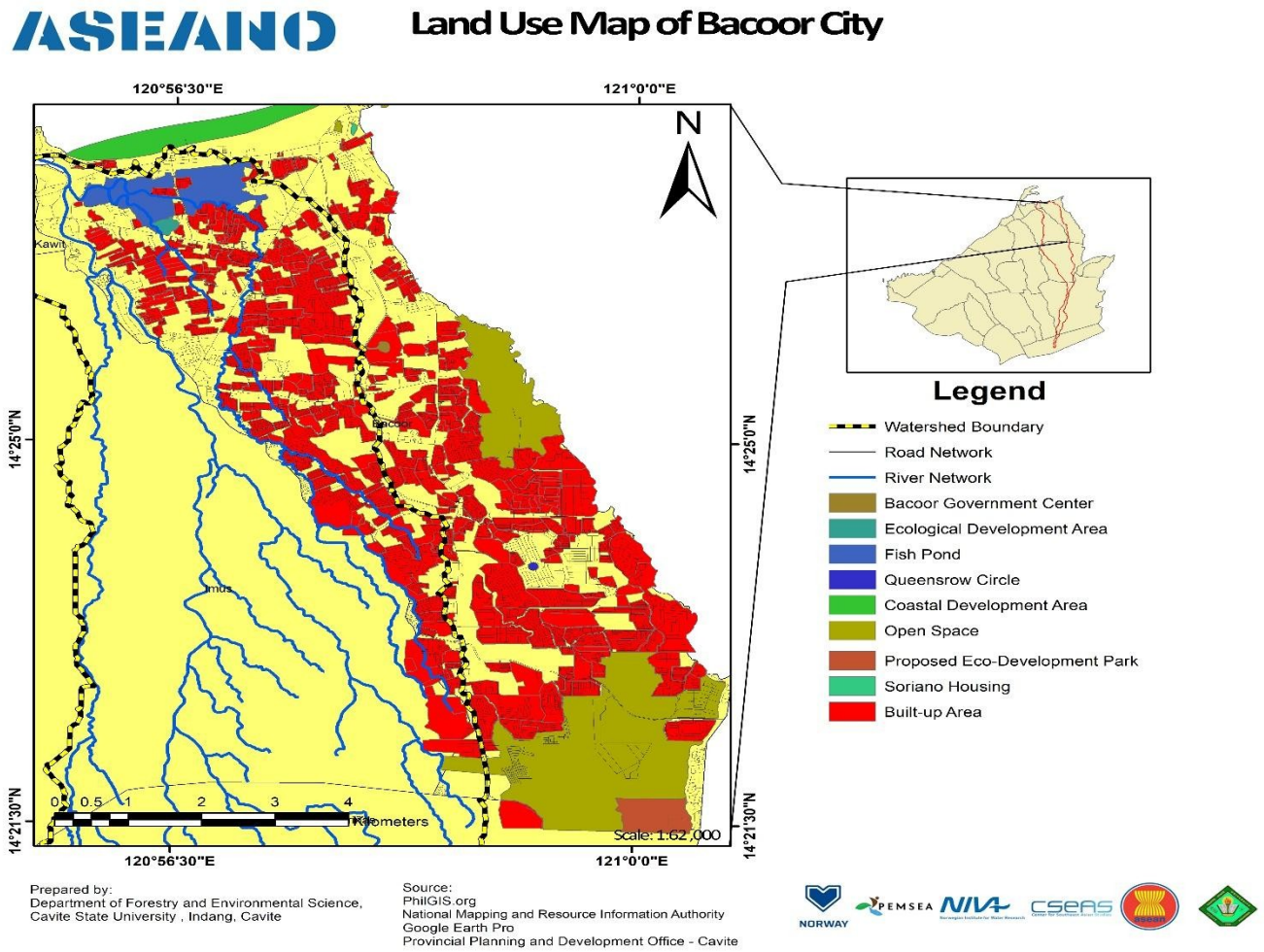

Figure 28. Land use within Bacoor City.

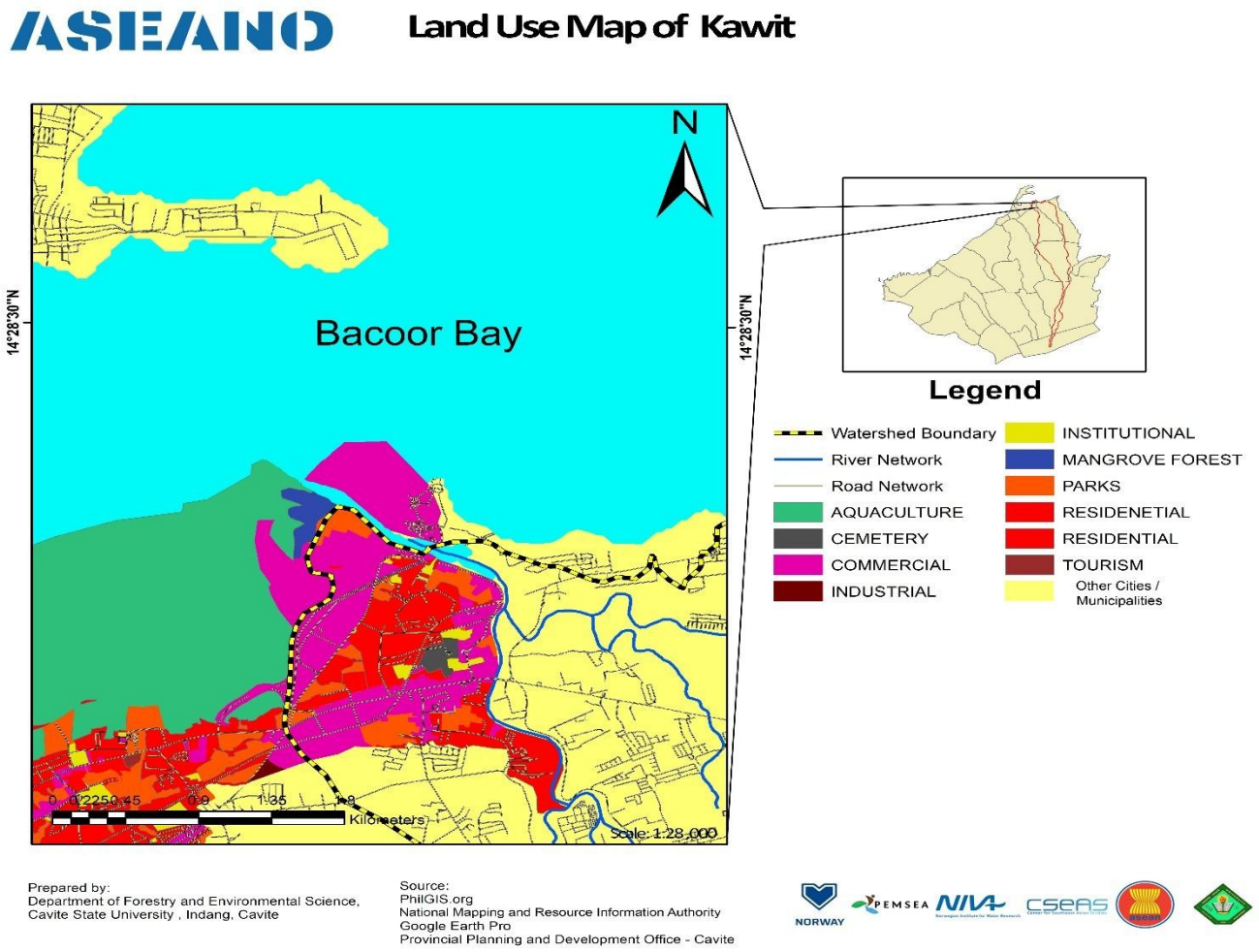

Figure 29. Land use within Kawit.

Hydroclimatic Conditions in Imus River Watershed

The analysis of hydroclimatic variables such as precipitation, temperature, and river flow dynamics in a given spatial-temporal scale is an emerging strategic research approach to better comprehend natural systems such as watersheds (Montanari, et al., 2013). Understanding the use and movement of water in a watershed will provide a strong foundation towards understanding and describing how the landscapes and water interact (Edwards, Williard, & Schoonover, 2015). Figure 30 shows the proximity of the two environmental monitoring stations to the IRW and their respective regions of influence.

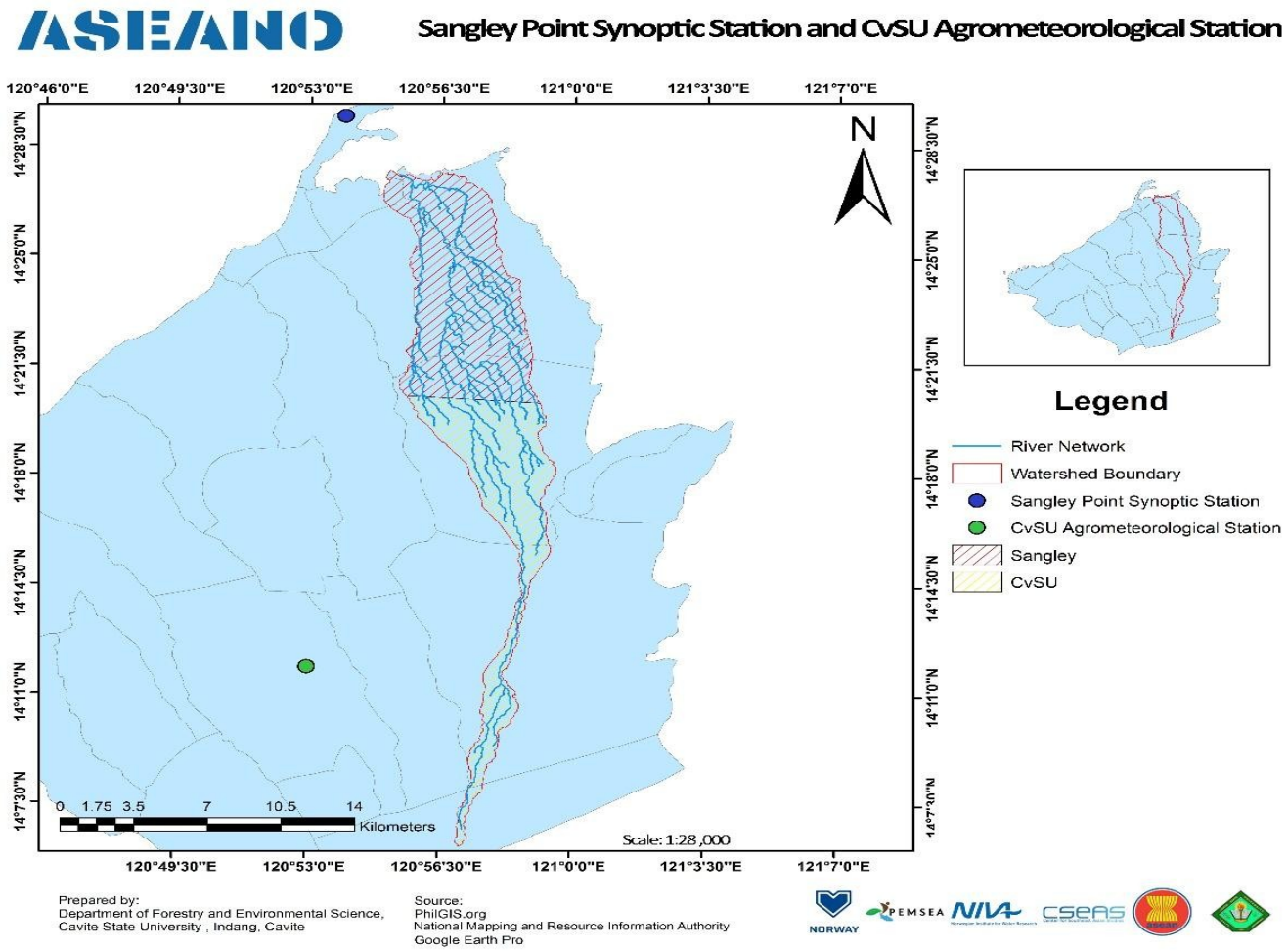

Figure 30. Sangley Point Synoptic Station (blue) and CvSU Agrometeorological Station (green), with Imus River Watershed coverage.

Air Temperature

Based on the 25-year temperature data from Sangley Point Synoptic Station, the normal mean temperature is 28.53°C, with a normal maximum temperature of 32.04°C and normal minimum temperature of 25.85°C. On the other hand, based on the 14-year temperature data in CvSU Agrometerological Station (also referred to as the CvSU-PAGASA Agromet Station), the normal mean temperature is 26.20°C, the normal maximum temperature is 30.46°C, and the normal minimum temperature is 21.70°C.

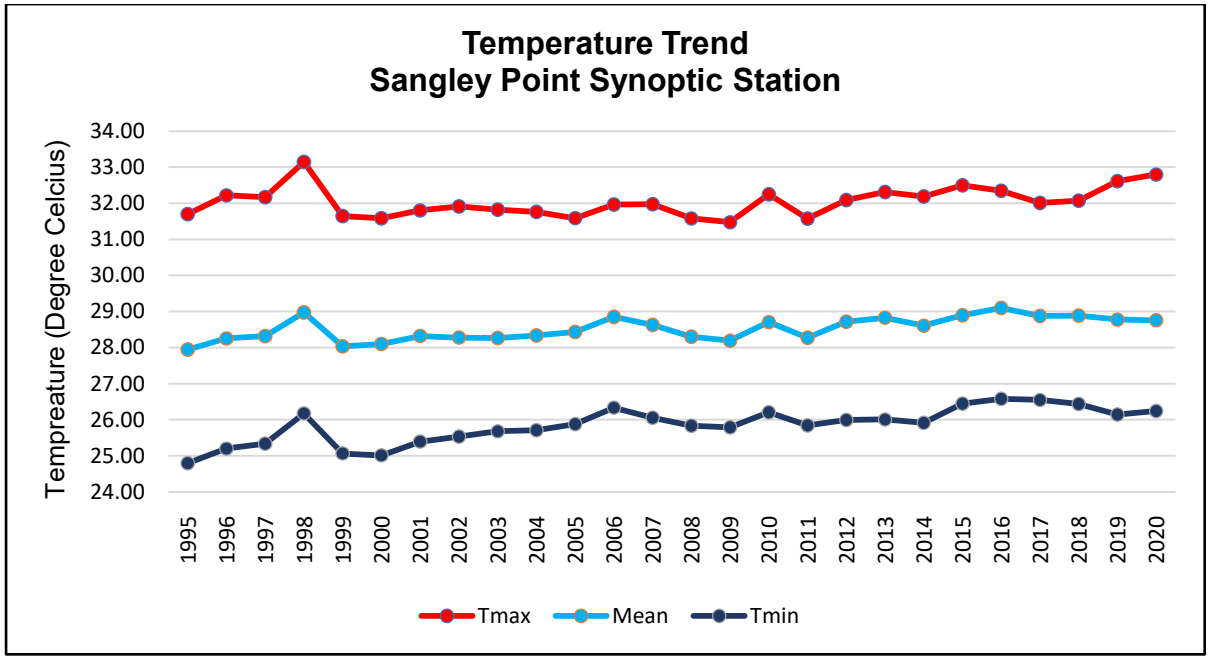

Figure 31. Temperature trend from 1995 to 2020 at Sangley Point Synoptic Station in Cavite City, Cavite.

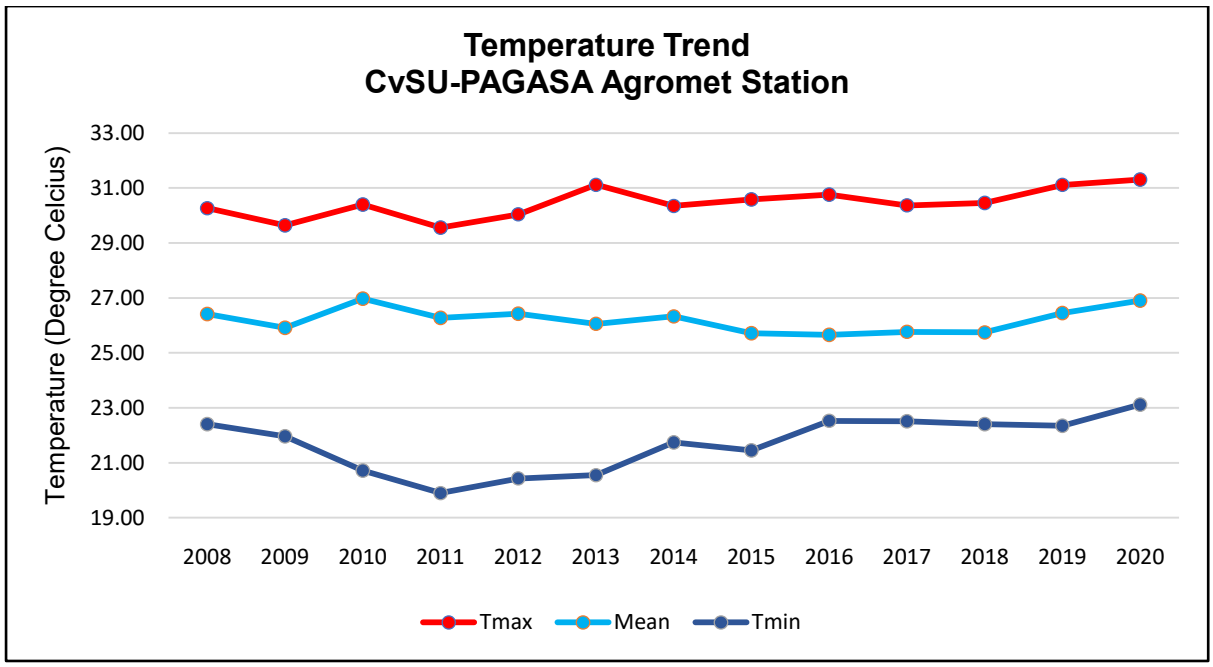

Figure 32. Temperature trend from 2008 to 2020 at CvSU Agrometeorological Station in Indang, Cavite.

The temperature anomalies for mean, maximum, and minimum temperatures are shown in **Figures 33** to **34**. A positive anomaly indicates that the observed temperature is warmer than the normal, while a negative anomaly indicates that the observed temperature is cooler than the normal. In Sangley Point Station, mean temperature anomalies had average values of +0.29°C and -0.29°C, In CvSU-PAGASA Agromet Station, the mean temperature anomalies had average values of +0.39°C and -0.34°C.

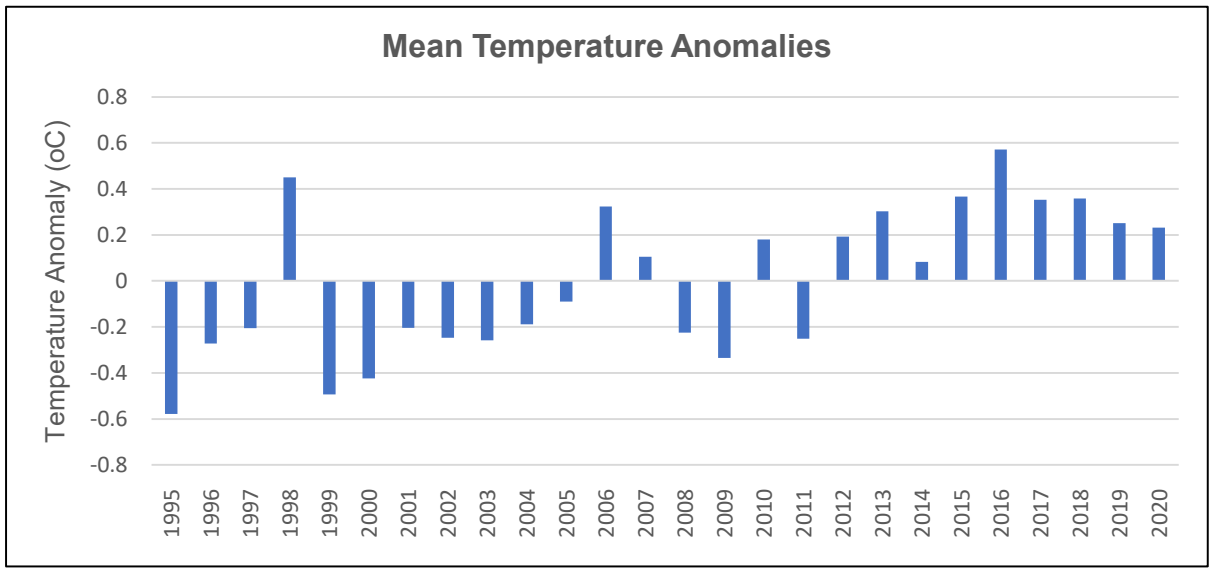

Figure 33. Mean temperature anomalies in Sangley Point Synoptic Station, Cavite City, Cavite.

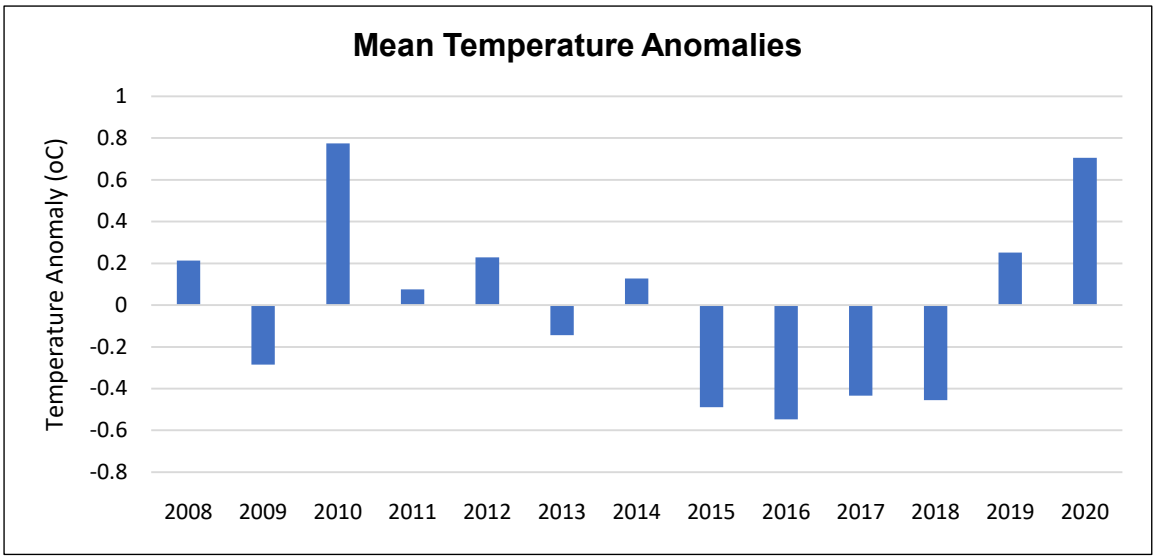

Figure 34. Mean temperature anomalies in CvSU Agrometeorological Station, Indang, Cavite.

May is, on average, the warmest month, while January is the coldest month. Sangley Point Station recorded mean temperatures for these months of 30.28°C and 26.94°C respectively (**Figure 35**). On the other hand, whilst May was also the hottest month recorded in CvSU Agrometeorological Station, February was the coldest month, with mean temperatures of 28.29°C and 24.10°C respectively (**Figure 36**).

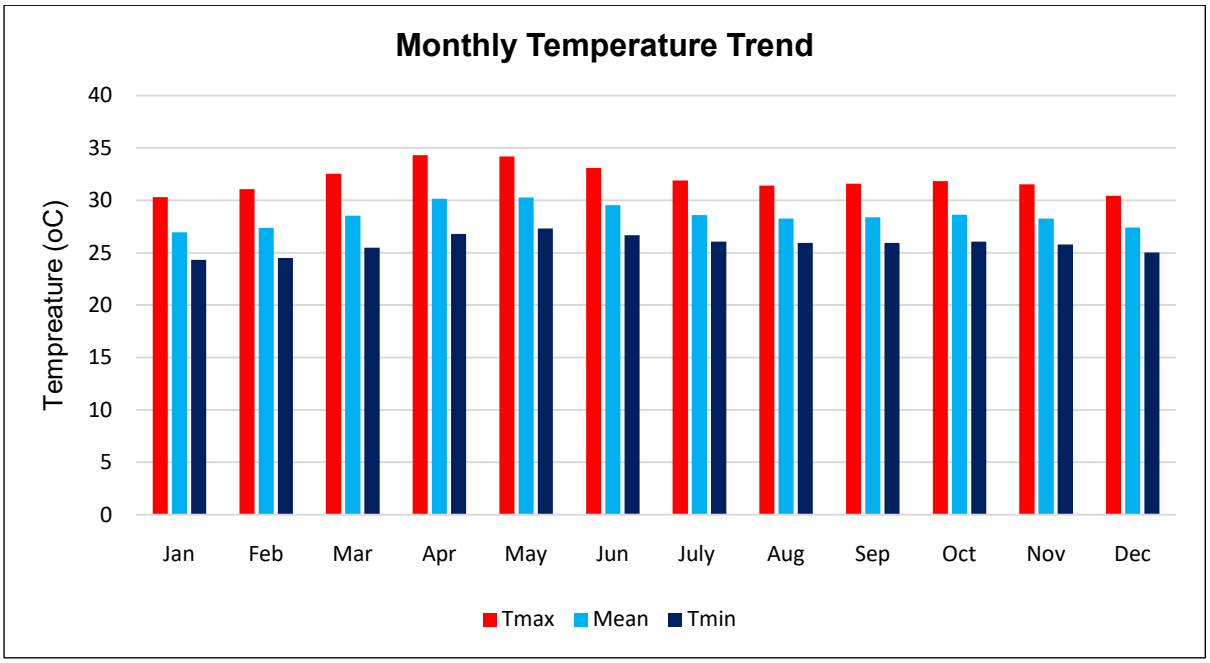

Figure 35. Monthly temperature trend in Sangley Point Synoptic Station in Cavite City, Cavite.

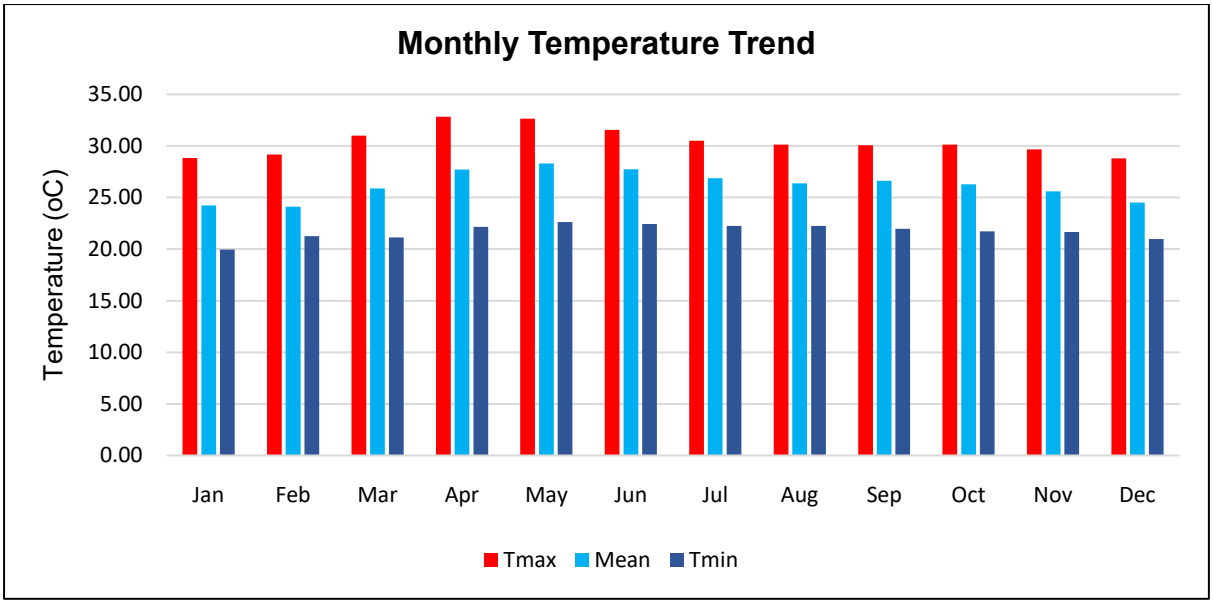

Figure 36. Monthly temperature trend in CvSU-PAGASA Agrometeorological Station in Indang, Cavite.

Rainfall and cloud cover are factors that greatly affect the diurnal temperature range variation because of their significant influence on surface energy and hydrological balance (Karolyn, et al., 2003). At Sangley Point Synoptic Station, the diurnal temperature variation was highest during the month of April and lowest during the month of December. At CvSU Agrometeorological Station, the diurnal temperature variation was also highest during the month of April and lowest during the month of December. Diurnal temperature variation thus seems wider in the upland areas than the lowland areas (**Figure 37**).

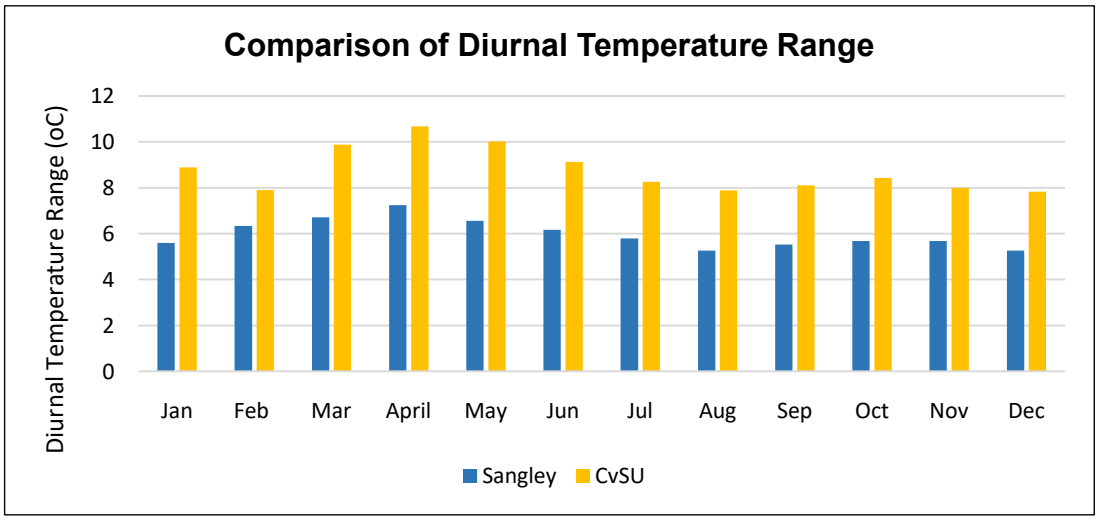

Figure 37. The diurnal temperature range of Sangley Point Synoptic Station and CvSU Agrometeorological Station.

Based on the 2008 – 2020 data of the two stations, the normal maximum temperature was higher at Sangley Point Synoptic Station than CvSU Agrometeorological Station, while the normal minimum temperature at CvSU Agrometeorological station was lower than the readings from the Sangley Point Synoptic Station. This indicates that the temperature readings were much higher in lowland areas than in the upland areas.

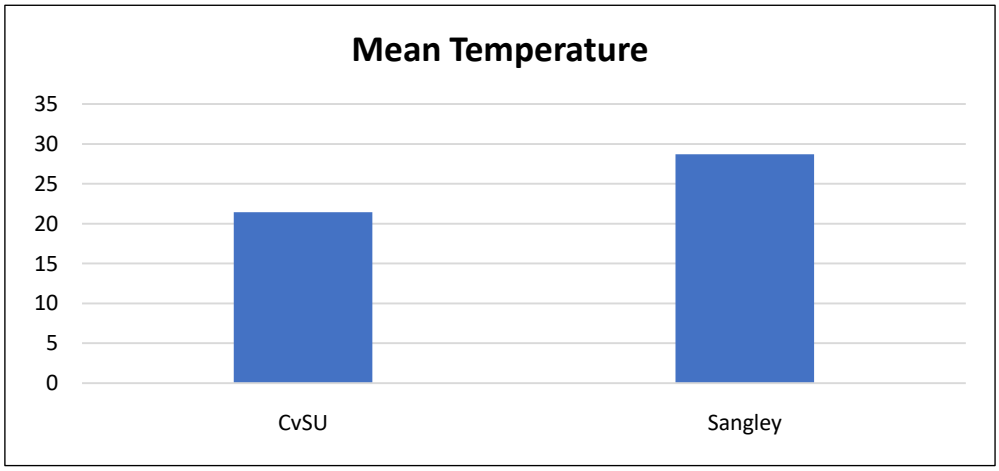

Figure 38. The average mean temperature of Sangley Point Station and CvSU Agrometeorological Station using 2008 – 2020 temperature data.

Rainfall

The average total annual rainfall recorded at Sangley Point Synoptic station and CvSU Agrometeorological Station were 2,265.69 mm and 2,483.05 mm respectively (**Figure 39**). April (17.39 mm) is the driest month recorded at Sangely Point Station while March (16.92 mm) was the driest month at the CvSU Agrometeorological Station. August, which had 518.10 mm, is the wettest month recorded at Sangely Point Station while July, which had 485.04 mm, was the wettest month at the CvSU Agrometeorological Station (**Figure 40**).

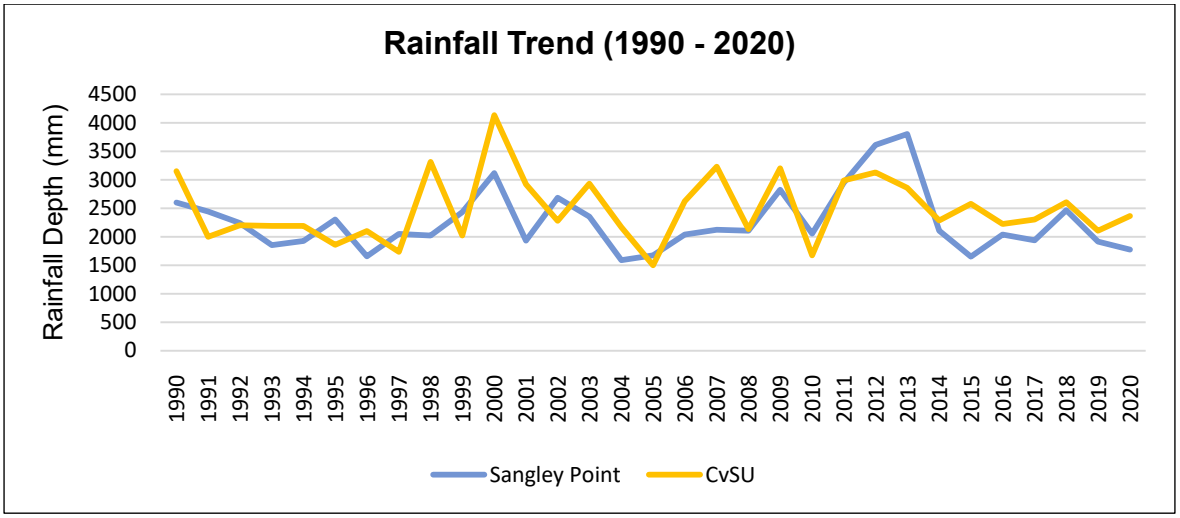

Figure 39. Rainfall trends in Sangley Point Station and CvSU Agrometeorological Station from 1990 to 2020.

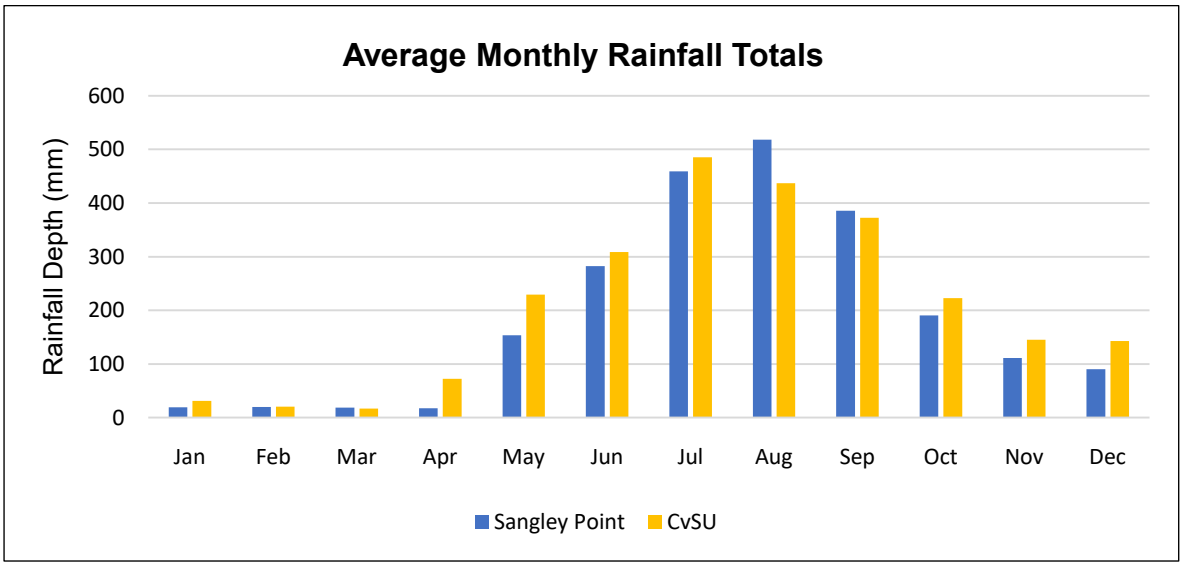

Figure 40. Average monthly rainfall in Sangley Point Station and CvSU Agrometeorological Station.

The readings between the two stations show the highest correlation during the month of December and the lowest correlation during the month of March (**Table 5**). This correlation coefficient value can be seen as a measure of the homogeneity of rainfall in the watershed from upland to lowland. Low values indicate less homogenous distribution, while high values indicate more homogenous distribution of rainfall within the watershed. The correlation coefficient of the rainfall readings was much higher during the wet season (0.70) than the dry season (0.54).

Table 5. The correlation coefficient of the monthly readings between Sangely Point Station and CvSU Agrometeorological Station.

Month	Correlation Coefficient
January	0.5
February	0.64
March	0.15
April	0.5
May	0.82
June	0.8
July	0.71
August	0.73
September	0.79
October	0.37
November	0.62
December	0.84

At CvSU Agrometeorological Station, the normal monthly precipitation was 206.92 mm. During wet season, the estimated monthly rainfall total was 342.50 mm, while the estimated monthly rainfall total during dry season was only 71.34 mm. There was a ±66% rainfall deviation from the normal value (**Figure 41**).

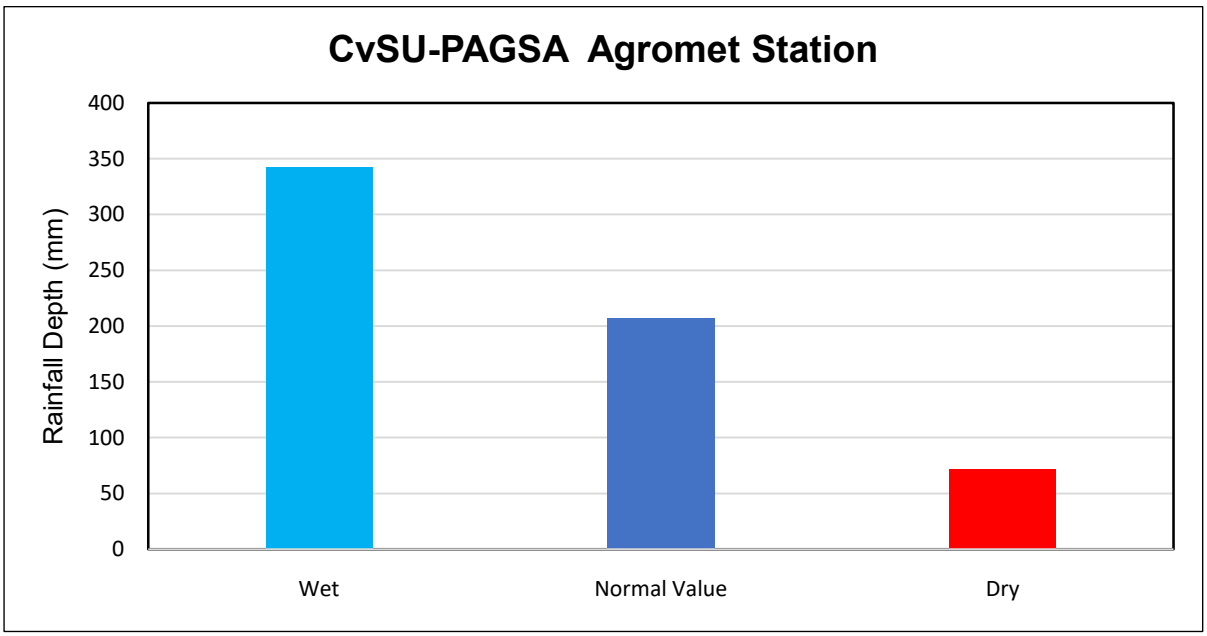

Figure 41. Seasonal rainfall deviation from the normal value in CvSU Agrometeorological Station.

The normal annual precipitation was 2,483.05 mm at CvSU Agrometeorological Station. During wet season, the estimated rainfall total was 2,055.02 m (83%) while the estimated rainfall total during dry season was only 428.03 mm (17%) (**Figure 42**).

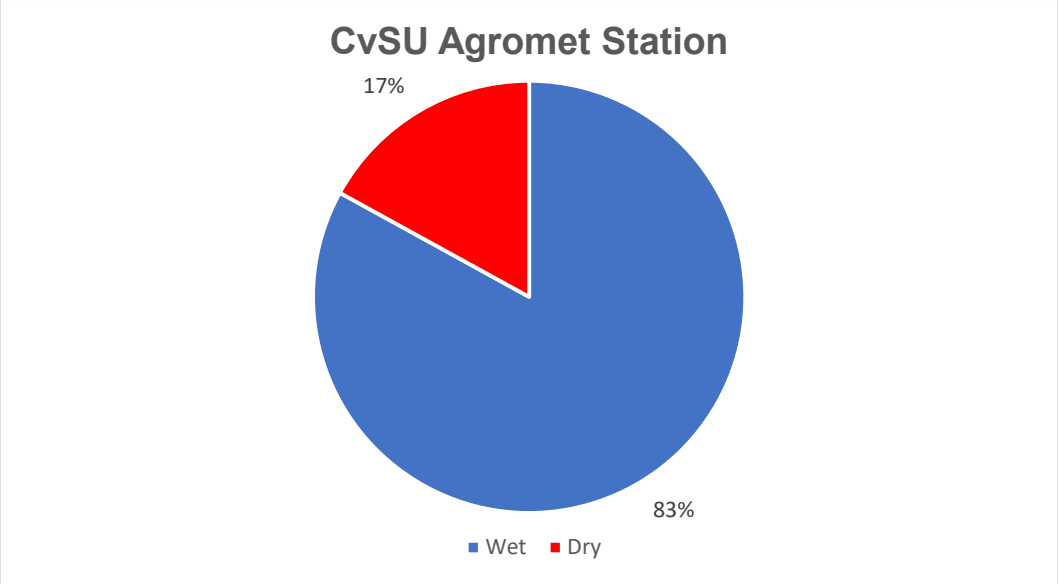

Figure 42. Seasonal rainfall contribution in CvSU Agrometeorological Station.

At Sangley Point Station, the normal monthly precipitation was 188.81 mm. During the wet season, the estimated total monthly rainfall total was 331.49 mm while the estimated total monthly rainfall during dry season was only 46.13 mm. There was a ±76% rainfall variation from the normal value (**Figure 43**).

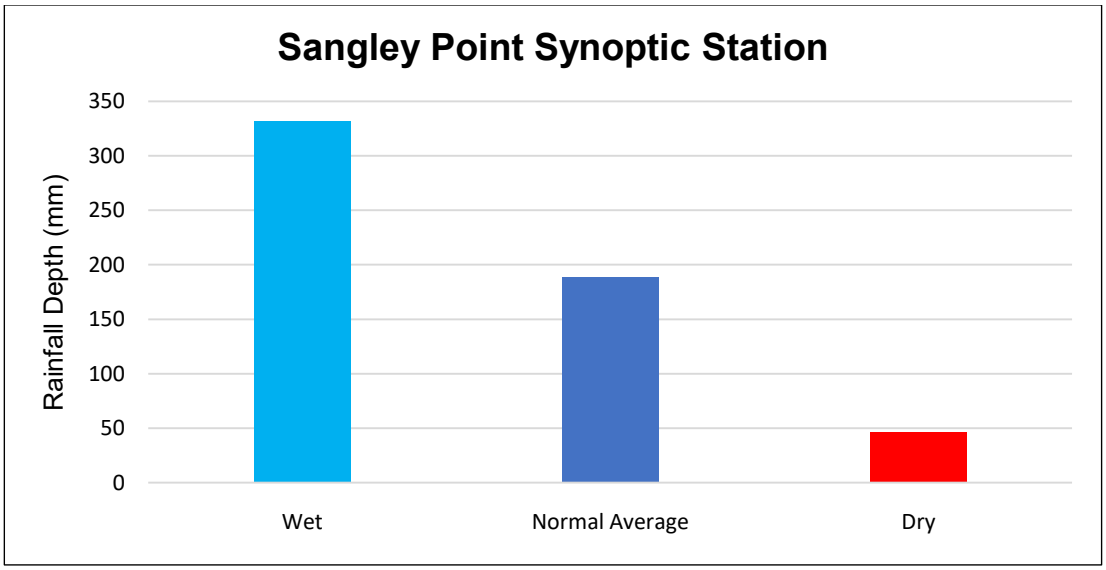

Figure 43. Seasonal rainfall deviation from the normal value in Sangley Point Synoptic Station.

The normal annual precipitation was 2,265.69 mm at Sangley Point Station. During wet season, the estimated rainfall total was 1,988.92 mm (88%) while the estimated rainfall total during dry season was only 276.76 mm (12%) (**Figure 44**).

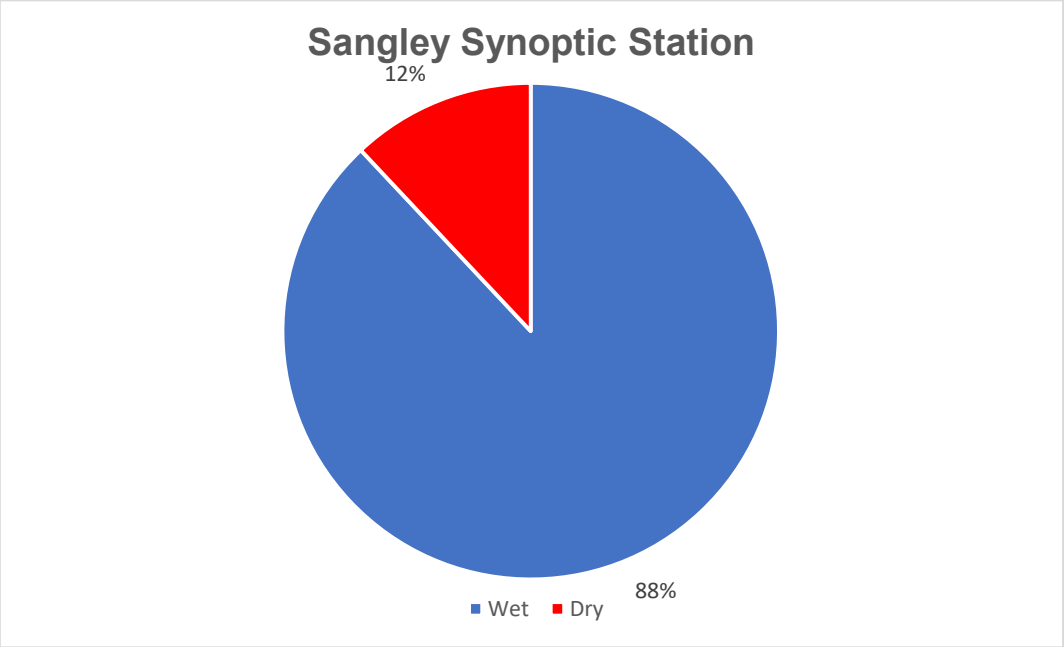

Figure 44. Seasonal rainfall contribution in Sangley Point Synoptic Station.

Streamflow

Streamflow is a volumetric discharge that takes place in a stream or channel and varies over space and time. Understanding the temporal and spatial distribution of streamflow is important in hydrology, emergency management, flood forecasting, water resources planning and management, and environmental protection (Wiche & Holmes, 2016). Rivers are considered as the main conduits of plastic waste to the seas, with most plastic waste carried by small rivers that flow through densely populated urban areas (Parker, 2021). Understanding the streamflow of rivers will help to explain the movement of plastic waste and inform potential solutions to reduce the amount that is released into the oceans.

Rainfall is the main factor to consider in the changes of streamflow. Other natural mechanisms that cause changes in streamflow are transpiration by vegetation, groundwater discharge and recharge, and natural sedimentation. Human induced changes should also be considered such as land use changes due to urbanization, surface withdrawals, reservoir sedimentation, and others. **Figures 46** to **51** show the daily average streamflow at Daang Hari Bridge (located in **Figure 45**) at different seasons.

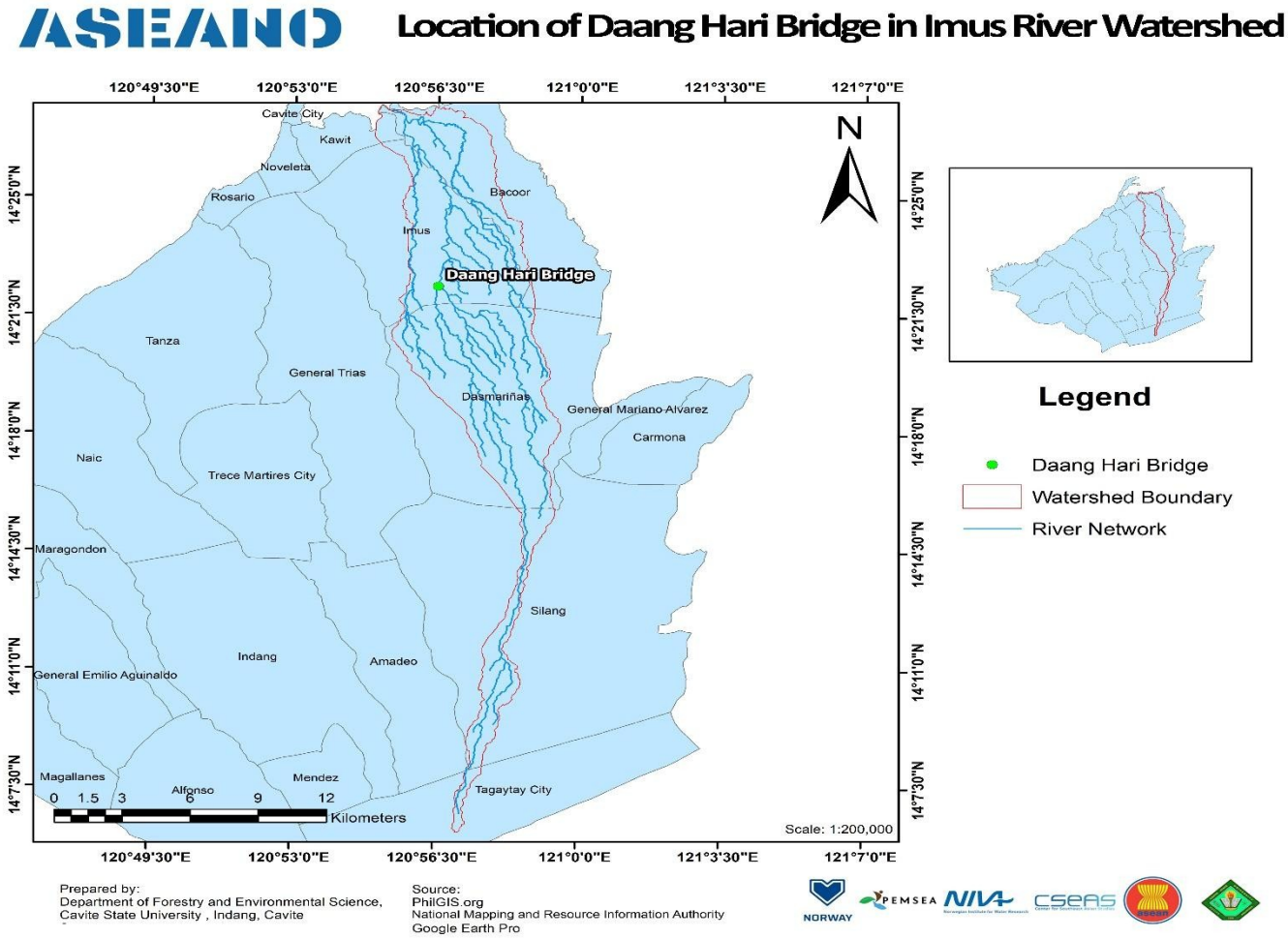

Figure 45. The location of Daang Hari Bridge in Imus River Watershed.

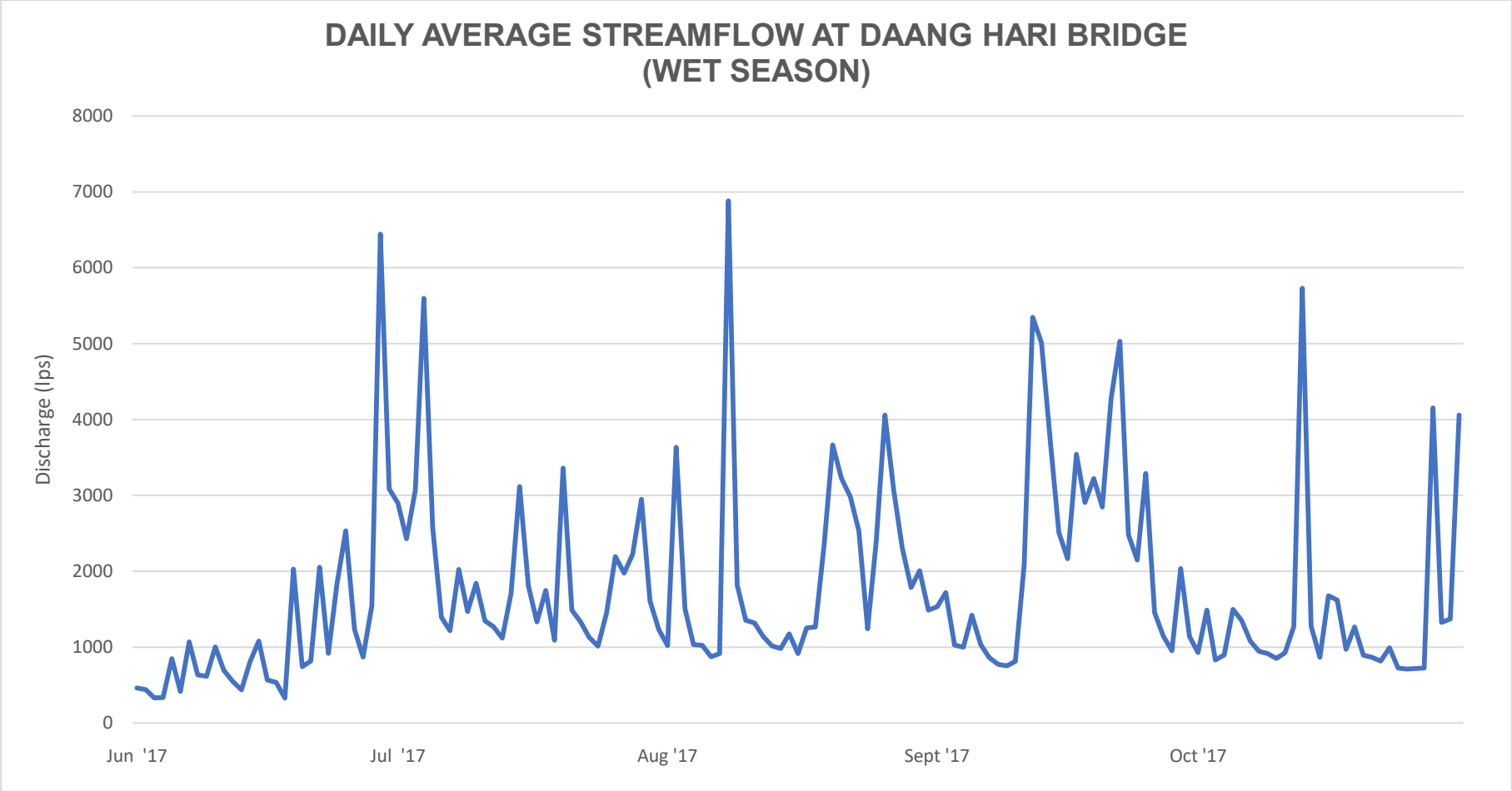

Figure 46. Daily streamflow trend at Daang Hari Bridge during the wet season of June 2017 to October 2017 (DOST-ASTI)

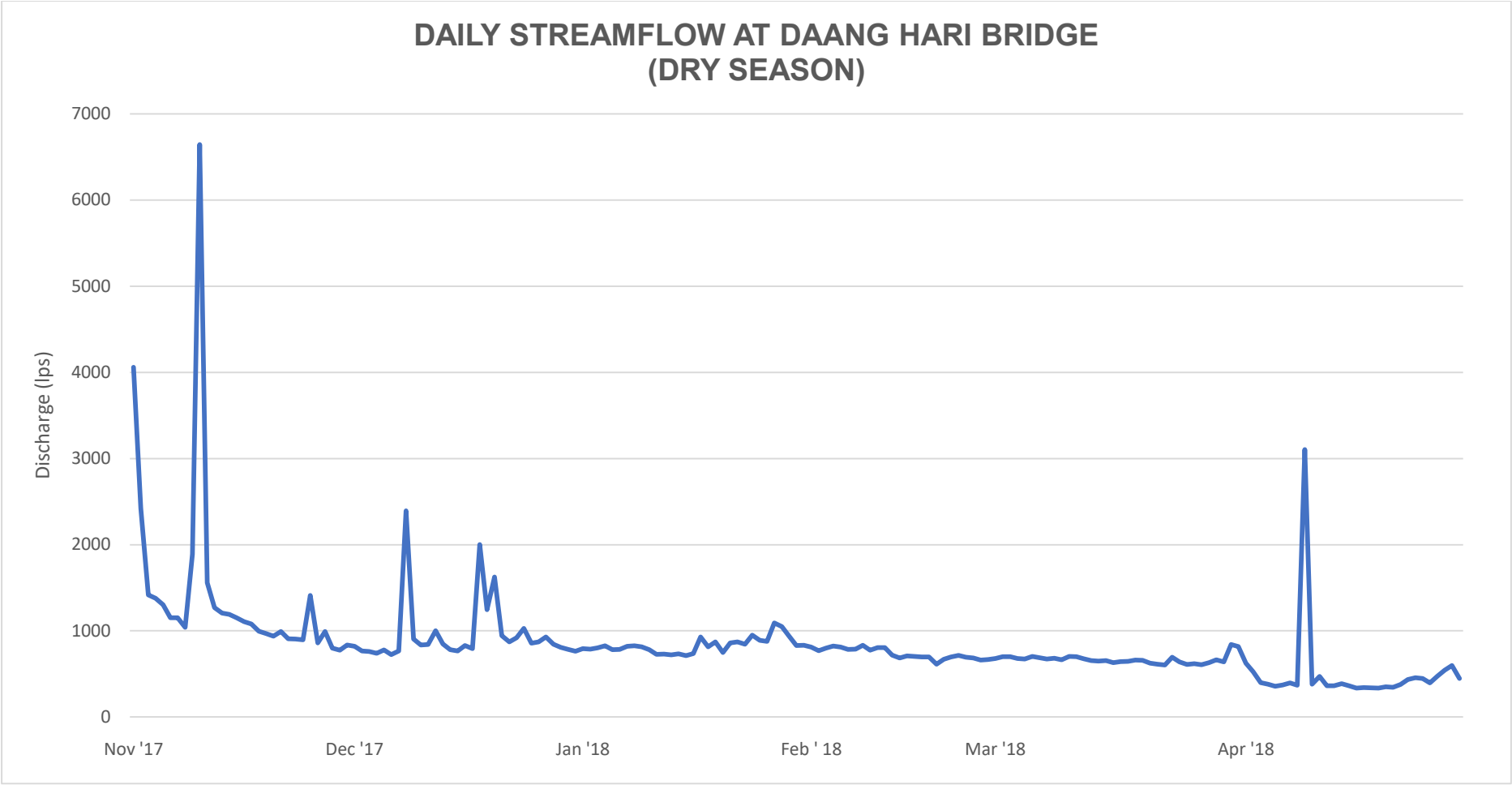

Figure 47. Daily streamflow trend at Daang Hari Bridge during dry season of November 2017 to April 2018 (DOST-ASTI)

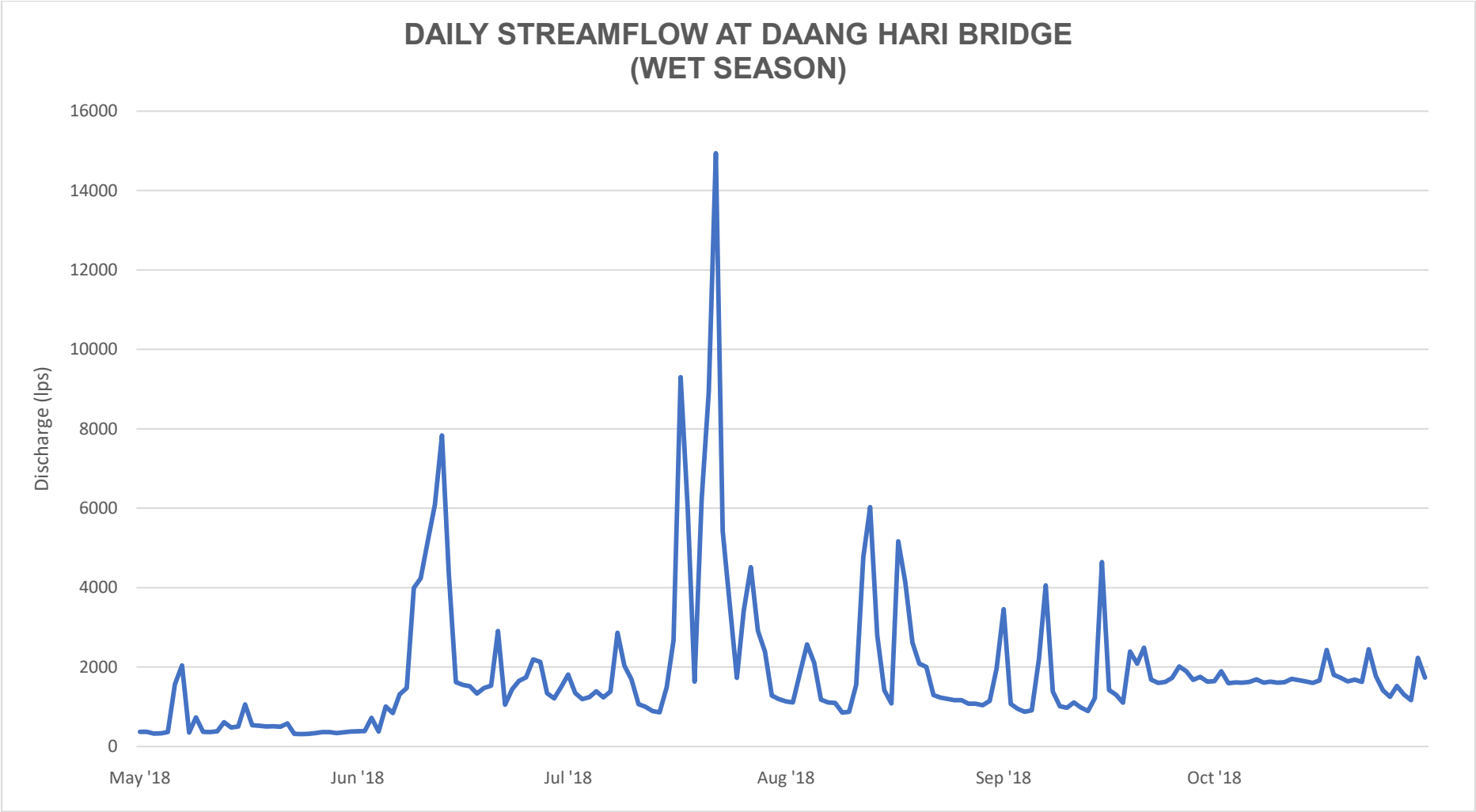

Figure 48. Daily streamflow trend at Daang Hari Bridge during wet season of June 2017 to October 2017 (DOST-ASTI)

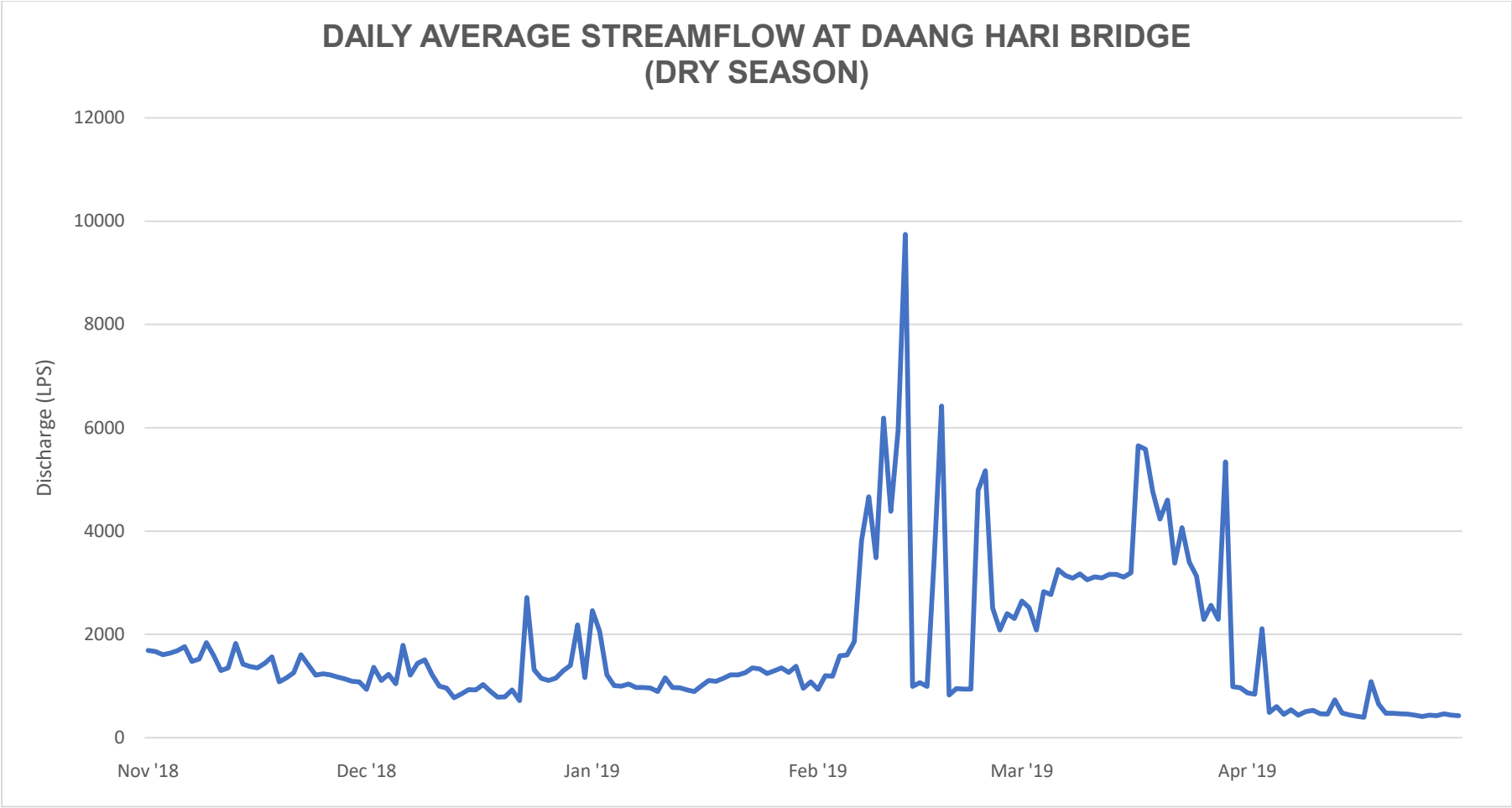

Figure 49. Daily streamflow trend at Daang Hari Bridge during dry season of June 2017 to October 2017 (DOST-ASTI)

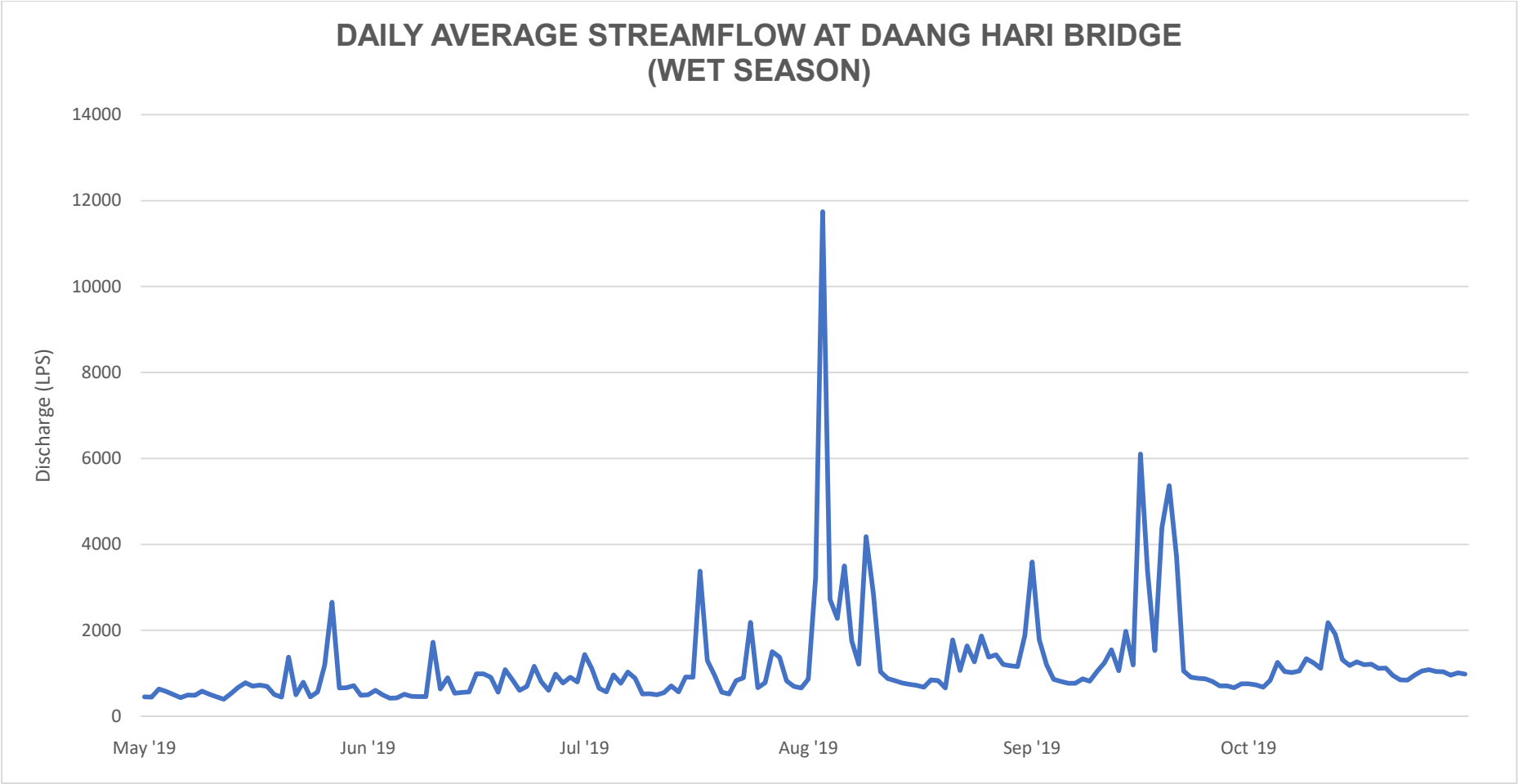

Figure 50. Daily streamflow trend at Daang Hari Bridge during wet season of May 2019 to October 2019 (DOST-ASTI)

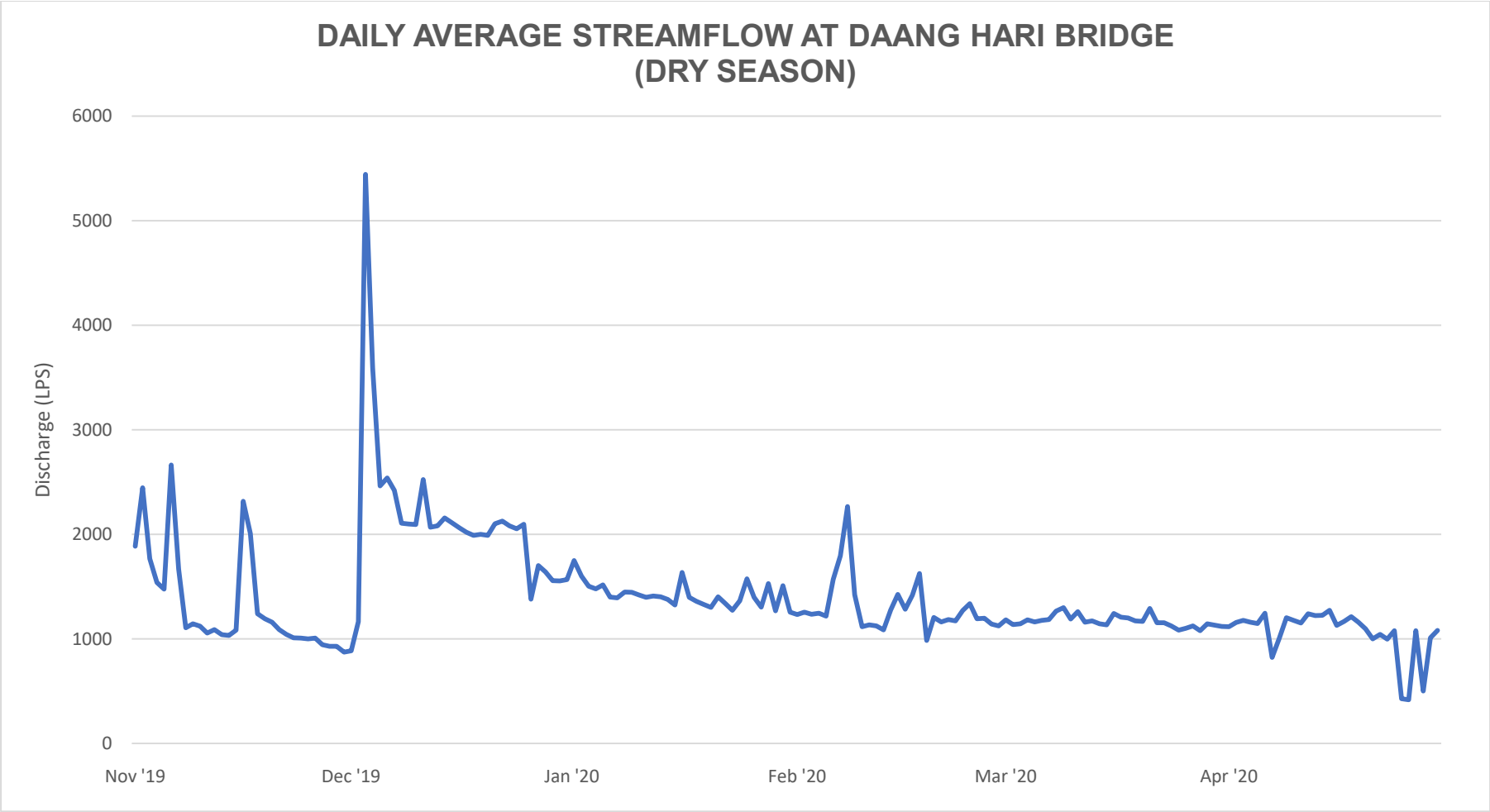

Figure 51. Daily streamflow trend at Daang Hari Bridge during dry season of November 2019 to April 2020 (DOST-ASTI)

Table 6 shows the average flow, minimum flow and maximum flow at the Daang Hari Bridge from June 2017 to April 2020. Based on the available data, the average flow during wet season was 1,601.84 liters per second (Lps), while the average flow during dry season was 1,337.42 Lps The extreme minimum and extreme maximum flow were 315.63 lps and 14,941.18 Lps and were both experienced during a wet season during May 2018 to October 2018.

Table 6. Streamflow at Daang Hari Bridge outlet during different seasons.

Period	Season	Average flow (Lps)	Minimum Flow (Lps)	Maximum Flow (Lps)
Jun 2017 – Oct 2017	Wet	1,767.18	326.24	6,883.20
Nov 2017 – Apr 2018	Dry	857.14	334.41	6,645.02
May 2018 – Oct 2018	Wet	1,862.79	315.63	14,941.18
Nov 2018 – Apr 2019	Dry	1,751.44	394.53	9,742.09
May 2019 – Oct 2019	Wet	1,175.55	392.97	11,741.99
Nov 2019 – Apr 2020	Dry	1,403.67	418.16	5,442.72

Conclusion

The total drainage area of IRW is 11,259.80 hectares and covers portions of Tagaytay City, Amadeo, Silang, Dasmariñas, Imus City, Bacoor City and Kawit. The elevation within the watershed ranges from 0 to 655 meters above sea level and can be subdivided into upland, central hilly, and lowland. The lowland area covers parts of Kawit, Imus City, and Bacoor City. The central hilly area covers parts of Imus City, Bacoor City, and the majority of the communities in Dasmariñas and Silang. The upland area covers parts of Silang, Amadeo, and Tagaytay City.

The Imus river originates in Tagaytay City. Its watershed contains 56 perennial streams with a total length of 186.15 km, divided between 36 river segments. These segments are a combination of headwaters and medium-sized streams. The sub-watersheds A, B, and C have drainage densities of 1.15 km/km^2, 1.95 km/km^2, and 1.41 km/km^2, respectively. The sub-watersheds A and C have stream frequencies of 0.20/km^2 and 0.25/km^2, which is considered a low value, while sub-watershed B has a high stream frequency of 0.39/km^2. Sub-watersheds A and B have bifurcation ratios of 5 and 3.31 while sub-watershed C has a bifurcation ratio of 2.5. The elongation ratio of sub-watersheds A, B, and C have values of 0.33, 0.26, and 0.43, respectively. The circulatory ratio of sub-watersheds A, B, and C have values of 0.18, 0.11, and 0.26, respectively.

A total of 222 barangay communities were located within the boundaries of the watershed with a total population of 1,351,057 in 2015. In terms of land classification, 90.67% of the province is classified as alienable and disposable land, while the remaining forest land represents only 9.33%. Alienable and disposable lands are further classified as production land (55.24%) and built-up areas (44.76%).

The Sangley Point Synoptic Station shows a normal mean temperature of 28.53°C, while the CvSU Agrometeorological Station recoded a normal mean temperature of 26.20°C. The average total annual rainfall recorded at Sangley Point Synoptic station and CvSU Agrometeorological Station was 2,265.69 mm and 2,483.05 mm, respectively. The average flow during the wet season was 1,601.84 liters per second (Lps), while the average flow during the dry season was 1,337.42 Lps.

The use of GIS and remote sensing had been found very useful in the fast and efficient delineation of the boundaries of the Imus river system and the identification of communities located within its boundaries. These are very useful for identifying and mapping potential sources of plastic waste within the watershed. Furthermore, such baseline data can help in measuring the magnitude of waste generation and monitoring the flow and transport of plastic waste from potential sources into the sea.

References

Andrady, A. (2011). Microplastics in the Marine Environment. *Marine Pollution Bulletin* , 1596 - 1605.

Chowdhury, M., Hasan, M., & Abdullah-Al-Mamun, M. (2020). Land use/land cover change assessment of Halda watershed using remote sensing and GIS. *The Egyptian Journal of Remote Sensing and Space Science*, 63 - 75.

Edwards, P., Williard, K., & Schoonover, J. (2015). Fundamentals of Watershed Hydrology. *Journal of Contemporary Water Research and Education*, 3-20.

Guzha, A., Rufino, M., Okoth, S., Jacobs, S., & Nobrega, R. (2018). Impacts of land use and land cover change on surface runoff, discharge and low flows: Evidence from East Africa. *Journal of Hydrology: Regional Studies*, 49-67.

Haque, S. (2013). *Watershed Management in Bangladesh. Degradation of Upland Watershed in Bangladesh Project- a USDA funded Project, Grant No. BG-ARS-123.* Chittagong 4331, Bangladesh.: Institute of Forestry and Environmental Sciences, University of Chittagong .

Horton, R. (1945). Erosional development of streams and their drainage basins; hydrophysical approach to quantitative morphology. *Geological Society of America*, 275-370.

Karolyn, D., Braganza, K., Stott, P., Arblaster, J., Meehl, G., Brocolli, A., & Dixon, K. (2003). Detection of a human influence on North American climate. *Journal of Science*, 1200-1203.

Kulkarni, M. (2015). The basic concept to study morphometric analysis of river drainage basin: a review. *International Journal of Science and Research* , 2277-2280.

Lambin, E., Geist, H., & Lepers, E. (2013). Dynamics of land-use and land-cover change in tropical regions. *Annual Review of Environment and Resources*, 205-241.

Local Government of Cavite . (2017). *Cavite Ecological Profile.* Trece Martires City: Province of Cavite.

Mahala, A. (2020). The significance of morphometric analysis to understand the hydrological and morphological characteristics in two different morpho-climatic settings. *Applied Water Science*, 33.

Montanari, A., Young, G., Savenjie, H., Hughes, D., Wagener, T., Ren, L., . . . Grimaldi, S. (2013). "Panta Rhei—everything flows": change in hydrology and society—the IAHS scientific decade 2013–2022. *Hydrologic Science Journal*, 1256-1275.

O'Keefe, T., Elliot, S., & Naiman, R. (n.d.). *Introduction to Watershed Ecology.* Retrieved from Watershed Academy Web: https://cfpub.epa.gov/watertrain/pdf/modules/watershedecology.pdf

Parker, L. (2021, May 1). *Environment: Plastic gets to the oceans through over 1,000 rivers*. Retrieved from National Geographic: https://www.nationalgeographic.com/environment/article/plastic-gets-to-oceans-through-over-1000-rivers

PEMSEA. (2020). *Baseline Report The situation and causes of plastic pollution in the Imus River, Cavite*. Quezon City, Philippines: Partnerships in Environmental Management for the Seas of East Asia (PEMSEA).

PEMSEA and Provincial Government of Cavite. (2017). *State of the Coasts of Cavite Province.* Quezon City, Philippines: Partnerships in Environmental Management for the Seas of East Asia (PEMSEA).

Prabhakaran, A., & Raj, N. (2018). Drainage morphometric analysis for assessing form and processes of the watersheds of Pachamalai hills and its adjoinings, Central Tamil Nadu, India. *Applied Water Science*, 31.

Sedigo, N., Hermosa, D., Villanueva, M., Espineli, M., & Panizales, J. (2015). *Bio-physical and Socio-economic Characterization and Vulnerability Assessment of Labac-Alemang River Watershed.* Trece Martirez City: DENR-PENRO Cavite and Cavite State University.

Sukristiyanti, S., Maria, R., & Lestiana, H. (2018). Watershed-based Morphometric Analysis: A Review. *Earth and Environmental Science*, 118-123.

USGS. (n.d.). *Watersheds and Drainage Basins*. Retrieved from USGS: Science for a changing world: https://www.usgs.gov/special-topic/water-science-

school/science/watersheds-and-drainage-basins?qt-science_center_objects=0#qt-science_center_objects

Wiche, G., & Holmes, R. (2016). Streamflow Data. In T. Adams, & T. Pagano, *Flood Forecasting: A Global Perspective* (pp. 371-398). Academic Press.

Annex

Correlation Formula for Climate Data Augmentation

For uncorrelated sequences ($r^2 \leq 0.8$), which was observed in the rainfall readings between the two stations, the dependent variable "y" can be solved using the formula:

$$y = mX_i + c + \sqrt{\quad}$$

Where: r = product – moment correlation coefficient

S_y = standard deviation of y from short sequence

ei = random normal variable the zero mean and unit variance.

The product – moment correlation coefficient (r) was obtained using the formula:

$$r = \left(1 - \frac{S_{yx}^2}{S_y^2}\right)^{\frac{1}{2}}$$

$$S_y^2 = \sum y^2 -$$

$$S_{yx}^2 = \frac{\sum \ y^2 - c\sum \ y - m\sum \ xy}{}$$

Where: x = basis

y = augmented

c, m = regression constant

Annex Table 1. Monthly maximum temperature (^{O}C) at Sangley from 1990 to 2020.

Year	Jan	Feb	Mar	Apr	May	Jun	Jul	Aug	Sep	Oct	Nov	Dec
1990	NR	NR	NR	NR	NR	NR	NR	NR	NR	NR	NR	NR
1991	NR	NR	NR	NR	NR	NR	NR	NR	NR	NR	NR	NR
1992	NR	NR	NR	NR	NR	NR	NR	NR	NR	NR	NR	NR
1993	NR	NR	NR	NR	NR	NR	NR	29.68	30.35	30.82	31.43	29.81
1994	30.03	31.04	32.22	34.15	33.92	32.88	30.20	31.59	31.60	31.48	31.88	30.76
1995	30.14	30.55	32.73	33.76	33.66	33.45	32.14	31.86	30.26	31.15	NR	29.00
1996	30.39	30.93	32.78	33.53	34.51	34.12	32.12	32.73	32.01	32.73	30.95	29.84
1997	29.97	31.07	32.10	34.50	33.85	32.99	31.35	30.67	31.89	33.18	32.83	31.66
1998	31.86	33.45	33.59	35.02	34.28	34.26	34.51	33.53	31.69	31.60	33.19	30.80
1999	31.62	31.34	33.36	33.52	34.40	31.81	30.73	30.83	30.64	31.39	30.28	29.86
2000	30.11	30.67	31.81	34.70	32.69	33.01	29.54	31.77	31.51	31.55	31.14	30.54
2001	30.73	30.71	32.23	34.26	33.28	32.69	31.26	30.67	31.91	32.18	31.61	30.08
2002	30.32	30.27	32.36	34.50	33.89	33.95	30.22	31.69	31.67	32.51	30.45	31.14
2003	29.84	30.98	32.63	34.68	33.69	31.91	32.68	31.42	30.61	32.22	31.76	29.45
2004	30.41	31.02	32.69	34.89	33.53	31.11	32.50	30.52	32.52	31.54	30.56	29.88
2005	29.78	31.30	31.78	33.82	34.82	32.45	32.40	31.07	30.78	30.80	30.88	29.17
2006	29.79	30.94	33.10	34.85	33.72	33.79	30.39	30.29	32.44	31.87	31.80	30.62
2007	30.75	31.30	32.94	34.36	34.51	33.60	33.24	30.95	31.41	30.68	29.78	30.16
2008	30.19	29.87	32.51	33.93	32.33	33.00	32.23	31.19	31.34	31.85	30.96	29.58
2009	28.92	31.24	33.04	32.49	32.55	31.65	31.75	31.87	30.35	30.75	31.60	MD
2010	30.26	31.06	32.47	34.29	34.09	33.95	32.90	32.25	32.51	31.65	31.31	30.26
2011	29.98	30.96	31.27	32.66	34.28	32.01	31.27	31.19	31.12	32.46	31.70	29.97
2012	30.80	31.19	31.60	34.46	34.52	32.24	31.66	30.44	31.54	31.68	32.99	32.00
2013	30.16	32.02	33.01	35.35	35.05	34.07	32.68	31.05	30.48	31.20	31.37	31.32
2014	29.48	31.33	32.45	34.66	36.00	32.91	31.66	32.01	31.69	32.00	31.93	30.13
2015	29.48	30.66	32.01	34.36	35.25	34.67	32.32	32.62	32.86	32.13	32.61	30.99
2016	31.28	30.79	32.82	35.00	34.81	33.45	33.07	31.07	32.31	31.96	30.73	30.89
2017	29.74	30.04	32.16	33.83	34.39	33.61	31.77	32.53	32.22	31.60	31.73	30.49
2018	30.32	31.57	32.15	34.32	35.45	31.57	30.41	31.17	31.84	33.14	32.38	30.57
2019	30.64	31.54	33.15	35.41	34.51	34.46	32.49	30.89	31.65	33.22	31.86	31.52
2020	31.04	31.05	33.32	34.98	34.93	34.11	33.85	32.21	33.68	31.80	31.59	30.99

*NR = No reading

Annex Table 2. Monthly minimum temperature (OC) at Sangley from 1990 to 2020.

Year	Jan	Feb	Mar	Apr	May	Jun	Jul	Aug	Sep	Oct	Nov	Dec
1990	NR	NR	NR	NR	NR	NR	NR	NR	NR	NR	NR	NR
1991	NR	NR	NR	NR	NR	NR	NR	NR	NR	NR	NR	NR
1992	NR	NR	NR	NR	NR	NR	NR	NR	NR	NR	NR	NR
1993	NR	NR	NR	NR	NR	NR	NR	26.06	NR	NR	NR	NR
1994	NR	NR	NR	25.89	26.39	25.62	24.19	24.61	24.55	25.55	24.89	24.89
1995	23.48	22.91	24.16	25.85	26.24	26.04	25.22	24.79	25.05	25.11	NR	NR
1996	22.69	23.14	25.19	25.84	26.79	26.58	25.66	25.81	25.46	26.18	24.90	24.90
1997	23.25	24.18	24.07	26.29	26.24	26.42	25.53	25.36	26.13	26.12	25.72	25.72
1998	24.45	25.53	25.66	27.14	27.05	26.95	27.28	26.73	25.67	26.30	26.34	26.34
1999	24.40	23.60	25.12	26.07	26.72	25.26	25.14	25.14	25.27	25.25	24.54	24.54
2000	23.93	24.18	24.78	26.32	25.51	25.74	24.75	25.49	24.79	25.22	24.94	24.94
2001	24.41	24.68	25.12	26.61	26.51	25.93	25.31	25.35	25.94	25.83	25.01	25.01
2002	23.36	23.92	24.82	26.22	26.86	27.05	25.37	25.95	25.68	26.22	25.54	25.54
2003	24.07	24.05	25.55	27.20	27.09	26.05	26.61	25.85	25.41	26.24	25.87	25.87
2004	24.39	24.87	25.83	27.32	26.80	25.91	26.01	25.25	26.15	25.95	25.42	25.42
2005	24.10	24.78	25.41	26.32	27.83	26.57	26.70	26.10	25.76	25.86	26.38	26.38
2006	24.89	25.40	26.44	27.31	27.08	27.17	25.90	25.70	26.41	26.49	27.14	27.14
2007	25.44	24.83	25.84	26.94	27.25	27.51	26.85	26.01	26.15	25.82	24.85	24.85
2008	24.82	24.61	25.69	27.14	26.03	26.89	26.38	25.49	25.94	26.32	26.02	26.02
2009	23.71	24.77	26.01	26.40	26.59	26.01	26.00	26.93	25.66	25.92	25.69	25.69
2010	24.34	24.61	25.52	26.83	27.33	27.25	26.91	26.51	26.68	26.60	26.24	26.24
2011	24.67	24.88	25.63	25.99	27.13	26.38	26.36	26.26	25.93	25.85	25.72	25.72
2012	25.26	25.35	25.59	27.00	27.49	26.71	25.88	25.25	25.80	25.60	26.20	26.20
2013	24.18	25.05	26.06	27.74	28.03	27.10	25.93	25.53	25.47	25.68	25.92	25.92
2014	23.37	24.13	25.37	26.80	28.32	26.98	25.83	26.50	26.32	26.20	25.92	25.92
2015	23.63	24.12	25.15	26.78	31.51	27.70	26.68	26.73	26.62	26.65	26.53	26.53
2016	25.34	24.86	26.34	27.87	28.32	27.24	27.01	26.65	26.78	26.65	26.08	26.08
2017	25.07	24.50	25.85	27.17	28.28	27.75	26.79	27.14	27.10	26.61	26.49	26.49
2018	25.45	25.44	25.70	27.24	28.45	26.52	26.04	26.58	26.54	27.04	26.57	26.57
2019	24.95	24.56	25.53	27.30	27.58	27.43	26.39	26.28	25.94	26.46	25.95	25.95
2020	24.82	24.13	26.17	27.38	27.82	27.50	26.64	26.30	26.89	26.08	25.59	25.59

*NR = No reading

Annex Table 3. Monthly mean temperature (^{O}C)at Sangley from 1990 to 2020.

Year	Jan	Feb	Mar	Apr	May	Jun	Jul	Aug	Sep	Oct	Nov	Dec
1990	27.15	28.57	29.03	31.32	31.40	29.32	29.20	28.82	29.07	29.07	28.79	27.91
1991	27.61	28.04	28.75	30.22	31.04	29.97	28.76	27.35	NR	28.05	26.87	26.69
1992	25.88	26.50	27.85	29.38	29.60	29.15	27.48	27.40	28.69	29.04	27.63	27.88
1993	27.44	27.78	28.72	30.42	31.13	30.75	29.21	27.75	27.79	27.98	28.40	27.07
1994	26.89	27.48	28.28	29.58	29.79	28.91	27.06	28.38	28.09	28.50	28.25	27.21
1995	26.34	26.39	28.26	29.83	29.45	29.37	28.26	28.05	27.50	27.97	NR	25.98
1996	26.28	26.48	28.49	29.28	29.98	29.83	28.38	28.85	28.16	29.13	27.57	26.61
1997	26.35	27.08	27.65	30.12	29.65	29.39	27.94	27.71	28.53	29.20	28.69	27.53
1998	27.44	28.61	28.78	30.37	30.25	30.02	30.28	29.32	27.99	28.36	28.92	27.37
1999	27.26	26.87	28.85	29.48	30.16	28.27	27.89	27.72	27.79	28.01	27.32	26.76
2000	27.00	27.20	28.20	30.25	28.78	29.12	27.03	28.45	28.02	28.17	27.70	27.28
2001	27.37	27.22	28.38	30.29	29.71	29.16	27.97	27.64	28.73	28.72	27.99	26.69
2002	26.45	26.73	28.12	29.86	30.02	30.10	27.51	28.41	27.87	28.93	27.61	27.72
2003	26.44	26.96	28.39	30.42	29.76	28.79	29.18	28.02	27.64	28.76	28.51	26.33
2004	26.97	27.30	28.69	30.65	29.82	28.25	28.76	27.70	28.89	28.35	27.64	27.02
2005	26.55	27.75	28.25	29.64	30.96	29.27	29.15	28.25	27.90	28.12	28.48	26.90
2006	27.21	27.80	29.24	30.54	30.16	30.20	27.88	27.76	28.92	28.99	29.27	28.19
2007	27.78	27.55	28.90	30.30	30.28	30.13	29.51	28.06	28.43	27.97	27.19	27.45
2008	27.04	26.84	28.53	30.11	28.82	29.53	28.67	27.96	28.31	28.72	28.15	26.93
2009	25.97	27.55	28.89	29.02	29.11	28.54	28.33	29.08	27.61	28.10	28.33	27.75
2010	26.91	27.34	28.53	30.08	29.81	29.74	29.29	28.78	29.20	28.73	28.41	27.63
2011	26.72	27.29	27.77	28.90	30.04	28.78	28.33	28.39	28.26	28.83	28.49	27.48
2012	27.76	27.88	28.34	30.54	30.57	29.05	28.38	27.63	28.34	28.47	29.17	28.48
2013	26.87	28.08	29.14	31.18	30.98	30.01	29.01	28.16	27.67	28.32	28.37	28.15
2014	26.10	27.30	28.45	30.47	31.79	29.95	28.83	28.18	28.24	28.52	28.25	27.21
2015	26.10	26.81	27.96	30.04	31.12	30.72	28.99	29.36	29.34	29.12	29.29	27.85
2016	27.99	27.53	29.15	30.97	31.05	29.99	29.53	28.53	29.04	28.98	28.19	28.20
2017	26.96	26.89	28.53	30.01	30.95	30.09	28.74	29.50	29.36	28.77	28.91	27.81
2018	27.48	28.13	28.51	30.38	31.46	28.67	28.00	28.56	28.74	29.69	29.18	27.80
2019	27.38	27.60	28.75	30.62	30.32	30.28	28.84	27.98	27.93	29.39	28.30	27.92
2020	27.31	26.87	29.00	30.41	30.65	30.23	29.71	28.75	29.67	28.33	28.07	27.73

*NR = No reading

Annex Table 4. Monthly rainfall depth (mm) readings at Sangley from 1990 to 2020.

Year	Jan	Feb	Mar	Apr	May	Jun	Jul	Aug	Sep	Oct	Nov	Dec
1990	5.50	0.00	5.50	8.40	179.90	513.30	534.40	633.60	389.70	389.70	179.10	51.80
1991	4.30	2.80	19.90	10.60	13.40	153.80	437.50	1324.30	320.70	49.40	98.50	6.00
1992	13.70	0.00	0.00	0.80	44.20	167.10	370.70	745.00	476.50	266.20	152.00	6.10
1993	2.30	0.00	0.00	16.30	11.80	334.20	410.20	400.60	242.90	158.00	153.50	122.20
1994	28.40	0.00	5.20	36.90	81.60	240.80	677.70	442.40	245.00	73.40	5.00	87.20
1995	4.60	26.60	0.00	1.20	139.90	270.30	340.00	525.40	544.60	290.90	71.10	84.30
1996	6.80	3.20	6.10	27.90	75.80	81.80	562.90	160.00	494.80	75.00	148.90	14.00
1997	7.20	24.40	2.00	7.80	523.50	186.10	351.10	754.50	135.10	52.40	3.20	0.20
1998	11.10	0.00	5.00	0.60	188.70	134.80	62.80	182.20	691.70	352.00	83.20	307.10
1999	17.70	5.80	48.30	44.00	58.20	241.00	558.80	539.60	314.20	315.10	99.20	188.50
2000	33.20	33.80	28.20	38.80	339.20	157.70	883.30	334.50	332.20	505.50	319.30	110.10
2001	48.60	75.60	18.80	21.40	135.20	292.20	281.60	605.50	198.10	104.10	83.00	65.40
2002	4.90	7.80	1.20	9.20	111.20	162.70	1596.70	197.80	313.40	84.70	179.00	13.00
2003	0.60	4.90	0.20	7.40	437.50	707.90	242.30	382.80	441.20	49.00	73.30	5.20
2004	3.20	34.40	0.00	2.70	282.40	295.40	182.10	405.30	111.40	59.10	165.40	49.20
2005	3.80	10.40	18.10	1.20	68.00	334.60	207.30	312.70	362.60	246.00	29.10	78.80
2006	77.60	1.40	30.50	0.00	65.20	93.40	559.10	377.70	437.70	132.70	83.10	177.60
2007	2.30	3.20	1.00	2.00	126.80	134.60	224.80	737.60	394.90	200.20	241.60	55.40
2008	52.60	18.20	0.80	5.60	258.40	325.70	234.20	411.80	433.10	215.40	95.60	51.30
2009	22.80	19.80	49.20	171.60	265.00	476.20	538.50	228.50	786.80	219.10	36.40	9.20
2010	5.80	0.00	10.40	45.40	36.80	151.20	355.90	375.20	291.80	444.70	240.90	98.00
2011	69.70	0.00	48.00	3.00	251.70	744.50	393.10	486.60	423.10	172.10	156.20	198.50
2012	25.20	104.20	88.50	10.50	294.30	232.00	748.00	1186.30	591.50	308.00	12.70	11.40
2013	37.60	110.00	58.40	1.40	47.40	290.90	533.00	1339.50	977.20	246.30	130.20	28.80
2014	0.40	3.30	7.20	1.20	84.50	321.40	523.40	296.80	460.30	212.90	27.80	163.20

*NR = No reading

Year	Jan	Feb	Mar	Apr	May	Jun	July	Aug	Sep	Oct	Nov	Dec
2015	31.80	1.00	8.80	0.00	10.20	166.80	352.80	312.60	359.20	103.60	9.20	294.70
2016	1.40	80.60	0.20	20.20	161.80	182.40	302.80	775.00	145.30	189.36	88.90	89.80
2017	52.50	5.40	6.40	39.30	186.40	105.10	467.20	323.00	382.70	196.10	116.40	57.10
2018	16.40	0.80	13.82	0.20	20.00	723.00	757.30	427.20	194.70	72.80	13.70	132.90
2019	5.70	2.00	2.40	3.60	61.90	271.10	309.80	622.90	330.10	33.20	149.80	119.50
2020	4.20	31.60	2.00	0.00	190.20	268.90	230.40	214.20	130.90	375.70	203.60	123.90

Annex Table 5. Monthly maximum temperature (^{O}C) at CvSU Agrometeorological Station from 1990 to 2020.

YEAR	Jan	Feb	Mar	Apr	May	Jun	Jul	Aug	Sep	Oct	Nov	Dec
2007	NR	NR	NR	NR	NR	NR	NR	NR	NR	NR	28.79	28.79
2008	28.85	28.66	30.92	32.66	30.21	31.01	30.43	30.42	30.51	31.39	29.76	28.36
2009	27.45	29.36	31.64	31.32	30.75	30.03	29.53	29.84	28.86	29.07	29.33	28.50
2010	28.33	30.93	31.25	32.99	32.64	31.07	30.85	30.35	28.92	29.60	29.55	28.33
2011	27.68	28.62	28.94	31.40	31.60	30.26	29.55	29.51	28.53	30.19	29.89	28.50
2012	29.08	28.92	29.66	32.57	31.63	30.53	29.25	28.83	29.72	29.74	30.53	30.05
2013	36.36	29.56	31.08	33.58	32.42	32.08	31.02	29.75	29.23	29.56	29.36	29.40
2014	27.41	29.79	31.02	33.51	33.36	31.47	29.86	30.31	29.69	29.79	30.04	27.92
2015	26.87	28.45	30.38	33.09	33.45	32.98	30.34	31.03	31.45	30.21	30.10	28.68
2016	29.35	29.10	31.88	32.91	33.40	31.79	31.77	29.82	30.72	29.86	29.33	29.13
2017	27.78	28.20	30.61	32.90	33.16	32.29	30.43	30.96	30.98	30.14	28.39	28.60
2018	28.46	29.48	30.60	33.09	34.06	30.24	29.27	29.62	30.44	31.35	30.33	28.55
2019	27.83	28.85	32.29	34.27	34.12	33.24	31.86	30.13	29.93	31.39	30.10	29.37
2020	29.28	29.06	32.81	32.54	33.63	32.99	32.10	31.05	31.83	29.39	29.69	NR

*NR = No reading

Annex Table 6. Monthly minimum temperature (^{O}C) at CvSU Agrometeorological Station from 1990 to 2020.

YEAR	Jan	Feb	Mar	Apr	May	Jun	Jul	Aug	Sep	Oct	Nov	Dec
2007	NR	NR	NR	NR	NR	NR	NR	NR	NR	NR	22.06	22.05
2008	21.17	21.06	21.69	23.96	22.09	22.56	25.10	22.48	22.28	22.72	22.51	21.27
2009	19.85	21.41	21.89	22.38	22.80	22.43	22.51	23.18	22.54	22.11	21.98	20.47
2010	20.62	20.83	21.87	21.63	21.56	20.98	20.38	20.15	20.23	20.64	20.15	19.51
2011	18.60	18.35	19.31	19.03	20.62	20.58	20.48	20.84	20.48	20.18	20.34	19.91
2012	19.40	19.46	19.80	20.71	20.79	20.53	20.38	21.99	21.01	20.36	20.73	19.97
2013	18.87	25.94	20.15	20.96	20.92	21.17	20.25	20.15	19.92	19.36	19.64	19.26
2014	16.45	20.00	21.54	22.77	23.78	23.50	22.87	22.53	22.25	22.12	21.81	21.23
2015	19.47	19.42	20.57	21.94	22.53	22.87	22.21	22.09	22.09	21.65	21.83	20.70
2016	20.34	20.85	21.31	23.35	23.93	23.59	22.87	23.43	23.06	22.94	22.36	22.27
2017	21.21	20.68	21.56	22.61	23.83	23.17	23.13	23.17	23.02	22.86	22.86	22.00
2018	21.56	21.24	21.62	22.97	23.98	22.81	22.88	22.85	22.65	21.76	22.43	22.06
2019	20.63	20.22	21.37	22.89	23.45	23.86	22.93	23.25	22.83	22.58	22.33	21.80
2020	21.07	26.83	22.05	22.93	23.89	23.34	22.98	23.00	23.07	22.87	22.27	NR

*NR = No reading

Annex Table 7. Monthly mean temperature (^{O}C) at CvSU Agrometeorological Station from 1990 to 2020.

YEAR	Jan	Feb	Mar	Apr	May	Jun	Jul	Aug	Sep	Oct	Nov	Dec
2007	NR	NR	NR	NR	NR	NR	NR	NR	NR	NR	24.69	25.95
2008	25.76	25.71	28.33	29.20	26.48	26.71	27.40	24.31	26.49	26.66	25.78	24.10
2009	23.40	24.69	26.05	27.08	27.30	26.92	26.79	27.06	26.23	25.81	25.37	24.29
2010	24.54	25.95	26.79	28.30	28.50	28.26	27.90	27.00	27.90	26.93	26.49	25.15
2011	24.35	24.82	25.64	26.96	28.08	27.21	26.55	26.09	27.00	26.56	26.44	25.61
2012	25.04	25.56	26.23	28.22	28.57	27.79	26.96	26.03	26.26	25.46	25.94	25.09
2013	23.49	24.17	26.05	28.10	28.26	27.86	26.66	26.38	26.00	26.03	25.46	24.21
2014	28.48	23.29	25.13	27.50	29.07	28.35	26.52	26.45	25.98	25.96	25.19	24.01
2015	22.13	22.47	24.35	27.26	28.29	28.05	26.72	26.61	27.13	26.01	25.39	24.14
2016	23.64	23.35	25.23	27.14	28.24	27.15	26.01	26.06	26.30	26.06	24.61	24.05

2017	22.97	23.04	24.96	26.98	28.31	27.72	26.53	26.53	26.47	26.07	25.56	24.07
2018	23.60	23.86	24.96	27.01		26.49	26.01	26.02	26.06	26.43	25.67	24.20
2019	23.13	22.58	25.83	28.35	29.15	29.37	27.47	26.69	26.47	27.33	25.98	25.07
2020	24.30	23.80	26.88	28.05	28.84	28.74	27.79	27.57	27.81	26.32	25.86	NR

*NR = No reading

Annex Table 8. Monthly rainfall depth (mm) readings at CvSU Agrometeorological Station from 1990 to 2020.

YEAR	Jan	Feb	Mar	Apr	May	Jun	Jul	Aug	Sep	Oct	Nov	Dec
1990	31.50	16.54	22.32	85.70	274.72	494.57	631.94	542.30	424.52	236.22	268.16	121.62
1991	11.55	0.97	7.96	40.92	105.53	190.36	385.33	781.92	277.95	105.63	87.89	1.21
1992	23.56	3.02	6.39	43.44	142.97	220.01	382.06	529.01	422.37	237.07	174.58	17.27
1993	17.99	5.05	8.47	67.00	125.89	336.32	431.59	371.47	258.84	199.18	185.76	180.58
1994	34.87	4.56	9.94	90.52	173.31	273.65	643.45	389.41	258.02	157.96	18.82	131.75
1995	7.51	10.37	3.96	19.15	182.15	250.94	269.31	371.63	423.16	191.53	37.38	91.14
1996	21.13	7.30	10.93	81.29	171.00	172.21	556.27	255.11	446.71	162.26	181.38	34.81
1997	9.81	9.51	2.61	28.48	451.60	198.09	283.31	486.04	121.84	86.19	35.19	20.72
1998	45.00	26.42	32.25	100.55	307.88	283.21	336.96	371.88	697.50	407.58	208.22	497.81
1999	15.80	3.70	13.89	69.44	123.94	230.30	442.35	376.42	249.93	200.17	66.55	230.65
2000	61.35	50.28	42.75	150.48	417.57	304.19	1014.28	454.40	438.73	486.90	477.91	236.81
2001	66.76	72.84	34.19	117.65	261.77	374.36	485.82	561.96	315.08	276.72	192.95	161.02
2002	4.42	5.28	6.90	20.61	153.03	168.79	1255.48	195.58	235.08	79.01	141.45	15.68
2003	28.26	19.78	20.34	84.55	454.66	621.60	396.18	420.31	462.86	214.25	150.93	58.69
2004	23.48	32.56	13.52	62.79	328.36	328.79	290.32	398.42	185.48	181.90	222.16	97.45
2005	8.73	1.51	4.71	23.50	136.80	299.28	177.57	276.95	296.72	181.06	0.85	89.29
2006	74.20	12.18	26.38	62.67	180.17	201.60	605.90	391.34	434.13	222.56	136.87	275.02
2007	42.18	31.59	33.88	109.75	273.05	294.12	494.50	657.57	492.14	355.70	324.80	117.00
2008	82.20	25.30	42.30	94.10	264.00	391.50	277.60	262.10	378.70	176.90	92.60	48.10
2009	37.60	34.10	74.50	275.00	286.80	420.90	516.80	331.70	791.50	350.10	66.20	13.80
2010	21.90	0.00	4.00	50.20	107.60	264.70	519.40	288.70	76.60	171.90	106.50	61.70
2011	25.40	5.20	18.00	18.60	254.00	613.10	459.10	636.80	404.70	259.90	134.60	154.90
2012	62.90	57.10	26.10	12.40	340.70	299.40	734.40	821.30	418.20	300.80	27.30	26.40
2013	56.20	118.70	28.40	78.90	246.70	195.80	151.40	733.90	811.00	185.20	215.60	37.30

2014	0.00	1.30	6.60	139.20	142.40	285.60	574.70	317.40	397.80	127.40	31.20	261.90
2015	39.60	5.30	1.80	33.80	149.20	322.60	660.50	344.80	311.40	251.20	30.60	428.20
2016	5.20	18.10	0.00	36.60	191.80	184.80	287.20	546.60	295.20	389.00	119.70	148.00
2017	43.90	18.80	16.80	86.20	304.00	240.50	342.60	354.10	404.90	194.80	190.40	106.90
2018	24.30	1.80	0.30	8.20	80.60	633.00	830.70	414.90	278.10	40.50	18.70	271.70
2019	18.60	6.20	0.00	36.10	134.30	297.20	455.60	501.70	298.00	68.10	92.20	197.10
2020	14.00	22.10	4.40	112.20	334.90	171.10	143.60	152.10	248.80	413.90	461.10	283.90

Annex Table 9. River segments and its stream order within the Imus River Watershed.

Stream Order	River Segment	Highest Point				Lowest Point				
		Point	Elevation	x	y	Point	Elevation	x	y	Length
1	1-3	1	619.2713	14° 6'42.92"N	120°57'8.71"E	3	463.8022	14° 9'24.35"N	120°57'39.62"E	5046.02
1	2-3	2	490.6514	14° 9'7.76"N	120°57'29.77"E	3	463.8022	14° 9'24.35"N	120°57'39.62"E	593.45
1	4-6	4	480.845	14° 9'22.49"N	120°57'57.96"E	6	374.6301	14°11'13.82"N	120°58'16.49"E	3455.91
1	5-7	5	393.1259	14°10'58.16"N	120°57'53.62"E	7	371.1261	14°11'22.03"N	120°58'9.85"E	869.47
2	3-59	3	463.8022	14° 9'24.35"N	120°57'39.62"E	59	31.22159	14°22'22.69"N	120°56'31.56"E	24004.50
1	13-14	13	145.0812	14°18'23.92"N	120°59'13.72"E	14	133.9903	14° 18.603'N	120° 59.055'E	480.09
1	12-14	12	148.613	14° 18.329'N	120° 59.118'E	14	133.9903	14° 18.603'N	120° 59.055'E	520.31
1	11-16	11	149.663	14° 18.044'N	120° 58.916'E	16	124.3484	14° 18.776'N	120° 58.920'E	1352.01
1	17-18	17	129.7673	14° 18.725'N	120° 58.789'E	18	113.1687	14° 18.826'N	120° 58.684'E	269.93
1	8-17	8	234.711	14° 15.488'N	120° 59.049'E	17	129.7673	14° 18.826'N	120° 58.684'E	6177.91
1	15-19	15	134.8011	14° 18.287'N	120° 58.290'E	19	106.6481	14° 18.642'N	120° 57.908'E	934.09
1	9-22	9	193.35	14° 16.528'N	120° 58.253'E	22	98.39375	14° 18.971'N	120° 57.705'E	4611.45
1	10-23	10	154.1908	14° 17.331'N	120° 57.734'E	23	80.96656	14° 19.516'N	120° 57.397'E	4133.18

2	14-21	14	133.9903	14° 18.603'N	120° 59.055'E	21	105.7208	14° 19.146'N	120° 58.691'E	1200.74
2	18-21	18	113.1687	14° 18.826'N	120° 58.684'E	21	105.7208	14° 19.146'N	120° 58.691'E	588.31
1	20-44	20	118.0377	14° 18.832'N	14° 18.832'N	44	41.54596	14° 21.588'N	120° 56.563'E	5743.63
1	30-39	30	81.90814	14° 19.637'N	120° 56.697'E	39	55.30947	14° 20.561'N	120° 56.031'E	2080.05
1	31-39	31	80.56731	120° 56.031'E	120° 56.344'E	39	55.30947	14° 20.561'N	120° 56.031'E	1864.71
1	40-47	40	63.21944	14° 20.400'N	120° 55.894'E	47	39.73262	14° 21.616'N	120° 55.748'E	2263.46
2	39-80	39	55.30947	14° 20.561'N	120° 56.031'E	80	0.7	14° 26.517'N	120° 55.910'E	10984.86
1	43-46	43	55.53639	14° 21.077'N	120° 56.297'E	46	39.55898	14° 21.500'N	120° 55.802'E	1181.87
1	35-38	35	83.22163	14° 20.285'N	120° 57.548'E	38	54.51525	14° 21.007'N	120° 57.260'E	1427.96
1	28-38	28	100.3311	14° 19.768'N	120° 58.062'E	38	54.51525	14° 21.007'N	120° 57.260'E	2071.82
1	32-34	32	89.2032	14° 20.251'N	120° 57.963'E	34	83.22689	14° 20.463'N	120° 57.917'E	398.58
1	29-34	29	95.72849	14° 20.002'N	120° 58.183'E	34	83.22689	14° 20.463'N	120° 57.917'E	975.71
1	33-42	33	98.33135	14° 20.313'N	120° 58.199'E	42	46.90046	14° 21.535'N	120° 57.526'E	2545.65
3	21-45	21	105.7208	14°19'8.76"N	120°58'41.46"E	42	46.90046	14°21'44.51"N	120°56'57.15"E	5696.84
1	27-36	27	109.9995	14°19'49.19"N	120°58'44.73"E	36	75.14953	14°20'55.02"N	120°58'41.76"E	2012.85
2	25-26	25	112.2812	14°19'40.95"N	120°59'4.33"E	26	95.35459	14°19'59.17"N	120°59'6.83"E	583.82
1	24-26	24	105.8878	14°19'41.86"N	120°59'12.98"E	26	95.35459	14°19'59.17"N	120°59'6.83"E	562.24
2	26-72	26	95.35459	14°19'59.17"N	120°59'6.83"E	72	7.604295	14°24'49.42"N	120°56'48.71"E	9833.47
2	34-41	34	83.22689	14°20'27.76"N	120°57'54.99"E	41	49.82454	14°21'13.66"N	120°57'13.20"E	1888.49
2	38-41	38	54.51525	14°21'0.42"N	120°57'15.60"E	41	49.82454	14°21'13.66"N	120°57'13.20"E	409.92
1	48-60	48	44.66206	14°21'39.67"N	120°56'8.90"E	60	29.25159	14°22'17.06"N	120°55'54.23"E	1233.53
3	41-45	41	49.82454	14°21'13.66"N	120°57'13.20"E	45	37.939	14°21'44.51"N	120°56'57.15"E	1064.68
1	37-52	37	68.0992	14°21'28.11"N	120°58'45.43"E	52	47.41051	14°22'16.19"N	120°58'22.07"E	1610.23

1	51-55	51	52.76982	14°22'6.98"N	120°57'45.77"E	55	30.73618	14°22'50.12"N	120°57'51.56"E	1344.09
1	56-66	56	37.26807	14°22'53.59"N	120°57'39.53"E	66	13.27068	14°23'50.29"N	120°56'46.92"E	2343.48
1	57-63	57	38.37227	14°22'39.23"N	120°57'28.07"E	63	18.47463	14°23'12.35"N	120°56'47.78"E	1576.16
1	58-62	58	35.36711	14°22'36.18"N	120°57'2.61"E	62	19.15739	14°23'9.71"N	120°56'46.15"E	1145.03
1	50-61	50	42.78047	14°22'8.49"N	120°57'15.23"E	61	21.46007	14°22'55.82"N	120°56'37.26"E	1845.97
1	49-49.5	49	46.88607	14°21'52.42"N	120°57'5.37"E	49.5	33.35084	14°22'6.19"N	120°56'46.05"E	720.53
4	45-83	45	37.939	14°21'44.51"N	120°56'57.15"E	83	0	14°27'36.61"N	120°55'20.80"E	11239.10
1	53-68	53	49.90404	14°22'32.34"N	120°58'37.75"E	68	23.32995	14°24'12.32"N	120°57'36.08"E	3614.09
1	54-68	54	48.21714	14°22'39.25"N	120°58'26.37"E	68	23.32995	14°24'12.32"N	120°57'36.08"E	3201.68
1	64-67	64	34.90218	14°23'28.40"N	120°57'58.58"E	67	15.87711	14°24'12.08"N	120°57'19.54"E	1777.35
1	65-71	65	30.7222	14°23'55.80"N	120°58'21.85"E	71	13.64192	14°24'56.61"N	120°57'19.85"E	2634.23
1	69-70	69	15.72534	14°24'28.48"N	120°56'45.31"E	70	10.06625	14°24'44.87"N	120°56'50.86"E	530.68
2	68-81	68	23.32995	14°24'12.32"N	120°57'36.08"E	81	0.76653	14°27'18.08"N	120°55'58.74"E	6713.32
1	73-74	73	11.90761	14°25'11.82"N	120°57'21.39"E	74	7.442218	14°25'49.65"N	120°56'54.36"E	1419.57
1	75-78	75	5.143465	14°26'8.40"N	120°56'47.03"E	78	2.561378	14°26'46.01"N	120°56'26.27"E	1311.24
1	77-78	77	3.051099	14°26'30.27"N	120°56'25.19"E	78	2.561378	14°26'46.01"N	120°56'26.27"E	492.98
2	78-81	78	2.561378	14°26'46.01"N	120°56'26.27"E	81	0.76653	14°27'18.08"N	120°55'58.74"E	1285.42
1	76-79	76	4.254199	14°25'55.45"N	120°56'4.57"E	79	1.035759	14°26'28.11"N	120°56'1.16"E	1019.98
3	81-82	81	0.77	14°27'18.08"N	120°55'58.74"E	82	0.20248	14°27'19.75"N	120°55'40.78"E	523.11